PREDICTION OF RESERVOIR QUALITY SANDS USING SEISMIC ATTRIBUTES AND GEOMORPHOLOGY DRIVEN BY MACHINE LEARNING FACIES CLASSIFICATION IN LOWER INDUS BASIN, PAKISTAN

By

SYED HAMZA SHAH BUKHARI

Department of Earth and Environmental Sciences
Bahria University, Islamabad

2024

PREDICTION OF RESERVOIR QUALITY SANDS USING SEISMIC ATTRIBUTES AND GEOMORPHOLOGY DRIVEN BY MACHINE LEARNING FACIES CLASSIFICATION IN LOWER INDUS BASIN, PAKISTAN

Thesis submitted to Bahria University, Islamabad in partial fulfillment of requirement for degree of Master of Science in Geophysics

SYED HAMZA SHAH BUKHARI

01-262222-025

Department of Earth and Environmental Sciences
Bahria University, Islamabad

2024

Bahria University

Department of Earth & Environmental Sciences
Islamabad Campus, Islamabad

Dated: 31-10-2024

C e r t i f i c a t e

A thesis submitted by **Mr. Syed Hamza Shah Bukhari** to the Department of Earth & Environmental Sciences, Bahria University, Islamabad in partial fulfillment of the requirements for the degree of **Masters in Geophysics** (Session **2022-2024**).

Committee Member	Name	Signature
Supervisor	Dr. Urooj Shakir	
Internal Examiner	Dr. Muhammad Iqbal Hajana	
External Examiner	Dr. Muhammad Kamal	*(signed)*
Post Graduate Coordinator	Dr. Muhammad Iqbal Hajana	
Head of Department (E&ES)	Dr. Syed Umair Ullah Jamil	

APPROVAL FOR EXAMINATION

Scholar's Name: <u>SYED HAMZA SHAH BUKHARI</u>

Registration No. <u>44660</u>

Programme of Study: <u>MS GEOPHYSICS</u>

Thesis Title: Prediction of Reservoir Quality Sands Using Seismic Attributes and Geomorphology Driven by Machine Learning Facies Classification in Lower Indus Basin, Pakistan

It is to certify that the above scholar's thesis has been completed to my satisfaction and, to my belief, its standard is appropriate for submission for examination. I have also conducted a plagiarism test of this thesis using HEC prescribed software and found similarity index **<u>18%</u>** that is within the permissible limit set by the HEC for the MS degree thesis. I have also found the thesis in a format recognized by the BU for the MS thesis.

Principal Supervisor's Signature: _____

Date: _____

Name: _____

AUTHOR'S DECLARATION

I, **"Syed Hamza Shah Bukhari"** hereby state that my MS thesis titled **"Prediction of Reservoir Quality Sands Using Seismic Attributes and Geomorphology Driven by Machine Learning Facies Classification in Lower Indus Basin, Pakistan"** is my own work and has not been submitted previously by me for taking any degree from this university **Bahria University Islamabad** or anywhere else in the country/world. At any time if my statement is found to be incorrect even after my graduation, the University has the right to withdraw/cancel my MS degree.

Name of scholar: Syed Hamza Shah Bukhari

Date: 07 November 2024

PLAGIARISM UNDERTAKING

I solemnly declare that the research work presented in the thesis titled **"Prediction of Reservoir Quality Sands Using Seismic Attributes and Geomorphology Driven by Machine Learning Facies Classification in Lower Indus Basin, Pakistan"** is solely my research work with no significant contribution from any other person. Small contribution/help wherever taken has been duly acknowledged and that complete thesis has been written by me.

I understand the zero-tolerance policy of the HEC and Bahria University towards plagiarism. Therefore, I as an Author of the above titled thesis declare that no portion of my thesis has been plagiarized and any material used as reference is properly referred to / cited.

I undertake that if I am found guilty of any formal plagiarism in the above-titled thesis even after the award of the MS degree, the university reserves the right to withdraw/revoke my MS degree and that HEC and the University have the right to publish my name on the HEC / University website on which names of scholars are placed who submitted plagiarized thesis.

Scholar / Author's Sign: _____

Name of the Scholar: Syed Hamza Shah Bukhari

DEDICATION

To my parents, whose unwavering support and boundless love have been the bedrock of my journey. Your sacrifices and encouragement have shaped every step I've taken, and this accomplishment is as much yours as it is mine.

To my family, whose collective love, support, and belief in my potential have been a source of endless motivation. Each of you has played a unique role in this journey, and for that, I am profoundly grateful.

To my friends, whose companionship, understanding, and laughter have made the journey not only bearable but truly joyful. Your belief in me has been a constant source of strength and inspiration.

And to all my teachers, whose guidance, wisdom, and dedication have illuminated my path. Your commitment to nurturing my growth and expanding my horizons has been instrumental in reaching this milestone.

Thank you all for being the pillars of my success and the light along the way.

ACKNOWLEDGEMENTS

ABSTRACT

Assessing reservoir quality plays an instrumental role in an oil / gas fields performance and lifecycle. Lower Goru gas fairway is a prolific producer in the Lower Indus Basin. This research is an effort to demarcate the reservoir quality within the different system tracts and parasequence sets. High energy depositional environments have better reservoir quality as a general rule, and we apply this concept to evaluate the East-West oriented progradation, parasequence stacks and system tracts. The hydrocarbon-bearing intervals of Miano gas field belong to the Early Cretaceous and are bounded by multiple flooding surfaces and other unconformities identified through well correlation. Overall, the NTG is good and porosity ranges from 12-16% in zones of economic water saturation (<30%). Seismic interpretation based on local flatness and semblance attributes highlights progradation and a basinward shift of facies. The upper shoreface facies deposited by wave-tide effect has better amplitudes and reflector continuity. The reservoir quality gets affected in lower sequences as the shale and heavy mineral content increases. Attributes including Grey Level Co-Variance Matrix (GLCM), 3D Curvature and Variance are rendered on the seismic volume for improved feature detection and holistic evaluation. These attributes are then blended for improved constraint on the deposition-facies association. In order to better quantify reservoir quality sands in the area, we run machine learning algorithms including Principal Component Analysis (PCA) and Self Organizing Maps (SOM's) on seismic attribute data and (MLP-SVM) Multilayer Perception Support Vector Machines model to predict facies using RGB logs with accuracy of 92.31%. The results add immense value by sharply amplifying subtle stratigraphic details and predicting reservoir quality across a varying stratigraphic ecosystem. To better understand the reservoir quality variation within our area of interest, seismic data is inverted to impedance and clay volume estimated from logs along with porosity is populated on the impedance volume. The sand is distributed as lenses with shale deposited in between them. With good porosities and low clay volume, these sand lenses provide good locations for future exploration endeavors. Furthermore, river ravinement, channels and lobe trends can also be observed on the inverted volume. The effective porosities are high, and clay volume is low in sand bodies in the upper inverted sequence, reflecting good reservoir quality. Evaluating log signatures for stratigraphic control over facies and seismic interpretation providing insights into the facies variation trend at different levels, the machine learning steered attribute analysis and inversion at the upper shoreface sequence above the flooding surfaces agree with each other thus encouraging the validity of results at the lower transgressive and regressive sequences in Miano.

ABBREVIATIONS

Abbreviation	Description
LGF	Lower Goru Formation
LIB	Lower Indus Basin
HC	Hydrocarbons
Fm	Formation
LSW	Lowstand wedge
LG	Lower Guru
HST	Highstand System Tract
LST	Lowstand System Tract
TST	Transgressive System Tract
MFS	Maximum Flooding Surface
LS	Lowstand
PNN	Probabilistic Neural Network
PCA	Principal Component Analysis
SOM	Self Organizing Map
MLP	Multilayer Perception
SVM	Support Vector Machines

CONTENTS

CHAPTER 1

INTRODUCTION

CHAPTER 2

GEOLOGY AND TECTONICS

CHAPTER 6

SEISMIC ATTRIBUTES AND MACHINE LEARNING BASED FACIES CLASSIFICATION

CHAPTER 7

RESULTS AND DISCUSSION

LIST OF FIGURES

TABLES

CHAPTER 1

INTRODUCTION

1.1 Research Background

With the advancement of reservoir interpretation in recent years and the need of 3D seismic data analysis, the industry has found out more and more new attributes on the basis of conventional seismic attributes. At the same time, methods and means used for the calculation and analysis of seismic attributes are increasing. Seismic attribute analysis has successfully been implemented in predicting reservoir lithology, hydrocarbon potential prediction as well as reservoir property estimates (Chopra et al., 2007).

To gain the desired output leading to pro-deltaic depositional environment (channels, linear bodies of sharp erosional contacts, turbidities, levees and tidal facies) seismic attribute analysis, this research will focus on frequency based, tensor based and geometric attributes to test results and screen the most insightful geomorphic extraction from the seismic volume (Oumarou et al., 2021).

In addition, machine learning models will be utilized which provides an excellent computing ability to classify and rank geomorphic features based on training the attribute volumes. Unsupervised learning algorithms, particularly Self Organizing Maps (SOM's) can be used to highlight and delineate multiple geologic features from the attributes volume (Marfurt et al., 2019).

The goal of a reservoir description study is identifying geomorphic features with reservoir quality facies (Chopra et al., 2007). This endeavor focuses establishing a sequence stratigraphic framework for clastic depositional systems as a predictor for reservoir quality sands within the geomorphic features of a paleo-delta in the Lower Indus Basin.

To achieve this, multiple clastic-deposition specific attributes are rendered to identify the sand bodies. Well log analysis further validates attribute analysis and also estimates the reservoir quality (Chopra et al., 2007). Once validated, machine learning models will be used to classify and rank the sand bodies within

the deltaic depositional system. Away from well prediction will be achieved through inversion and validated by geomorphology manifested through attributes.

Inversion is an effort to use seismic data to predict the characteristics of rocks, such as their porosity, thickness, fluid content, hydrocarbon saturation, etc. The three basic kinds are attribute, elastic, and acoustic. Each varies in their capacity for prediction as well as in the needs for data input. The data and the stage of exploration or development of an area determine which inversion is best to utilize. When we discuss inversion as a particular process, we typically refer to a numerical method that predicts rock characteristics like density, porosity, velocity, and water saturation by utilizing the seismic response. Numerous approaches assert that they can achieve this (Pandrel et al., 2006).

Seismic measures only four fundamental rock-physics properties:

i. P-wave velocity,

ii. S-wave velocity, density, and

iii. Anisotropy.

Only the above-mentioned three properties are the ones that can be predicted with high accuracy which is required for inversion. Inversion of the seismic data to other rock properties assumes a relationship between the property and one or more of these fundamental properties implicitly. A reliable estimation of the reservoir properties is of significant importance to E&P in making decisions (Pandrel et al., 2006).

Seismic inversion benefits include better seismic resolution and improved seismic interpretation as the layer-oriented impedance displays more complete constraints for reservoir models. Model based inversion is envisaged to capture the reservoir quality within the sequence stratigraphic framework.

The outcome of this research endeavor will be a ranking of geomorphic sequence stratigraphy-based targets with reservoir quality sands which can be readily up-scaled into a static model or evaluated for fluid contacts / saturations.

Key in utilization of sequence stratigraphy as a tool for interpretation of the sedimentary section are the major bounding and subdividing surfaces as these

surfaces are commonly created by changes in relative sea level and from the moment the oceans were first created, they have varied in distribution of water volume across the globe. This has resulted in transgressions that caused the shore and the near-shore being flooded so transgressive surfaces (TS) formed.

Once the rate of sea level rise reaches its most rapid change stage, the rate of sediment accumulating seaward of the shore slows down. From the onset of the Phanerozoic, the pelagic and benthic organic matter continued to accumulate, and these organisms isolated radioactive elements in the water column. As a result, from the Phanerozoic onwards, the sediments have strong radioactive signal on gamma logs with matching condensed sections of fossils that accumulated on a surface or in a thin zone which is known as the maximum flooding surface (mfs).

For establishing depositional setting of the sedimentary section, sequence stratigraphy utilizes geometric arrangement of sedimentary fill, particularly the vertical succession of sedimentary facies geometries and their enveloping surfaces known as stacking patterns. There is a similarity between Geometries and stacking patterns of un-cemented carbonates and clastic sediments as both respond to changes in base level and both can be subdivided by similar surfaces as well as both respond to wave and current movement similarly and as a result they may be transported

In quantitative interpretation, seismic attributes are transformed (primarily but not exclusively, amplitudes) into physical quantities which can be related to properties of rocks. Seismic attributes are characteristics of seismic waves which includes geometry, kinematics, dynamics and statistical characteristics, they are derived from seismic data through mathematical transformation (Delaplanche et al., 2006)

1.2   Literature Review

Early Creataceous clastics of the Lower Goru Formation in the Lower Indus Basin have been studied by different researchers with varying perspectives from both the academia and oil industries. Detailed research work on petroleum resources within the Sembar-Goru/Ghazij Composite total Petorleum System (TPS) was conducted by Wandrey et al in 2004. Sequence stratigraphic analysis of the Lower Goru Formation in the Lower Indus Basin was performed for fair play analysis by a few authors including Ahmad et al in 2004, Ahmad & Khan in 2010 and Weihua et al in 2005. Several authors have also worked for reservoir characterization by utilizing petrophysical techniques in the LGF, these authors include Shahid et al in 2008, Nadeem et al in 2016, Hussain et al in 2016, Siyar et al in 2017, Khan and Khan in 2018, Khalid et al in 2018, Qadri et al in 2019, Ali et al in 2019, Asad and Rahim in 2019, Yasin et al in 2019, Dar et al in 2021. Reservoir properties of the LGF have been analyzed based on integrated analysis of seismic and core data by various authors which includes Parvez et al in 2003, Riaz and Ibrahim in 2008, Ahmed et al in 2010, Munir et al in 2011, Ashraf et al in 2020. Diagenesis impact on the reservoir quality of LGF has been studied by various authors which includes Baig et al in 2016 as well as Dar et al. Various authors evaluated depositional facies based on petrography, well cuttings and wireline log motifs for the Lower Goru Formation, Lower Indus Basin, Pakistan, authors include Sahito et al in 2013, Nazeer et al in 2016, Dar et al in 2021. With the help of seismic, image logs and wireline logs, subsurface structural analysis in the Lower Indus Basin, Pakistan, were performed by Wasimuddin et al in 2005, Abbas et al in 2015, Khan et al in 2016, Nadeem et al in 2016 and Qureshi et al in 2021. Ahmad et al in 2015 identified reservoir geometries of C-Sand member of LGF in the Sawan Gas Field and discussed reservoir properties on the basis of well correlation seismic data and well correlation panels.

The Miano gas discovery in the block 20 situated in the province of Sindh is a geological curiosity as its appraisal represents a model driven exploration case history The Miano-1 discovery well was drilled to a prospect originally mapped as a structural/ stratigraphic combination trap within the LGF. Several sands from 3160-3900m were tight or produced water with some gas and while drilling Gas was produced at high rates only from one interval; the "B" sand (Krois et al., 1998).

The Miano area contains several gas fields having both structural and stratigraphic traps, according to various studies. The extensional regime located within Central Indus Basin, an area with normal faulting as a result of rifting of the Indian Plate from Africa then Madagascar & Seychelles. Miano area is located in the proven petroleum province with Cretaceous extensional tectonic history overprinted by Tertiary strike-slip tectonics. This may soon change, whilst the area is largely undrilled or explored in detail but has some modest production and substantial prospectivity with potential for hydrocarbon accumulation both structurally and stratigraphically by means of pinchouts. Widespread NW-SE aligned echelon arrays of linear gravitational sector elements are found throughout the faulted sedimentary rock and basement terrains covering almost 1000 km geographic distance area. Khairpur and Mari Highs are main structural features affording major control over the underlying freshwater resource system. The sand is of Lower Cretaceous age in arrangement and provides clothing as a tank, at the moment in Pandora area. The area is perspective to hydrocarbons and needs more wells with better understanding of structural, stratigraphic traps (Jadoon et al., 2017)

Pakistan lies in the tectonic plate boundary area and many wells have discovered giant hydrocarbon zones from traps located beneath these non-successions that are heterogeneously developed. Miano Gas field is one of a unique zone producing tons of oil, gas; however, it does not fit into conventional trap classes. The Fluvio-deltaic facies of the deltaic depositional setting contain Lower Goru which is also known as Principial Hydrocarbon reservoir. Geophysical researches have been comprehensive in this area for the exploration of these clastic reservoirs. For geoscientists, predicting thin reservoirs in these lateral heterogeneous environments is a challenge. In order to resolve this issue, we have utilized spectral decomposition; robust seismic interpretation tool for detail mapping of channel geometries and possibility of thin beds hydrocarbon bearing sands (Solangi et al., 2015).

This is where unconventional resource shales have a key role to play in global economic expansion. In case of unconventional prospect generation HC potential in Faults and Fractured shales is a significant challenge. For shale gas prospects exploration within the regional modeling in Indus platform, SW

Pakistan, this study applies the spectral decomposition (SD) technology of continuous wavelet transforms on high resolution 3D seismic data from the Miano area. The Schmoker method delineates 9.2% TOC containing high-quality shales in the western part of this platform. Seismic amplitude, root mean square (RMS) and most positive curvature attributes have restricted capability in defining the zones that contain prospective fractured shale lithological constituents (Naseer et al., 2017).

Sequence stratigraphy is a powerful tool for understanding the spatial and temporal relationships of sedimentary deposits. It focuses on the identification and correlation of genetically related sedimentary units, known as depositional sequences, which are bounded by surfaces of erosion (unconformities) or non-deposition (subaerial exposure surfaces). These surfaces represent significant changes in the relative sea level and can be recognized across different sedimentary basins, providing a framework for interpreting the stratigraphic record in terms of eustasy (global sea-level changes), tectonics, and sediment supply dynamics (Vail et al., 1977). The methodology of sequence stratigraphy involves detailed analysis of sedimentary facies and their stacking patterns within these sequences. By understanding the facies associations and their vertical and lateral variations, geologists can reconstruct the paleoenvironmental conditions during deposition. This approach allows for the recognition of systems tracts within depositional sequences, such as lowstand systems tracts (LST), transgressive systems tracts (TST), and highstand systems tracts (HST). Each systems tract represents a distinct phase of relative sea-level change and associated sedimentary response (Posamentier & Veil, 1988). One of the key applications of sequence stratigraphy is in hydrocarbon exploration. By correlating depositional sequences and identifying their systems tracts, geoscientists can predict the distribution and quality of reservoir rocks and seals within sedimentary basins. This predictive capability is crucial for optimizing drilling locations and maximizing hydrocarbon recovery. Sequence stratigraphy has been instrumental in improving the success rate of exploration and development efforts worldwide (Mitchum et al., 1977). In addition to its applied significance, sequence stratigraphy contributes to our understanding of Earth's history and dynamics. By analyzing sequences on a global scale, researchers can reconstruct past sea-level changes, understand climate

variability, and infer the tectonic evolution of continents and ocean basins over geological time scales. This holistic approach integrates data from various disciplines, including sedimentology, stratigraphy, paleontology, and geophysics, to unravel the complex interactions that have shaped our planet's surface through time. Sequence stratigraphy represents a fundamental paradigm shift in the study of sedimentary basins, providing a unified framework for interpreting stratigraphic records in terms of environmental and tectonic controls. Its applications range from practical exploration strategies in the petroleum industry to broader implications for understanding Earth's geological history and its response to environmental change. Continued research and application of sequence stratigraphy promise further insights into the dynamics of sedimentary systems and their role in shaping the Earth we inhabit today (Haq et al., 1987).

Based on previous work and this literature review, it is concluded that Lower Goru Formation has been thoroughly studied for the structural analysis as well the reservoir properties by using conventional petrophysical techniques. However, a handful of authors went as far to study it for application in predicting play placement through sequence stratigraphic techniques providing geomorphic views.

1.3   Research Gap

A sequence stratigraphic approach has been previously used in several studies for different objectives. However, quantitative interpretation integrated with machine learning driven facies classification for reservoir quality geomorphic sand bodies in the deltaic system has not been attempted before. Furthermore, there has been no research towards a reservoir quality (populating sand bodies with well properties) based ranking of sand bodies within the early cretaceous pro-delta in lower Indus basin.

1.4   Objectives

1. To evaluate fluvial / tidal dominated cretaceous sand deltaic geomorphology through selected seismic attributes within a sequence stratigraphic framework

2. To evaluate reservoir properties pertaining to reservoir quality, i.e., clay volume, total and effective porosity (higher PHIE translates to higher reservoir performance).

3. To classify and rank sand geomorphology in terms of reservoir quality and predict higher quality sands within various system tracts.

1.5 Acquired Data

Miano field data was acquired from DGPC for the purpose of this study. The data included:

Table 1.1. Acquired data.

Seismic Data	Wells
12 Sq.kms of 3D Seismic data	Maino 2, 9, 10

1.6 Study Area
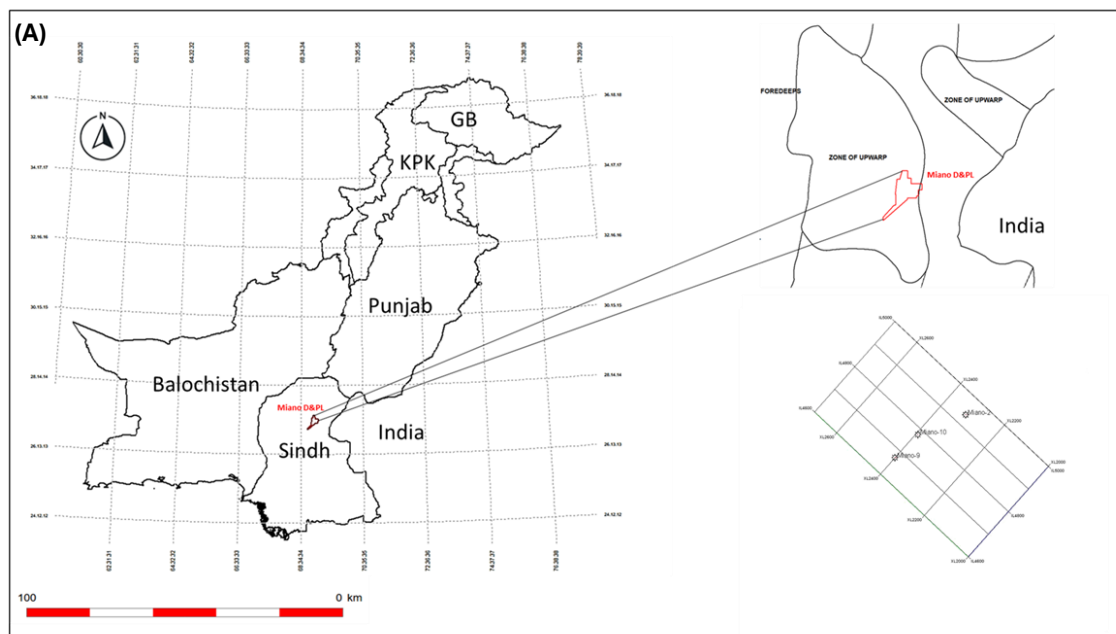
Fig 1.1. Lower Indus Basin, Sindh Province, Miano Block, Lower Goru (Modified after Yang et al., 2023)

Miano field (Fig 1.1) is situated in the Lower Indus Basin, Pakistan and it is confined by Indian shield towards east, while Sulaiman Range arc to its west. The open westward dipping of the Sind platform is locally broken by north to south trending elevated Khairpur High interpreted as large basement induced structure. The Sindh

platform resumes its westward dip to the west of the Khairpur High, forming a monocline dipping towards the Kachhi foredeep. This foredeep is an asymmetric Molasse basin with the deepest part near to Kirthar Fold Belt (Smewing et al., 2002).

1.7   Exploration history of study area

Miano Gas Field was discovered in the year 1963, from which multi zone hydrocarbon bearing formation penetrated interval of three peak groups at a depth range between 2922 meters and it corresponds to early Cretaceous Age. They are enclosed by shale intervals that are known as organic rich with maximum flooding surfaces (MFS). Hydrocarbons bearing intervals have two reservoir units, a tight gas and an overlying conventional unit. The reverse trend of two reservoirs makes it difficult for the production in forecasting and well proposal design to be developed by them using tight gas technology. For this purpose, detailed Miano gas field reservoir characterization is conducted in order to infer a reliable predictive model of the overburdened that should be valid for further exploitation. Geological genesis analysis integrating cores, borehole logs and 3D seismic data demonstrates that the productive zone of tight gas reservoir is tidal-influenced shore facies deposition with intergranular pore space reduced by mineral cement during burial diagenesis while overlaying conventional reservoir shows an incised fluvial channel sand body derived from deltaic deposition and abundant well-connected macropore network in the bulk volume), resulting excellent drillability (Karanovich et al., 2021).

Shelf-margin deltas tend to normally develop during the falling-stage and lowstand periods of relative sea level (Szczepan et al., 2003). In some cases, the shelf-edge deltas can also accumulate in periods of relative sea level highstand and can even rise if it is associated with an unusually high supply of sediment or narrow shelves (Szczepan et al., 2003). The formation of shelf-edge deltas however, requires shoreline regression across the entire shelf which mostly occurs in periods of forced regression (Posamentier et al., 1992). Since they were initially recognized in Quaternary shelf-margin sequences, interest in shelf-edge deltas has been on the rise as they usually form sand-rich accumulations (Suter and Berryhill, 1985), and thus prolific hydrocarbon reservoirs (Mayall et al., 1992). Furthermore, transportation of fluvial-derived sands from the shelf to deep-water occurs

preferentially in periods of falling-stage and lowstand (Posamentier & Vail, 1988) and it is considered that the shelf-edge deltas are the main driving force behind the delivery of sand to the slope and basins (Steel et al., 2000), (Porebski & Steel, 2003). Shelf-edge deltas accumulating in higher accommodation / sediment supply conditions, or which lacks significant fluvial incisions have proven to be inefficient in delivering sands to the slope and basins. Therefore, presence of shelf-edge deltas does not systematically guarantee formation of coeval turbidite reservoirs (Plink-Björklund & Steel, 2002), (Uroza & Steel, 2008), (Steel et al., 2003), (Dixon et al., 2012).

CHAPTER 2
GEOLOGY AND TECTONICS

2.1   History of plate tectonics

The concept of plate tectonics has been revolutionary in developing a better understanding of the Earth's geological processes as well as the dynamic nature of its crust. The history of plate tectonics goes all the way back to the early 20th century when a scientist named Alfred Wegener proposed his theory of the continental drift in 1912. It was hypothesized by Wegener that continents were once joined together in a single supercontinent called Pangaea and had since drifted apart to their current positions. This theory was based on the fit of continental coastlines, distribution of fossils, and geological similarities between continents on opposite sides of the Atlantic Ocean (Wegener, 1915). However, Wegener's continental drift hypothesis faced significant skepticism and criticism as he could not give a plausible explanation for how the continents move through solid oceanic crust. Advancement in geophysics in the middle 20th century, particularly the development of paleomagnetism and seismic studies, provided critical evidence supporting the concept of moving lithospheric plates. In the 1950s and 1960s, discoveries in marine geology and geophysics, particularly mid-ocean ridges mapping and the identification of magnetic striping on the seafloor, they provided key insights into the dynamic processes at work beneath Earth's surface. The Vine-Matthews-Morley hypothesis in 1963 proposed that alternating magnetic striping observed along mid-ocean ridges was the result of seafloor spreading, where new oceanic crust is formed at spreading centers and older crust is subducted back into the mantle (Vine et al., 1963). The integration of these findings culminated in the development of the theory of plate tectonics, which was formally articulated in the late 1960s and early 1970s, this theory proposes that lithosphere of the Earth is divided into several large and rigid plates which float on semi-fluid asthenosphere beneath them. Interaction of these plates takes place at their boundaries, which can be either divergent (plates moving apart), convergent (moving towards each other, colliding) or transform (sliding past each other).

2.2   Plate tectonics and drift of continents through ages

Plate tectonics process forms new oceans by rifting, and it also creates oceanic ridges and forms new oceanic crust, causing the continents to collide and destroy the ancient oceans through subduction of their lithospheric plates, giving rise to some of the earth's most notable physical features, such as the oceanic ridges, trenches, chains of volcanic islands, island arcs, and their associated basins and the large mountain chains of the world. The plate tectonic process leads to the concentration of valuable elements and forms significant ore deposits. Paleomagnetic data from Proterozoic (750 Ma), suggest that there was one Super Continent surrounded by the ocean, and the Indian plate was a part of it (Dietz & Holden 1976). During the Late Permian from 250 Ma ago to Miocene about 20 Ma ago, several continental blocks broke from the northern part of Gondwanaland and drifted across. Kohistan Island Arc collided with and accreted onto the southern margin of Eurasia, which was a fragment of the Laurasia. The whole process was accompanied by the replacement of the Paleo-Tethys by several oceanic spaces (Dietz & Holden, 1976). Earlier, the Indian plate was part of the Gondwanaland, which later separated from it about 130 Ma, followed by its drift northwards. While India was drifting, intra-oceanic subduction started ahead of it, which resulted in volcanic arcs in a series that includes the Kohistan Ladakh, and the southern boundary includes Arabian and Afghan microplate. About 102-85 million years ago, the back-arc basin started closing and eventually closed completely. Later the Kohistan Ladakh collided with Eurasia. After accretion to Eurasia, the Kohistan arc formed Andian-type passive margin. Later about 55-50 million years ago, Indian Plate eventually collided with the Kohistan-Ladakh part of Eurasia and formed the Karakoram and the Himalayas and controlled the evolution of basin (Dietz & Holden, 1976).

Figure 2.1. Pangea reconstruction with a relative plate motion hierarchy depicted at 200 MYA (Modified after Seton et al., 2012)

The Theory of Plate Tectonics Unification elucidates Earth's surface evolution through continental breakup, supercontinent amalgamation, and subsequent continental breakup episodes, leading to creation of new oceanic basins at cost of the older oceanic gateways. The configuration of continents serves as a primary control on long-term oceanic circulation, influencing the hydrosphere's capacity in order to reduce the thermal gradient from poles to equator.

Plate boundary reconstructions uses seafloor magnetic anomalies to reverse seafloor spreading and then create snapshots of the historical setting/arrangement of continents and oceanic crust. When there is lack of seafloor spreading histories, geological data from the continents can be utilized to deduce their past positions. This information allows for estimating the required seafloor spreading rate and direction needed to move these continents. This method enables the restoration of continents to a Pangea configuration, where all (or most) continents were united into a single supercontinent (Seton et al., 2012).

Indian plate was part of the Gondwanaland, which later separated from it about 130 Ma, followed by its drift northwards. While India was drifting, intra-oceanic subduction started ahead of it, which resulted in volcanic arcs in a series that includes the Kohistan Ladakh, and the southern boundary includes Arabian and Afghan microplate. About 102-85 million years ago, the back-arc basin started closing and eventually closed completely. Later the Kohistan Ladakh collided with Eurasia. After accretion to Eurasia, the Kohistan arc formed Andian-type passive margin. Later about 60-65 million years ago, Indian Plate eventually collided with the Kohistan-Ladakh part of Eurasia and formed the Karakoram and the Himalayas and controlled the evolution of basin (Dietz & Holden, 1976).

2.3   Geology of Pakistan

Pakistan is in the convergence area of the Indus Basin between Eurasia and India. Indus Basin has a sedimentary fill of the Precambrian age to recent. Based on sedimentation history, Indus-basin has been divided into three units, Upper Indus Basin, Middle Indus Basin, and the Lower Indus Basins. Sargodha High and Pizu uplift separate the Middle Indus Basin from Upper Indus Basin. The Punjab platform is a monocline structure which is dipping very gently towards the west, and the Sulaiman Fold belt has been resulted from the of Ind-Eurasian plates, the collision took place in the Paleocene to Mio-Pliocene. In the south of Mari Kandhkot High, the Lower Indus Basin is located, and the Indian Shield bounds it towards the east of the Indian Plate, and the southern border of LIB is along the offshore of the Indus Sub-basin (Iqbal & Shah, 1980).
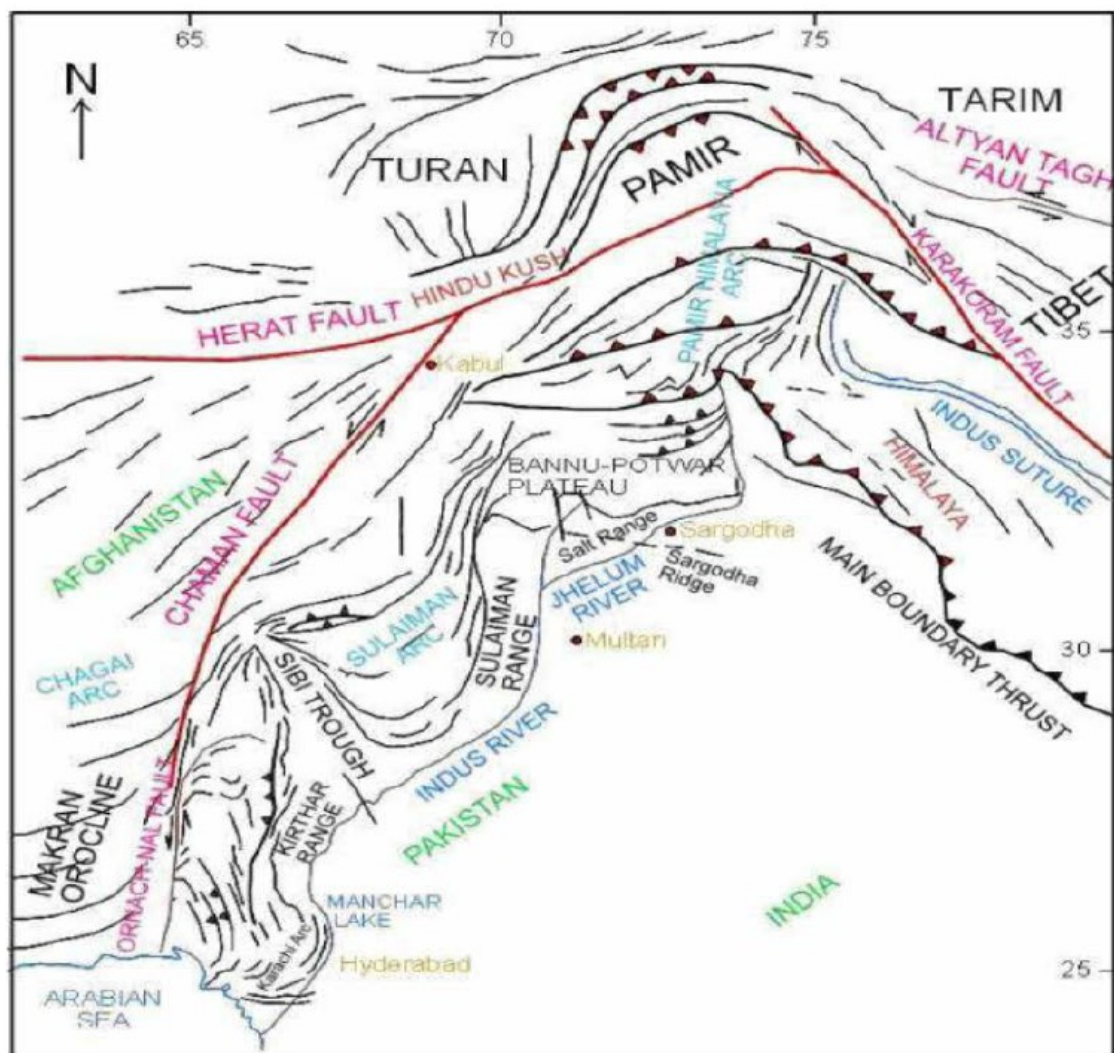
Figure 2.2. Tectonics map of Pakistan (Haleem et al., 2014).

Miano Field lies on the eastern flank of Khairpur High. Khairpur High, during its geological history of rifting and compression, went through number of phase if inversion and subsidence. The Proterozoic basement beneath the Khairpur High is also marked by high geothermal gradients because of recent uplift and / or higher heat flow. Schematic east to west stratigraphic cross-section showing a generalized basin architecture, with the thickening and thinning of the Cretaceous succession towards the E-W (Haleem et al., 2014).

The above contributes to the evidence of onlapping Paleocene clastics overlying this Basal Tertiary Unconformity and there is dramatic thickness, facies changes within. There are significant Eocene to thick Oligocene to Pleistocene Molasse deposits in the foredeep on western end near Kirthar Range. There is a

hiatus, or erosional phase of variable length between the Jurassic platform carbonates and the basal clastic. The Whitehorn was last deposited in the Miocene to Pliocene, outcropping over most of its entirety with minor hypothetical exception on a high arm at Kakela. Sediments of the Cretaceous. In general, Lower Cretaceous sediments comprise the Sembar Formation and Lower Goru Member of the Goru Formation. Sembar clinoforms show a westwards pro-grading history, aging basin ward and becoming younger towards the top. A time gap 30my, connected with the Late Aptian/Base Albian sea-level low stand is observed in-between Lower Goru Member and Sembar Formation (Haleem et al., 2014).

The Lower Goru Member in its lower part is subdivided (in the base upwards) as "A", "B" and "C". Lower Goru "A', "B" and 'C" intervals were deposited in a ramp type setting unlike the seismic geometries with relatively steeply dipping clinoforms which shows shelf type margin developed by Sembar Formation. These three intervals account for a modest 7 MY of the total time scale. This section can be dated within the time span of global sea level rise from Albian into Cenomanian. The Lower Goru Member shows a rise in carbonate content, finally becoming stabilized within the upper member. The paleontological record shows a deepening of the water for these deposits. The Upper Goru Member contains basal shales and marls succeeded by limestones, absent in the outcrops but rumored to attain a thickness of up to 500 feet (150 m) within basin (Krois et al 1998).

2.4 Generalized stratigraphy

Table 2.1. Generalized stratigraphy of Lower Indus Basin. (Khalid et al., 2014)

Age	Formation	Thickness (m)	Lithology	Description	Source	Reservoir	Seal	Overburden	Trap	Generation Migration Accumulation	Preservation
MIOCENE PLIOCENE	Alluvium	39									
MIOCENE PLIOCENE	Siwalik	430		Sandstone Shale Siltstone				▌	▯	▮	▮
EOCENE	Habib Rahi	49		Limestone		▬	▐		▯		
EOCENE	Ghazij	250		Sandstone Shale Limestone		▬			▯	▮	
PALEO-CENE	Ranikot	30		Sandstone Shale		▬		▐		▮	
CRETACEOUS	Goru	900		Sandstone Shale Limestone Marl		▬ ▬					
CRETACEOUS	Sember	150				▬					
JURASSIC	Chiltan / Samanasuk	300		Shale Limestone Marl		▬					
JURASSIC	Shinawari	200		Shale Limestone Marl							
JURASSIC	Datta	80		Sandstone Shale		▬					
PERMAIN	Warcha/ Dandot	110		Shale Conglomerates		▬					
PERMAIN	Tobra	60		Sandstone Shale		▬					
CAMBRIAN	Baghanwala	120		Sandstone Shale Silt		▬					
CAMBRIAN	Jutana	70		Dolomite Shale							
CAMBRIAN	Kussak	150		Sandstone Shale Dolomite							
CAMBRIAN	Khewra	150		Sandstone Shale Dolomite		▬					
INFRA CAMBRAIN	Salt Range	210		Shale Sandstone Dolomite Salt		▬ ▬					
INFRA CAMBRAIN	Basement										

2.4.1 Chiltan Limestone

Chiltan Limestone consists of massively bedded limestone, which is dark gray and forms a thick band on the rough surface. These limestones have unique property; they are highly resistant, and they also form the highest mountain valley around the Quetta and Chiltan Formation is underlain by the Shrinab Formation (Shah, 1977; Shah, 2009).

2.4.2 Sembar Formation

Sembar Formation is deposited in a passive margin geological setting, and its sediments have derived from the uplifted Indian Continent towards the Southeast (Hedleyetal, 2009). At present, the Formation's distribution indicates that it had been deposited in a large sedimentary basin, which most likely extended from the Indian Shield in the East (Raza et al., 1990). The term Sembar Formation was coined by Williams in the year 1959 (Raza et al., 1990). The Sembar Formation passes through the Mari hills, which are composed of clastic rocks, mainly shale and with a less amount of siltstone and sandstone in the lower Indus platform. In the southern part of the Platform, the sand content gradually increases. Sembar Formation consists of black to dark grey silts in the northeast towards the Sulaiman Fold Belt and the Formation gradually becomes sandy towards the Eastern part of the fold belt within the lower part. Glauconite is found very commonly in the Formation in the Formation, and sandy shales, phosphatic nodules, and pyrite are also developed locally (Shah, 2009). The color of shale tends to be light to dark grey and its hardness being medium hard (Raza et al., 1990). The thickness of the Formation in the type section is approximately 133 meters, although it increases up to 265 meters towards the Mughal Kot section of the Sulaiman Range (Shah, 2009). The depositional environment of Sembar Formation is open marine (Qadri et al., 1986). The lower contact of the Formation is with several Jurassic formations, e.g., Mazar Drik Formation, Chiltan L.S., and a disconformable contact with Shrinab Formation. Its upper contact however, is gradational with Guru Formation (Shah, 2009). Age of the Sembar Formation is Neocomian mostly. Sembar Formation consists of shale, which is black and silty, and shale is interbedded by siltstone, which is also black; argillaceous limestone beds are also present but on the top of their surface nodular rusting weathering also

occur. The greenish color of weathering is due to the presence of glauconite mineral, pyrite phosphatic nodules sandy shales are also present at the basal part, and Goru Formation overlies Sembar Formation (Shah et al., 2009).

2.4.3 Goru Formation

Goru Formation consists of shale, siltstone, and interbedded limestone of light-medium grey and olive-grey. The size of limestone is fine grain and thin-bedded of shale, and siltstone is quite different like grey to greenish-grey, and sometime in maroon color, they are present locally. The concentration of limestone is quite high in the lower and upper part of Formation, while shale changes its proportion throughout the Formation (Shah, 1977; Shah, 2009).

2.5 Petroleum system of Lower Indus Basin

Indus Basin's petroleum system with all of its formations is given in a generalized stratigraphic column (Table 2.1). Success rate is highest in Lower Indus Basin as strings of discoveries have been made in a relatively short time in a small fault block of the Goru reservoir. During the 1980s, several oil and gas discoveries were made in the Lower Goru Formation. Exploration efforts were pushed further later in the 1990s at the time when major gas discoveries were made in the rocks of Late Cretaceous, Bhit and the Zamama are two examples of those discoveries (Raza et al., 1990).

2.5.1 Source Rocks of Lower Indus-Basin

Sembar Formation is the main source rock for majority of the Indus Basin, although there are also other source rocks with potential (Table 2.2).

Table 2.2. Source Rocks of Lower Indus Basin (Shah, 1977; Shah, 2009).

FORMATION	LITHOLOGY	AGE
Laki	Shale	Eocene
Ranikot	Shale	Paleocene
Mughalkot	Shale	Cretaceous
Goru	Mudstone/Shale	Cretaceous
Parh	Shale/Packstone	Cretaceous
Sembar	Mudstone/Shale	Cretaceous

| Chiltan | Limestone | Jurassic |
| Wulgai | Shale/Limestone | Triassic |

2.5.2 Reservoir Rocks of Lower Indus Basin

Reservoir rocks are shown in table 2.3.

Table 2.3. Reservoir Rocks of Lower Indus Basin (Shah, 2009).

FORMATION	LITHOLOGY	AGE
Chiltan	Limestone	Jurassic
Sembar	Shale	Early Cretaceous
Lower Goru	Sandstone/Mudstone	Cretaceous
Pab	Sandstone	Cretaceous
Ranikot	Limestone Fracture	Paleocene
Laki	Limestone	Eocene
Nari	Sandstone	Oligocene
Gaj	Sandstone	Miocene
Sui Main LS	Limestone	Eocene
Habib-Rahi LS	Limestone	Eocene

2.5.3 Seal and Trap of Lower Indus Basin

Sembar Formation serves as a seal-rock for the Chiltan Limestone while the upper Goru Formation comprises of marl and shale; therefore, the reason that it acts as a seal rock. Its upper part is known to be an excellent cap for the lower Goru reservoir which underlies it. The fault traps in LIB resulted from extension caused by rifting (Raza et al., 1990).
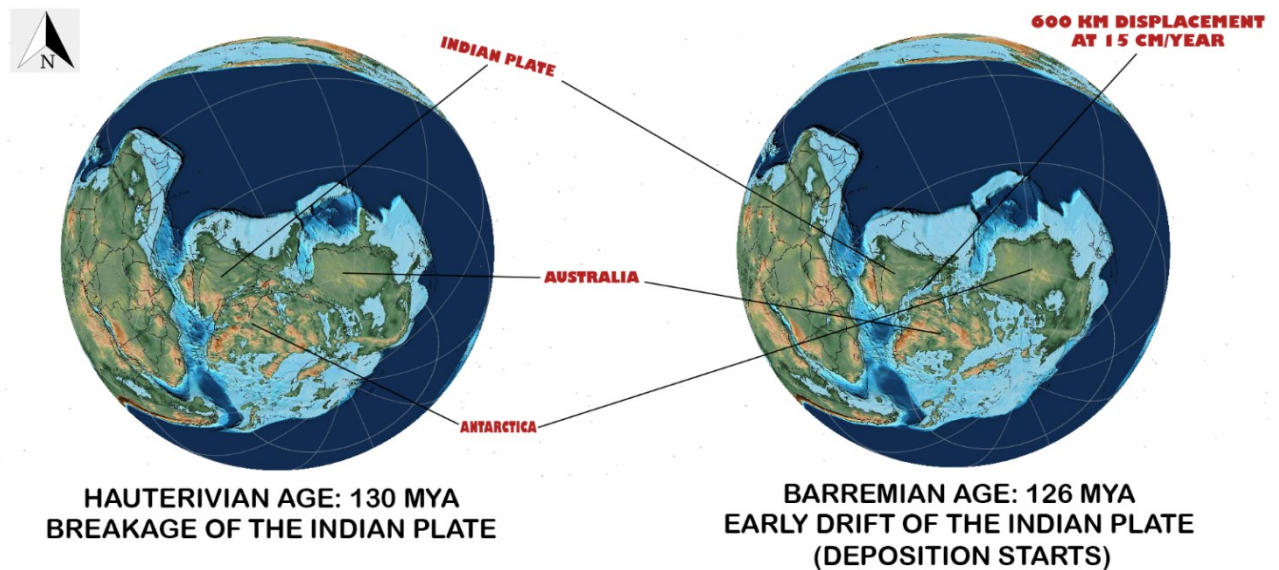
2.6 Environment of deposition

HAUTERIVIAN AGE: 130 MYA
BREAKAGE OF THE INDIAN PLATE

BARREMIAN AGE: 126 MYA
EARLY DRIFT OF THE INDIAN PLATE
(DEPOSITION STARTS)

Figure 2.3. Position of the Indian plate Hauterivian and Barremian Age (Modified after Seton et al., 2012)

2.6.1 Hauterivian Age

The Indian Plate had separated from the supercontinent Gondwana a long time ago, some 130 million years during Hauterivian age and started colliding with Asia about 40 to 50 million years back. At that time, the Indian Plate was much farther south than it is now. These low-lying areas marked the environments of the Indian Plate at that time:

1. Marine Influence: The shallow regions of the Indian Plate were largely occupied by marine environments. This was the province of marine sedimentation-dominated epicontinental seas. Proof that swamps and forests can be submerged enough comes from the presence of marine fossils, as well as the deposition of limestones, shales and marls which are clearly marine in origin.

2. Coastal and Shelf Environments: Regions of Indian Plate coastal and shelf environments had been previously sedimented by terrestrial and marine material which resulted in deposition of combinations of carbonates, siltstones, sandstone as is observed at many places.

3. Fluvial and Deltaic Systems: Terrestrial environments were also significant, including deltaic environments and river systems. These conditions resulted in the

deposition of clastic sediments such as sandstones and mudstones carried by rivers into floodplains, deltas etc.

4. Vegetation and climate: Climate of the Indian plate in the Hautervian age was warm and humid which supported a range of diverse vegetation. The presence of plant fossils like ferns, conifers etc., indicates very lush vegetation in some areas which contributes to the formation of coal and other organic-rich deposits.

5. Tectonic Activity: Indian plate experienced tectonic activity as a result of Gondwana separation from Laurasia. Sedimentation patterns and formation of depositional environments were influenced due to the tectonic movement. Sea levels were influenced by rifting and initial stages of plate separation which created new basins as well.

In short, Indian plate was a mix of deltaic, coastal, fluvial and shallow marine settings and was influenced by warm and humid climatic conditions and the active tectonic processes associated with the breakup of Gondwana (Dietz & Holden, 1976).

2.6.2   The Barremian Age

The Barremian age (roughly 129.4 to 125 MYA), when the Indian Plate continued a process of breaking away from Gondwana it was causing active geological and climatic changes. The environment of the Indian Plate at that time is characterized by the features given below.

1. Marine Environments: During this period, significant portions of the Indian Plate were under shallow marine environments similar to those during Hauterivian age. They were continental shelves and epicontinental seas, where was predominant one marine sedimentation. Limestones, shales and marls were deposited in those areas, and they contained marine fossils as well in some cases.

2. Coastal and Shelf Environments: Margins of the Indian plate had coastal and continental shelf environments. Marine and terrestrial processes interacted in these dynamic areas, resulting in mixed sedimentary deposits which included sandstones, siltstones and carbonates.

3. Fluvial and Deltaic Systems: There is a major role of river systems and deltaic environments in sedimentation on the Indian Plate. Clastic sediments like mudstones, sandstones and siltstone were deposited by rivers mostly in floodplains and deltas.

4. Vegetation and Climate: The Barremian climate was warm, humid with abundant vegetation. Plant fossils (ferns, conifers and cycads) demonstrate that the area accommodated rich vegetation. This vegetative debris ultimately resulted in the formation of coal and other organic-rich deposits occurring at different places.

5. Tectonic Activity: The tectonic activity that led to the breakup of Gondwana continued in part as stresses acting upon India itself due to Plate Tectonics. Mechanisms of rifting and basin forming, were producing factored sea-level changes generated by progradation stacked sequences. Tectonism: this created rift valleys and a variety of fault systems.

6. Lagoonal and Coastal Plains: In some regions, lagoon & coastal blanketed were usual. This created a range of sediment types (evaporites, for example, formed in the drier areas) and variable freshwater/saline/hypersalinity systems. Marine deposits are part of the continental shelf, suggesting a warm, humid climate on the Indian Plate throughout Barremian time. Associated with the breakup of Gondwana, tectonic activity further influenced sedimentation and depositional environments (Dietz & Holden, 1976).
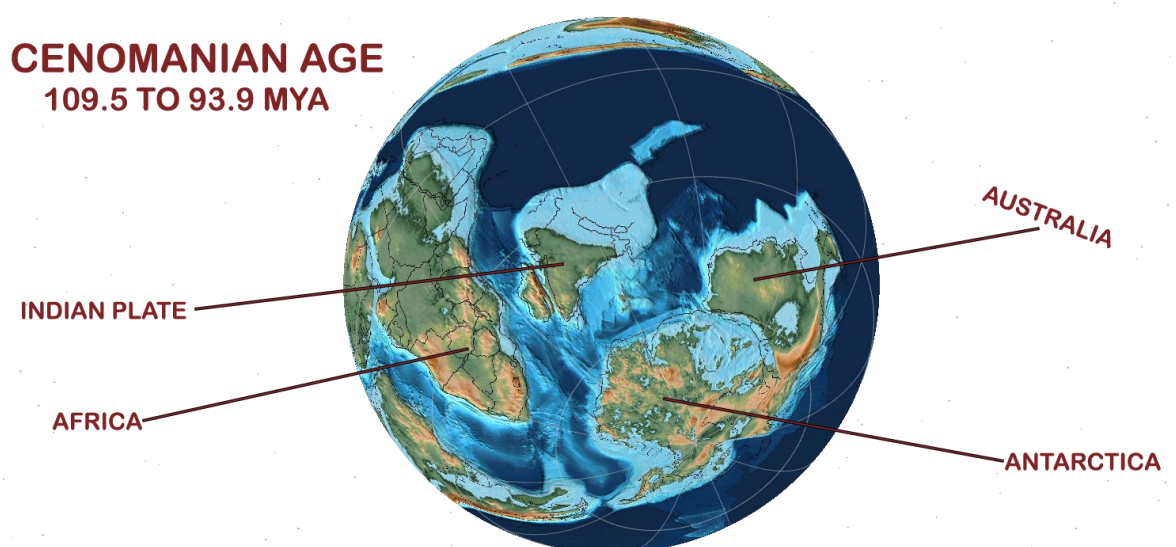

Figure 2.4. Position of the Indian plate in the Cenomanian age ((Modified after Seton et al., 2012)

2.6.3 The Cenomanian Age

By the Cenomanian epoch (about 100.5 to 93 Ma) of the Late Cretaceous, as it became further north from its later apparent position throughout even larger a part of middle and early cretaceous periods at other million year. All this movement along with global sea level changes and climatic conditions affected the depositional environment in Indian Plate. Some notable features of the Cenomanian age depositional environments are as discussed below.

1. Marine Environments: Wide portions of the Indian Plate remained under extensive shallow-marine environments. These settings are the result of deposition in margin parts of what was essentially a tethys sea existing between surrounding north continents and migrating Indian Plate. The diversity of benthic and planktonic microorganisms also attests to a sea that was high in nutrients throughout scapulite-time marine sedimentation, which is generally characterized by the accumulation of limestones, marls and shales richly loaded with species like ammonites.

2. Carbonate Platforms: warm, tropical to subtropical climate favored the formation of vast carbonate platforms & reefs. These platforms were areas of significant carbonate sedimentation— and the depositional environment is said to have cleared up for calcareous algae, stromatoporoids, crystals resembling calcite. The result was large buildups of limestone materials including reefs, rudistids; reef building organisms like corals, rudists with thick sequences of exogenic material produced in shallow seas.

3. Coastal and Shelf Environments: Around the margins of the Indian Plate, coastal (littoral) and continental shelf environments prevailed. They are characterized by interbedded sands, siltstones and mudstone deposited from both marine and terrestrial sources. In addition, tidal flats with lagoons and estuaries were characteristics of these environments.

4. Fluvial and Deltaic Systems: River systems and deltas remained the major depositional areas. These were areas of clastic sediment transport and deposition, with widespread sandstone-siltstone-claystones. Floodplains with fine-grained sediments also characterized many fluvial and deltaic environments as well.

5. Climatic influence: The climate during the Cenomanian age was relatively warm, with high sea levels that caused extensive transgressions. An array of marine life flourished in these tropical waters, and fertile land provided wide ranging vegetation which dictated the sediments that were laid down.

6. Organic-Rich deposits: In some regions, the Cenomanian age was associated with deposition of black shales (organic-rich sediments). The conditions for the preservation of organic matter were created by anoxic or low-oxygen environments in restricted basins where these deposits accumulated. Together with the black shales, they also form promising source rocks for hydrocarbons.

7. Tectonic Activity: The continued tectonism related to the breakup of Gondwana, and northward drift of Indian Plate also influenced sedimentation patterns. Tectonic activity created new basins and reconfigured existing depositional environments.

The middle Cenomanian stage was characterized by a shallow marine to carbonate platform sedimentation with important influxes of fluvial and deltaic systems, influencing the Indian plate margin. These environments and the sedimentary record are equally shaped by warm climate, high sea levels of this thinner crust period in combination with ongoing tectonic activity (Dietz & Holden, 1976).
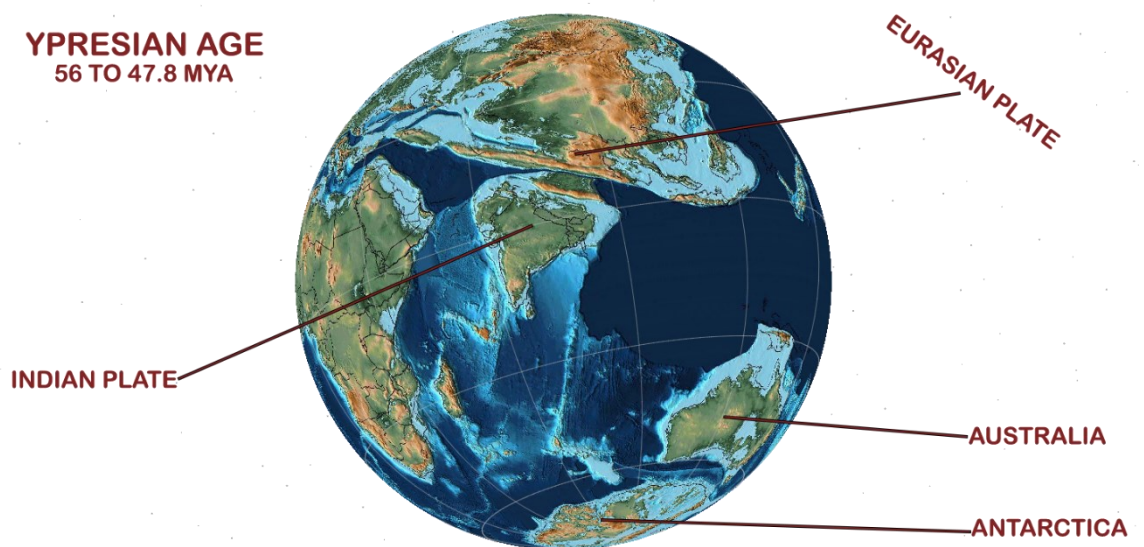

Figure 2.5. Position of the Indian plate in the Ypresian Age ((Modified after Seton et al., 2012)

2.6.4   The Ypresian Age

The Indian plate was continuing its northward march towards Asia and this crash continued well into the subsequent Oligocene epochs that lasted between 34-23 million years ago, eventually leading to the uplift of rocks in what is now called Western Ghats due forced thrust coming from southwards growing mantle forming a bulge somewhere around vicinity of Chanda Mountain region. This tectonic activity, along with climatic and sea level changes affected the depositional environments on the Indian Plate during this stadial Epoch (Ypresian age). Some key things to know about the environment during this period of deposition:

1. Marine Environment: extensive shallow-marine platform deposits are known on Precambrian strata especially in North plate while evidence for carbonates and evaporites indicate formation of restricted basins. These regions laid in the greater Tethys Ocean which was a marine sedimentary environment. These environments were sites for depositional formation of limestone, marl and shales with coral reefs usually found in the equatorial sea belt together limestones rich in fauna e.g., numerous species marine fossils including ostrocods, nummulites etc.

2. Carbonate Platforms: Substantial ditches progressing in creation are shown as carbon stages. These platforms were centers of intense carbonate sedimentation, including reef-building and the deposition of biogenic carbonates. These settings also held abundant nummulitic limestones, defined by the presence of large foraminifera.

3. Coastal and Shelf Environments: The coastal and continental shelf environments were common along the margins of Indian Plate. This caused these regions to have a combination of marine and land deposition with sandstone, siltstone or mudstones forming the deposits. These were often dominated by coastal plains, tidal flats and estuaries.

4. The river systems and deltas: Fluvial and Deltaic Systems played a major role in sedimentation especially in the southern, central part of Indian Plate The sediments transported and deposited in these environments were clastic (i.e. they consist of sandstones, siltstones and claystones). While rivers deposit their sediments from the interior regions into coastal lands, vast floodplains and deltaic deposits built up.

5. Terrestrial Environments: Indian Plate terrestrial deposition is varied and includes fluvial, lacustrine, paludal settings. This region was marked by an accumulation of fluvial and lacustrine sediments such as conglomerates, sandstones and shales. It is likely that these coal aggregates were deposited in swamplands where dense vegetation existed.

6. **Climate Influence:** The warm, humid climate of the Ypresian age with its high precipitation rates. This climate allowed for a mix of plant life, including tropical forests that helped make the different types of sediments found in lake and river deposits. The warm conditions also allowed the deposition of huge marine carbonate platforms.

7. Tectonic Activity: The continued northward motion of the Indian Plate that was to collide with Eurasian plate in future resulted for depositional environment tectonic activity. Foreland basins formed by tectonic activity and controlled the location of depositional environments. This tectonic event uplifted also the Himalayas, changing local drainage patterns and supply sediment.

The different sedimentary systems observed in the Indian Plate during the Ypresian age as fluvial, deltaic and terrestrial environments related to a coastline that extended along what is now northern Pakistan, where salt pans were developed later. These climate conditions combined with active tectonic processes would have strongly influenced the nature of environments in which these sediments were deposited and hence what is preserved within sedimentary record (Dietz & Holden, 1976).

CHAPTER 3
FORMATION EVALUATION

3.1   Introduction

The primary objective of any formation evaluation effort is to assess, measure and characterize the spatial arrangement of petrophysical parameters including shale volume, porosity, permeability and saturations in order to define flow units within it. For effective development, management and prediction of future performance of gas-field, precise understanding of these factors is needed. Analysis of wireline logs allows for the determination of petrophysical parameters (Aadil et al., 2011).

The process for achieving a reservoir description through open-hole logs requires:

i.   Data quality control via environmental corrections for logs.

ii.   Estimation of petrophysical properties via logs data.

iii. Calculation of net pay of studied reservoir.

For the purpose of this study, open-hole wireline data acquired within the Cretaceous Lower Goru Formation was used from the following wells:

1. Miano-02

2. Miano-09

3. Miano-10

3.2 Log QC and Conditioning

Acquisition of data, as we all know, has its own limitations as a result of various pitfalls in the acquisition methods which can reduce overall accuracy and precision, and therefore can result in reduced confidence & robustness. Also, the fact that datasets are often incomplete is one of the main reasons for most operators to put effort in maximization and full integrating the available information (Shekaili et al., 2012).

In order to do this, all geoscience workflows should start with rigorous QC and data conditioning. Performing QC and data conditioning may seem like a thankless task and is often given to junior geoscientists. However, it is a very important step, laying the foundations for the subsequent workflows to be performed with as much precision and accuracy as possible. Data that hasn't undergone QC & rigorous conditioning can lead to large errors to be carried forwards and results in expensive mistakes, and misinterpretations later on. Issues such as rough borehole conditions and gas effects are among the most common effects that should be repaired; however, there are other effects that may also cause errors. There are common practices that may be applied for each type of log, and often logs are checked against each other for errors (Shekaili et al., 2012).

3.3 Logplot Display

After stringent QC, the logs from the wells are displayed below. VGS, a proprietary software from Vizdom Solutions Oil and Gas Services is utilized for formation evaluation in this study.
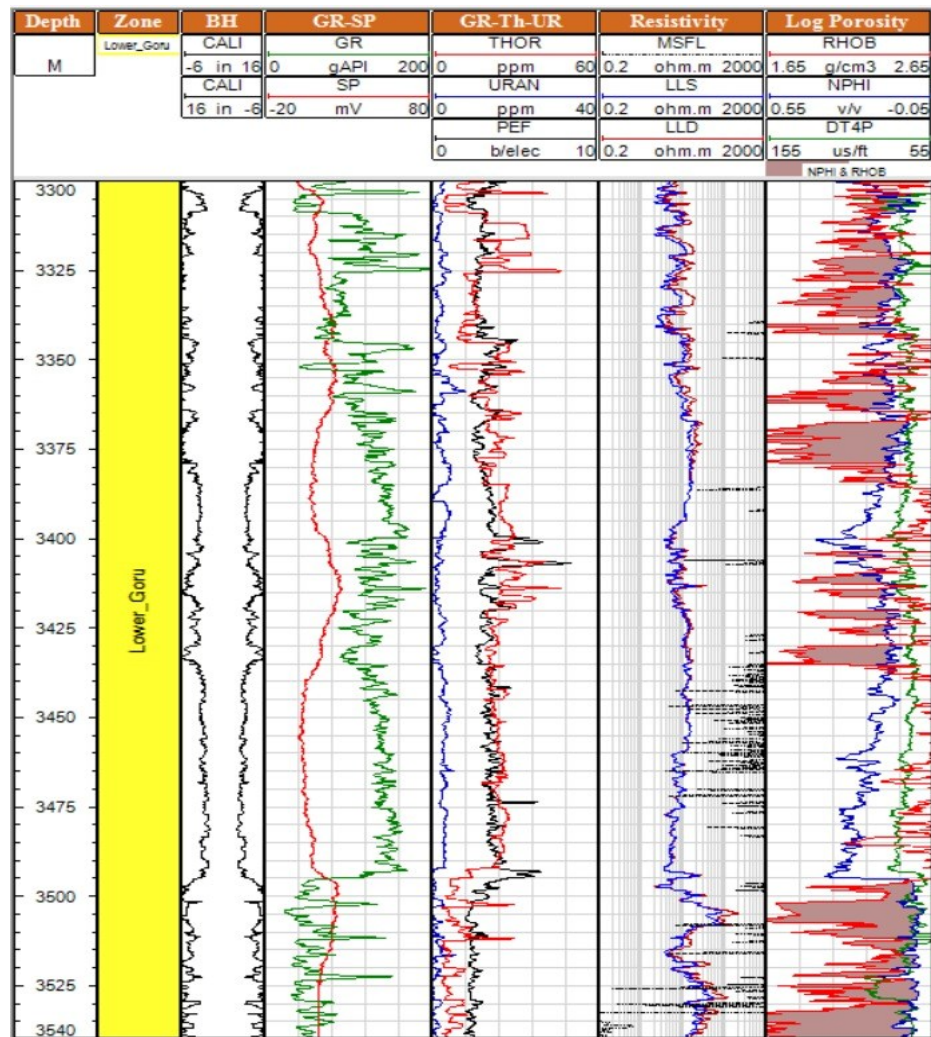
Figure 3.1. Logplot of Miano-02 with caliper, GR, SP, spectral GR, resistivity, porosity and acoustic log suites.

Notice that in the above fig 3.1 the density log is not reflecting the Compton scattering as it should within the formation due to stick and pull of the tool in bad-hole conditions. This means that density will give an under-compensated porosity, therefore cannot be used for porosity estimations. Sonic and neutron are used instead.
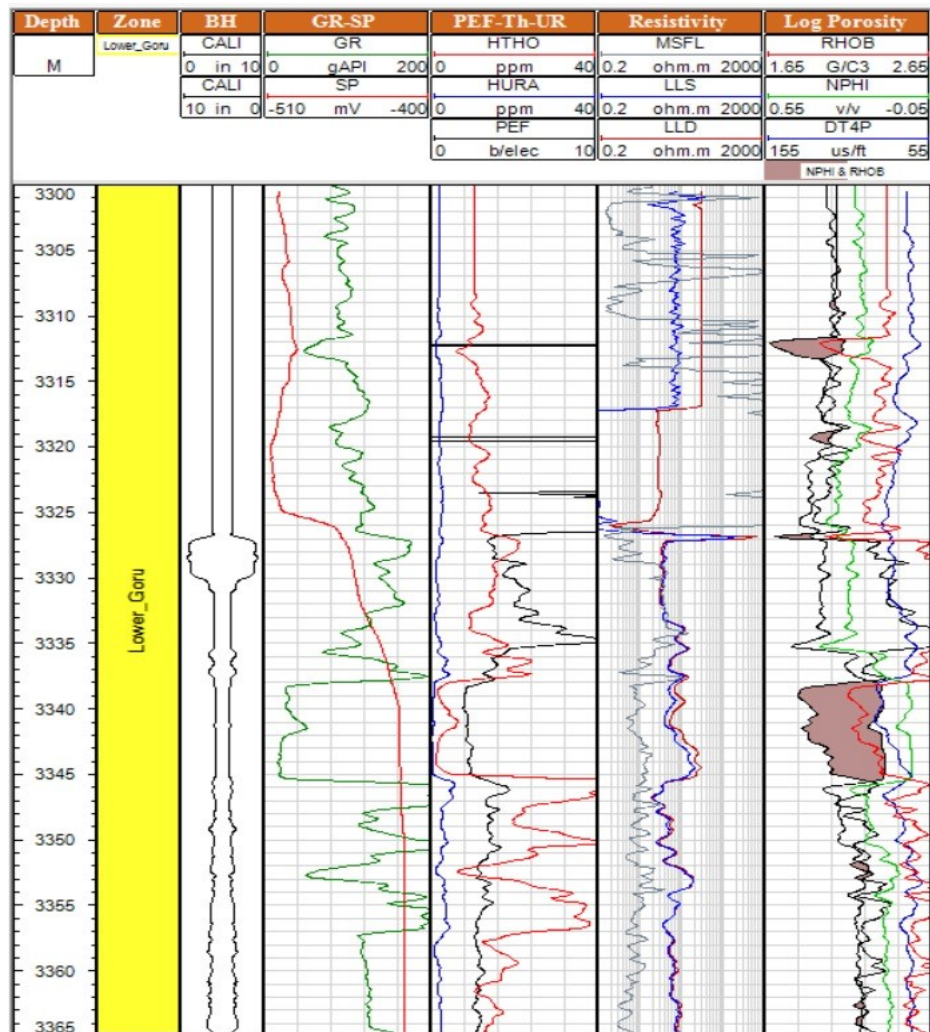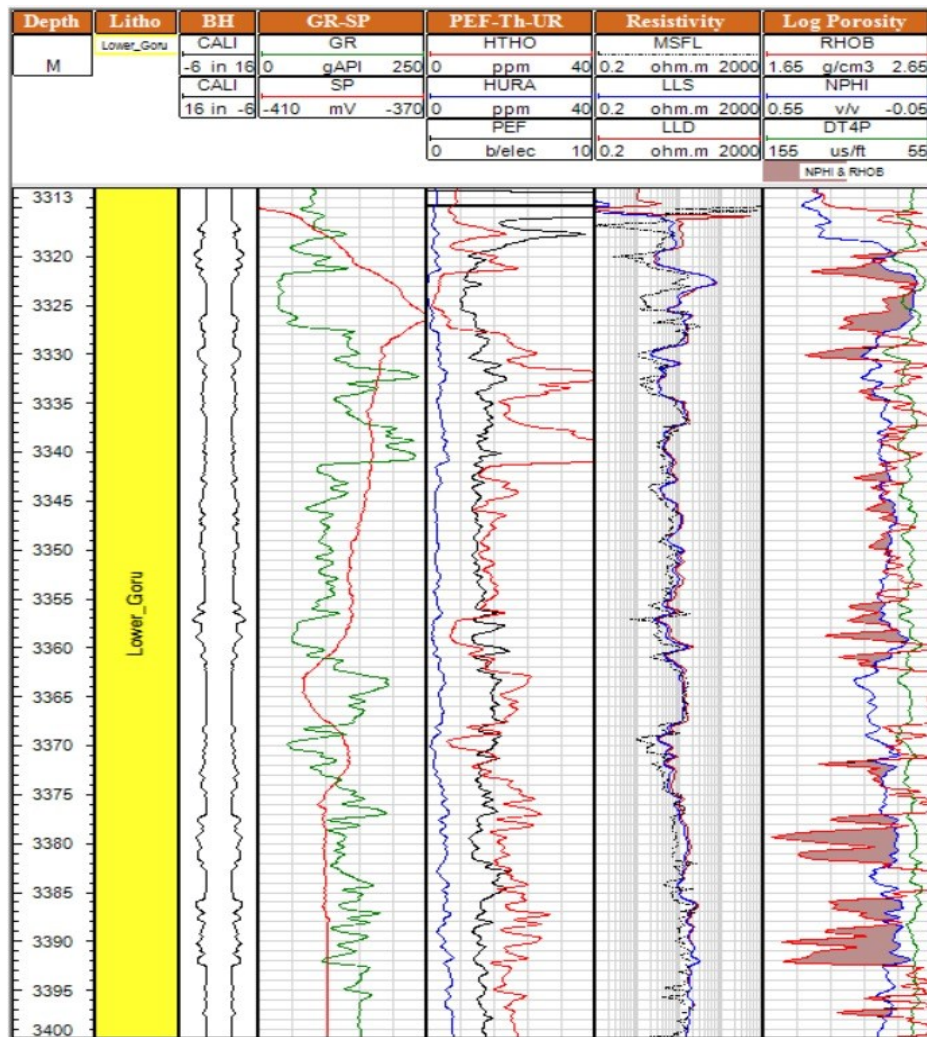
Figure 3.2. Logplot of Miano-09 with caliper, GR, SP, spectral GR, resistivity, porosity and acoustic log suites.

In case of Miano-09, bad-hole condition from 3325 to 3332 m have caused error in measurements in density and shallow-focused resistivity tool did not work in the upper section, evident by discrete spikes in intervals. In the lower section as well, data quality is not optimal. GR values are overcompensated in general and density log is not reliable. In such a scenario, it is advisable to take parameters from reliable logs i.e. accoustic, neutron and deep resistivity.

Figure 3.3. Logplot of Miano-10 with caliper, GR, SP, spectral GR, resistivity, porosity and acoustic log suites.

Logs acquired in Miano-10 are relatively poor quality in all of Lower Goru Interval. In this case, it is not a good idea to use over compensated or under compensated measurements which were recoreded due to poor borehole conditions; i.e. higher shaliness which causes swell / breakouts within the borehole. The tool gets stuck in this situation and the measurements are detrimentally affected. Therefore, density log cannot be used for porosity estimation, rather acoustic and neutron is utilized in this scenario.

3.4 Correlation and Interpretation
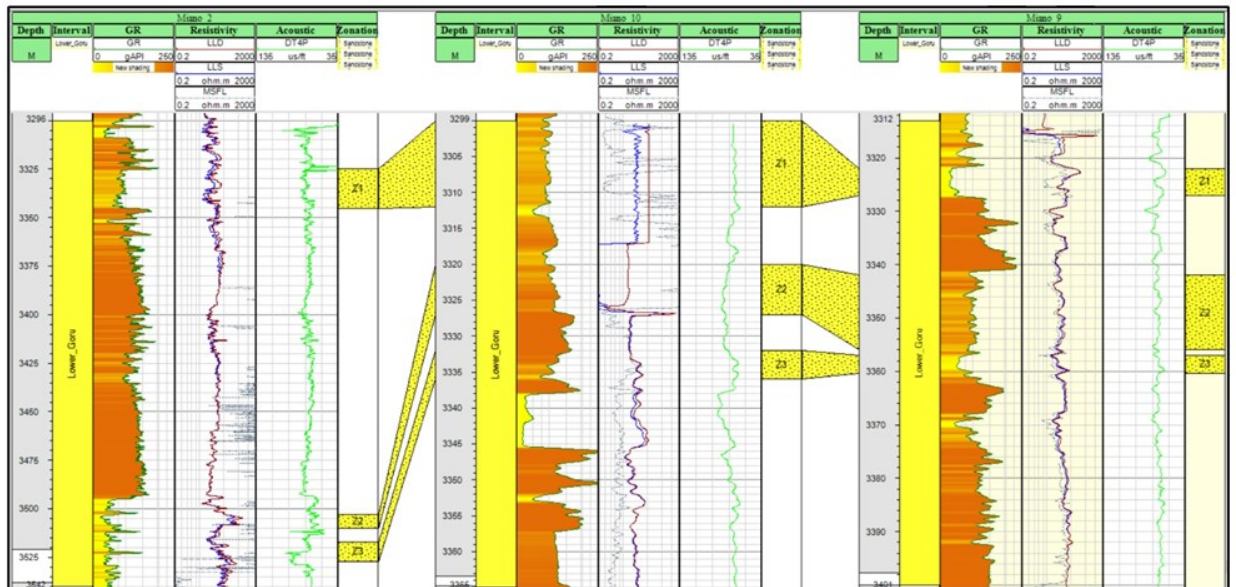
Figure 3.4. Correlation of sand units within the Lower Goru Interval of Miano-02, Miano-09 and Miano-10 wells.
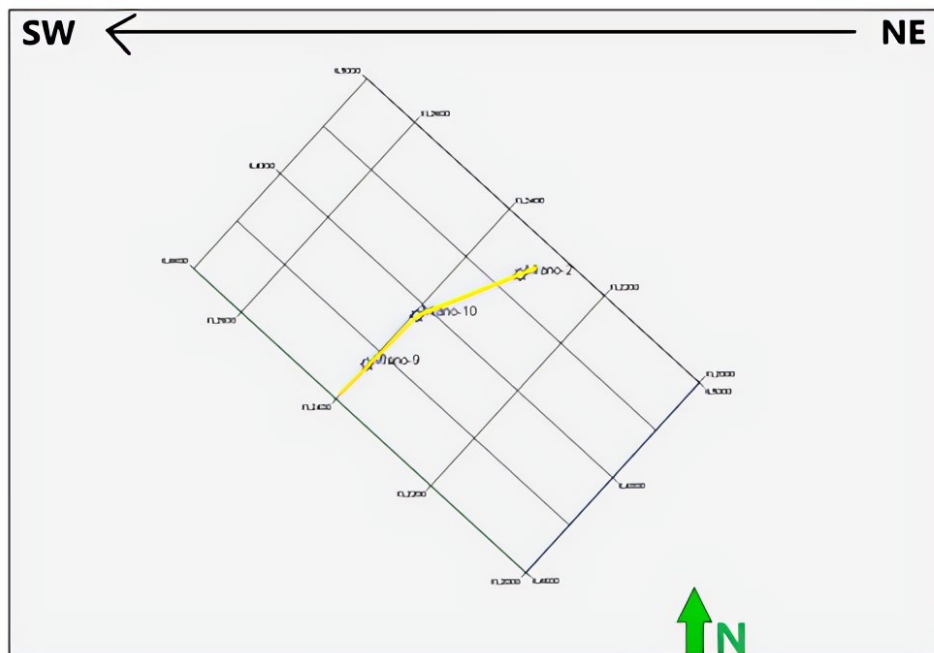
Figure 3.4.1. Index map showing trend of wells.

Sand units Z1, Z2 and Z3 are conformbale in all three wells and can act as potential reservoirs. The depositional facies of the reservoir horizons is related to shoreline and estuarine sedimentation. A wave dominated prograding barrier bar system, frequently overwashed by storm waves, describes the observed features best. Reservoir quality sands are developed in the high energy shoreface to

foreshore facies of the prograding shoreline. In order to define the stratigraphic boundaries based on log responses, we first take the wells that are closer to each other in an southwest-northeast i.e. Miano-09 and Miano-10. Based on the above correlation. The log trends indicate higher shaliness as we move from southwest to northeast reflecting a basinwards change of facies.

When dealing with stratigraphic prospects, the most difficult challenge is accurate prediction of medium to coarse grained sand body. Its reservoir quality and the extent of its lateral and updip shale-out. The eastward tilt of the strata or a valid structure closure is the other pre-requise for such prospect.

When it comes to the Lower Goru stratigraphic possibilities, predicting with precision whether a medium- to coarse-grained sand body will exist, the quality of the reservoir, and the degree of lateral and updip shale-out are the biggest challenges. The other requirement for such prospects is an overall tilt of the strata towards the east or a good structural closure.

3.5   Sequence Boundary indentification
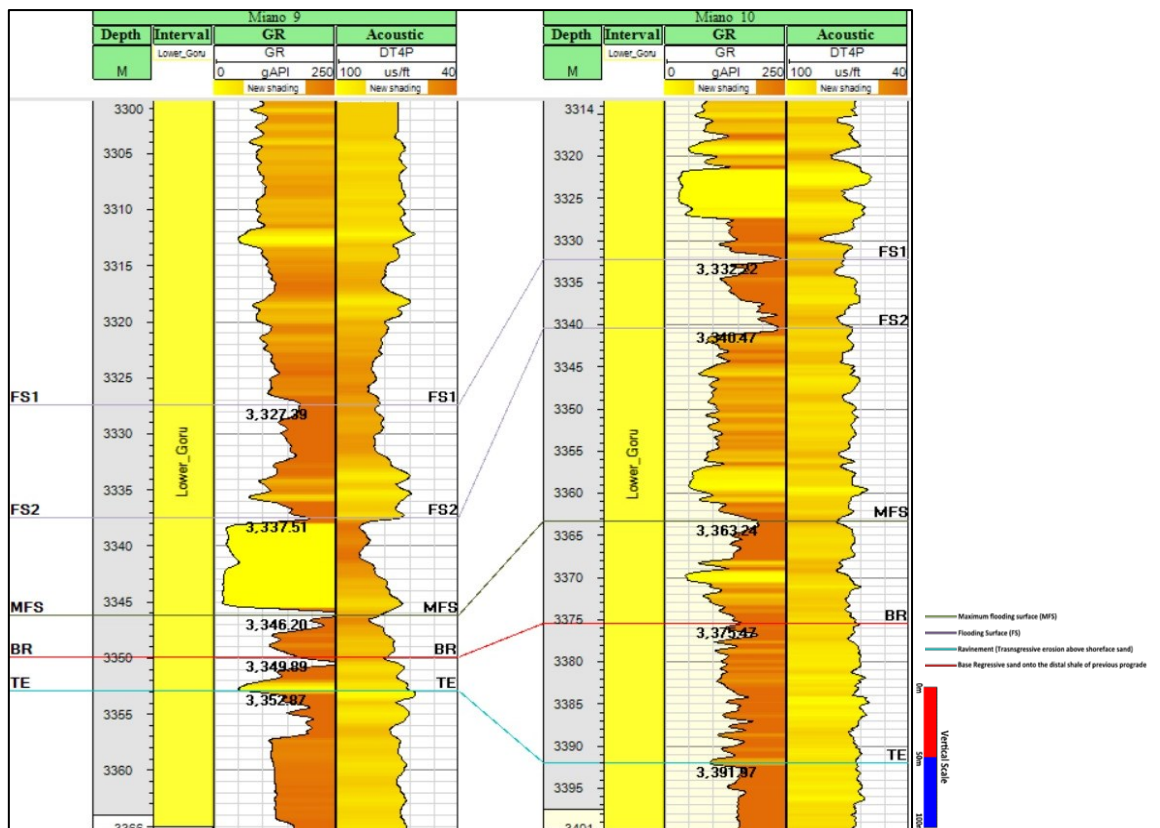
Figure 3.5. Stratigraphic boundaries marked based on log motifs (GR and DT) using data from Miano-09 and Miano-10 wells.

In the context of high-resolution seismic reflections of sand progrades, the GR log motif elucidates sequence stratigraphic surfaces identification on well logs and the interpretation of detached shoreface wedges. Transgressive shales, as defined in the preceding section, are observed as regionally widespread stratigraphic markers of high GR character and comparatively reduced acoustic impedance (slow DT) on the GR logs (including spectral GR logs K, Th and U) from wells that are widely separated. Shales are located above a reworked lithoclasts-bearing chamositic mudstone lag layer with high GR and high acoustic impedance (fast DT). A low-grade coarsening-upward, blocky or fining-upward sand-prone interval is located below, which represents the sands classified as Facies type 1 and 2. Seismic analysis identifies these transgressive events as sequence flooding surfaces that occur above the sequence boundaries.

Therefore, the high GR shales (high Th) define the basin-wide genetic stratigraphic packages within the LG mega-sequence. The transgressive shale seismic event (mfs) overlies a positive or negative reflectivity event (peak or trough on zero phase seismic data) that on the proximal areas towards the east marks the sequence boundary in each case depending on cemented or porous nature of the upper-most last regressive sand within each of the sequence. In the distally steepened ramp setting, the sequence boundary is located on the bottom of the forced regressive sand which exhibits a sharp-based fining upward log motif.

The high-GR shales also occur at other stratigraphic levels within the "Z1", "Z2" and "Z3" sequences and overlie fining-up, coarsening-up or blocky GR log motifs. These transgressive shales bound genetic stratigraphic packages comprised of further smaller scale, multiple coarsening and / or fining-upward trends representing the multiple regressive sand wedges. Each smaller scale sequence is comprised of the coarsening-upward or blocky sand capped by the ravinement erosion surface in the form of thinner high gamma counts, followed by the high gamma counts transgressive event and shaly bottom sets of the following prograding paralics.

The parasequences and PS sets are represented by these small sequences and sequence sets. High resolution correlations and regional seismic stratigraphic interpretations show that a marine incursion happened above the Sembar and that

a lowstand wedge was followed by a regression within the Z1 sand. A sediment supply and relative sea level rise equilibrium resulted in an aggradational stack of coastal plain and shallow marine deposits within the Z1 sand.
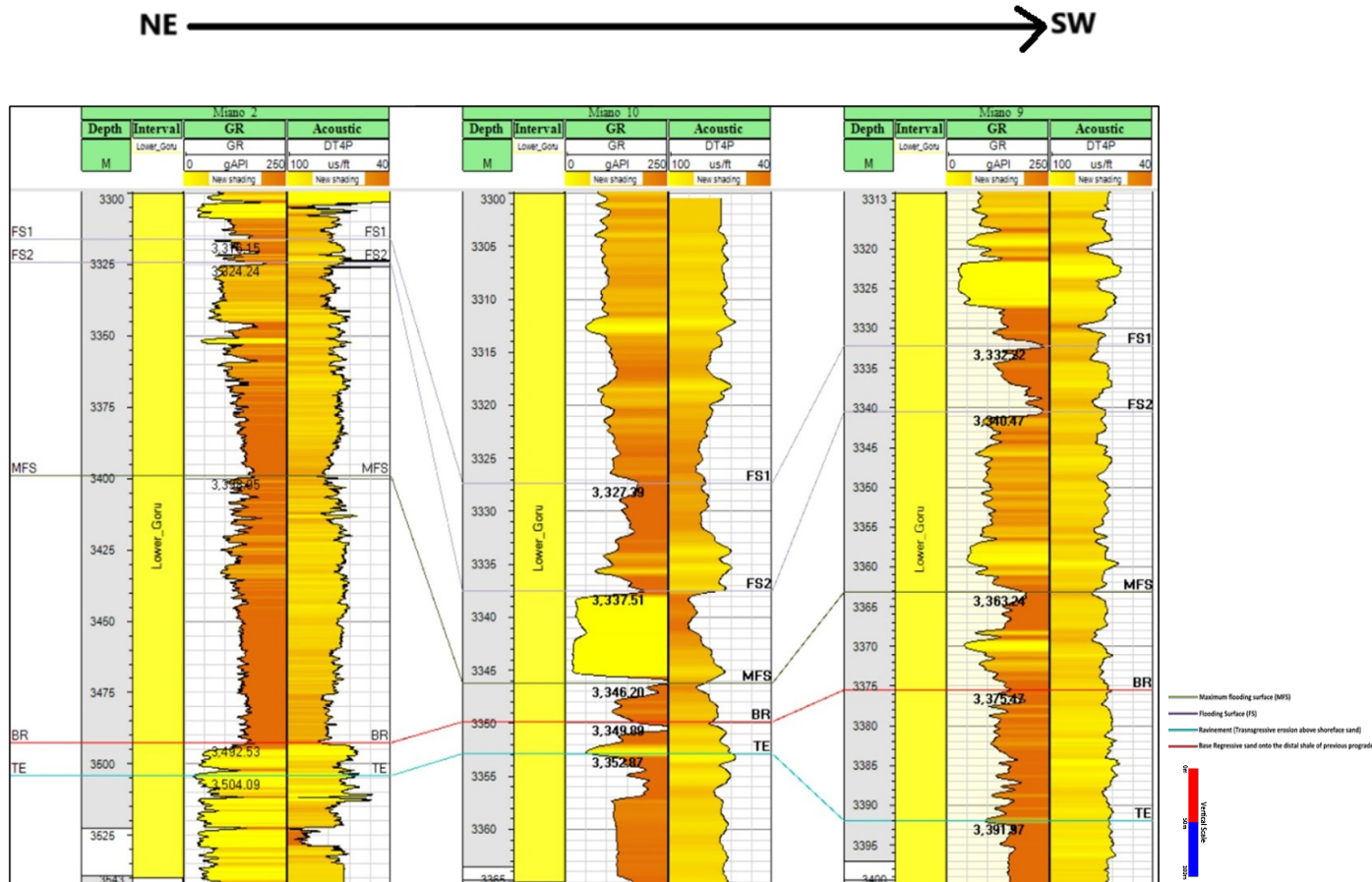

Figure 3.6. Stratigraphic boundaries marked based on log motifs (GR and DT) using data from Miano-09 and Miano-10 wells and translated to Miano-02.

Facies vary in Miano-09 and Miano-10 wells in a southeast-northwest orientation, whereas, in Miano-02, the correlation is not quite evident since it is north-east of Miano-09 and Miano-10 respectively. However, similar stratigraphic events are picked on log responses and correlated with the other wells.

3.6   Cross Plots

Cross plots of log data are an indispensable tool for the well log analyst for interpreting both logging while drilling (LWD) and wireline well log data. The basic idea behind a cross plot is a 2D representation of the variation of log data points with respect to two or more properties.

Cross plots of Sonic versus Density logs are preferred for shaly sands. For carbonates formations, Density versus Neutron cross-plots are commonly utilized.

The Neutron - Sonic cross-plot shows neutron values on x-axis which increases from left to right and the sonic transit time on the y-axis which decreases from top to bottom. Lithology lines which are present on the plot shows the increasing neutron porosity with increasing transit time and the large separations between lithology lines on the plot indicate good resolution of the main lithologies using this cross-plot, and it also indicates that the porosity is very much independent of lithology.

3.6.1 Neutron Sonic Cross-plots

NS cross plots for the Lower Goru interval are generated using overlay lines from SLB considering $1g/cm^3$ density of water filled porosity. The cross-plot values are constrained by gamma counts for understanding lithology variation.
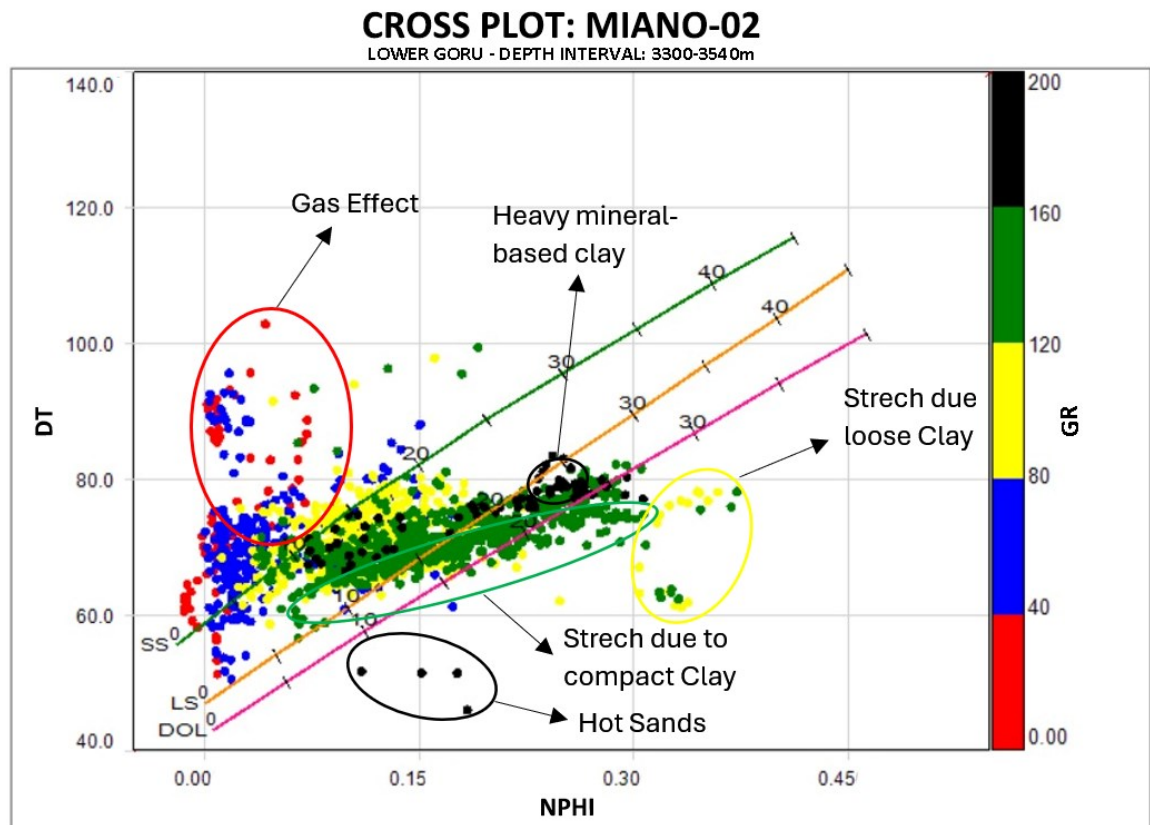
Figure 3.7. Neutron Sonic Xplot of Miano-02.
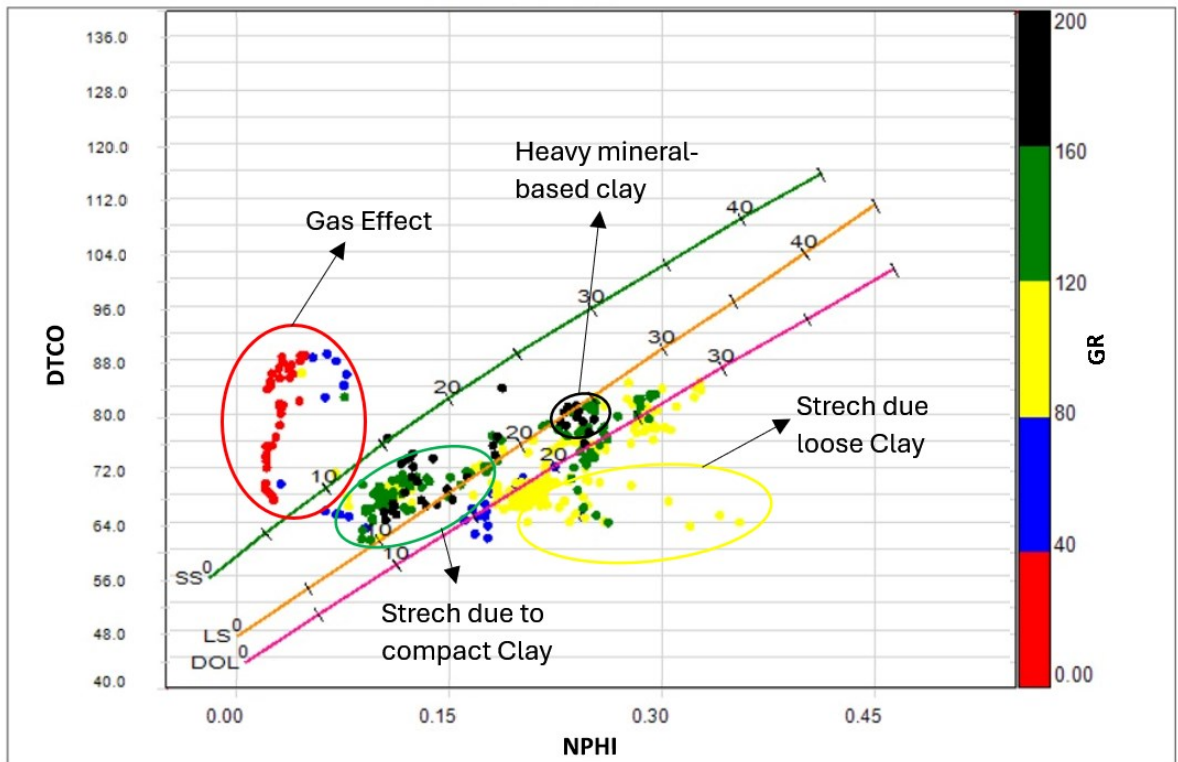
Figure 3.8. Neutron Sonic Xplot of Miano-09.
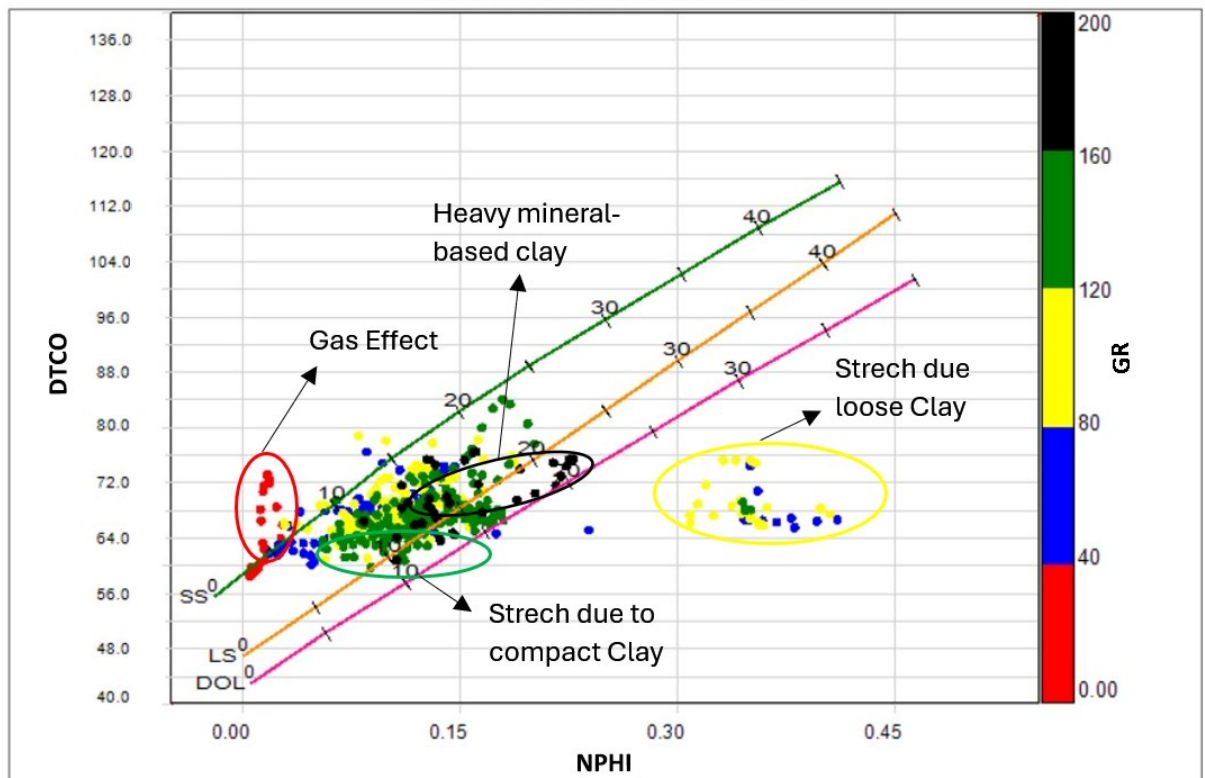
Figure 3.9. Neutron Sonic Xplot of Miano-10.

3.7   Workflow, Parameters and Interpretation

Workflow, parameters and interpretation is discussed as below.

3.7.1   Workflow

The formation evaluation workflow is based on identifying minerals, building lithology, estimating and separating clay volume from sands, estimating clean lithology porosities and finally estimating the saturation of water for the subsequent NTG & pay. In this analysis, we have used the deterministic clastic model in the software which has the lab calibrated end points for Quartz.

The petrophysical parameters and model selection varies and depends on whether the values of shale and knowledge of matrix is desired. The values of fluid for different interpretation methods are generally acquired in a laboratory environment and are calibrated for temperature, pressure and salinity needed.

The values of rock matrix are generally available from interpretation charts, book or data tables. The values of 'end point' usually shows readings of log for pure 100% minerals, which are rare in real environments. These values may also be found on inspecting logs if they are relatively pure, zero- porosity zones are also found.

3.7.2   Parameters

3.7.2.1 Clay Volume

Clay volume is calculated by GR and Neutron log overlay method. The best match has been finalized for porosity estimations.

Statistics setting:
Curve: VCL_MIN ☑ MinValue ☑ MaxValue ☑ Average ☑ Median ☐ P10 ☐ P50 ☐ P90

Final:

Zone				Final			
Name	Top	Bottom	Average Method	Min	Max	Average	Median

	Use	Method	Curve	Min	Max	Average	Median	P10	P50	P90
⊟ 1		3313	3321.583 Mean							
▸	☑	Gamma	VCL_GR	0	0.325	0.1069	0.0887	0	0.0887	0.256
	☐	Neutron	VCL_NEU	0	1	0.5559	0.7804	0.0521	0.7804	0.9101
⊟ 3322		3321.583	3327.3049 Mean							
▸	☑	Gamma	VCL_GR	0	0.1467	0.0502	0.0343	0.0153	0.0343	0.1174
	☑	Neutron	VCL_NEU	0	0.189	0.0738	0.0661	0.0402	0.0661	0.1136
⊟ 3327		3327.3049	3337.0583 Mean							
▸	☑	Gamma	VCL_GR	0	0.7496	0.1599	0.0868	0	0.0868	0.4137
	☑	Neutron	VCL_NEU	0	0.347	0.1597	0.1592	0.05	0.1592	0.2869
⊟ 3337		3337.0583	3340.9596 Mean							
▸	☑	Gamma	VCL_GR	0	0.5421	0.2782	0.2337	0.0796	0.2337	0.5207
	☑	Neutron	VCL_NEU	0.0178	0.155	0.1086	0.1231	0.0457	0.1231	0.1493
⊟ 3341		3340.9596	3361.1166 Mean							
▸	☑	Gamma	VCL_GR	0	0.5321	0.1547	0.1639	0	0.1639	0.2448
	☑	Neutron	VCL_NEU	0	0.2409	0.1313	0.1312	0.0474	0.1312	0.2134
▸ ⊟ 3361		3361.1166	3400 Mean							
▸	☑	Gamma	VCL_GR	0	0.4893	0.1447	0.1468	0	0.1468	0.2938
	☑	Neutron	VCL_NEU	0	0.4262	0.0799	0.0459	0	0.0459	0.218

Output:
Dataset [said] VCL_Minimum [VCL_MIN] VCL_Average [VCL_AVE] VCL_Final [VCL_AVE]

Show Logplot ✓ Apply ◉ Run ⊗ Close

Figure 3.10. Clay volume parameters from GR and NEU overlay.

3.7.2.2 Porosity Estimation

Porosity is estimated through density and neutron readings where the borehole data is not affected by bad borehole condition. DSI measurements are utilized in case of bad borehole conditions. A temperature log is also generated using average geothermal gradient and bottom hole temperature i.e. 0.3 / 100m and 120 degrees respectively. Total porosity and effective porosity curves are finalized as a last step.

s

Figure 3.11. Porosity estimation parameters.

Figure 3.12. Temperature log generation to estimate Rw.

3.7.2.3 Water Saturation

Using the temperature curve and a known salinity of formation water @110PPK Rw is calculated to be 0.3316 ohm-m. Clay volume, effective porosity and Rw are used with saturation exponents a=1, m=2 and n=2 in Indonesian Equation.

Figure 3.13. Water saturation estimation parameters.

3.8. Interpretation
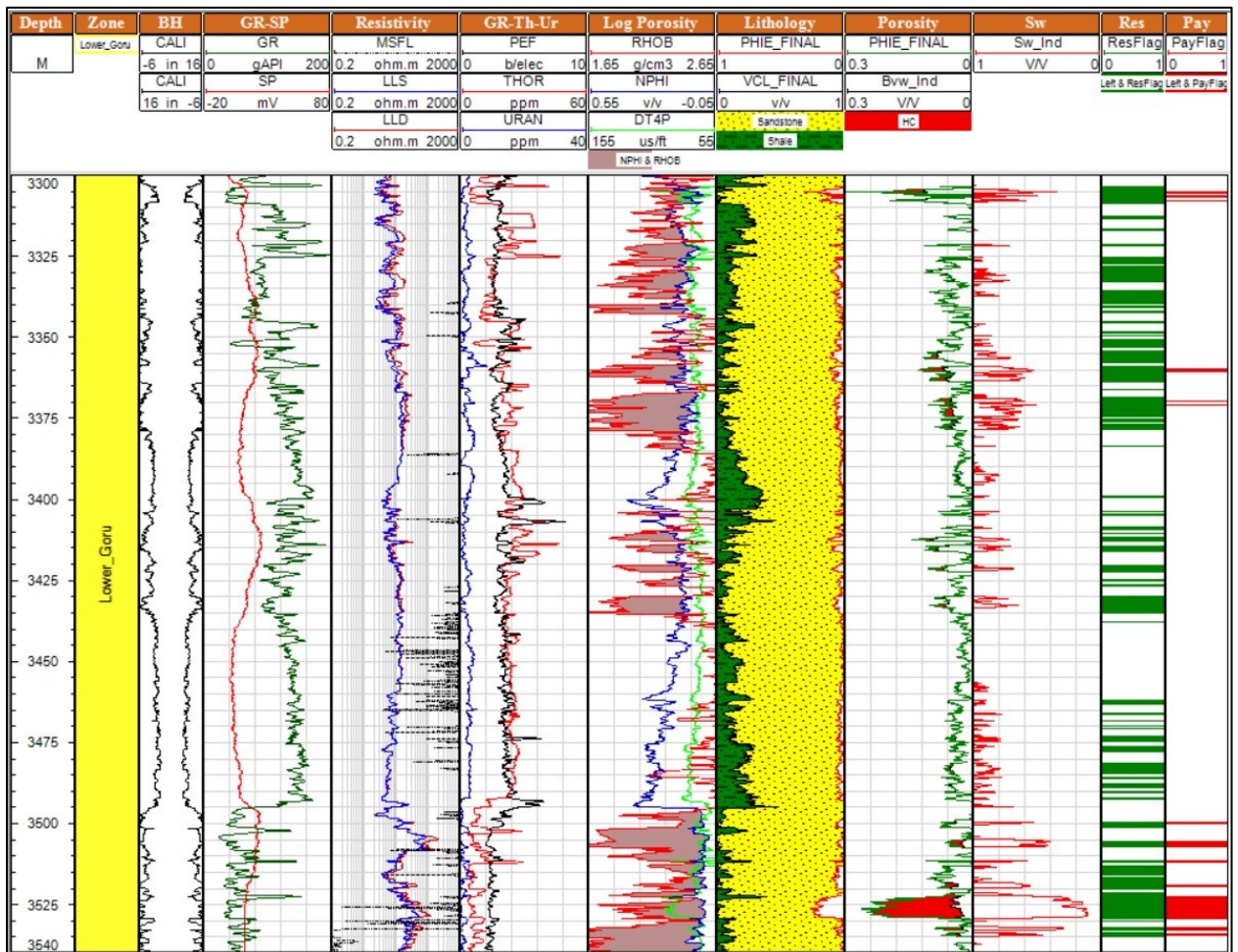
Figure 3.14. Interpretation of Miano-02, lithology; porosity, saturation and pay estimation at Lower Goru Level.

Figure 3.14 shows Interpretation of Miano-02, lithology; porosity, saturation and pay estimation at Lower Goru Level.
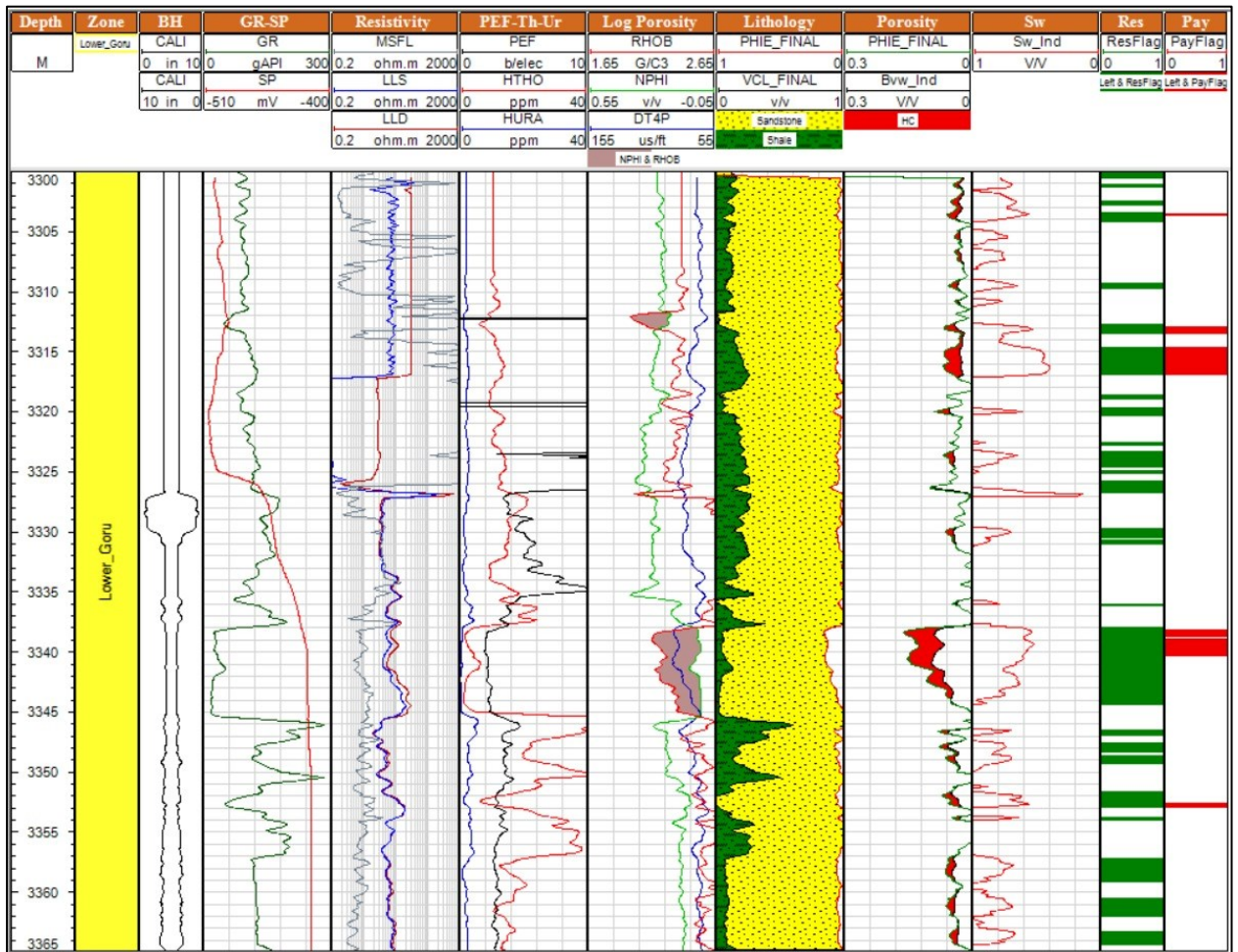
Figure 3.15. Interpretation of Miano-09, lithology; porosity, saturation and pay estimation at Lower Goru Level.

Figure 3.15 shows interpretation of Miano-09, lithology; porosity, saturation and pay estimation at Lower Goru Level.
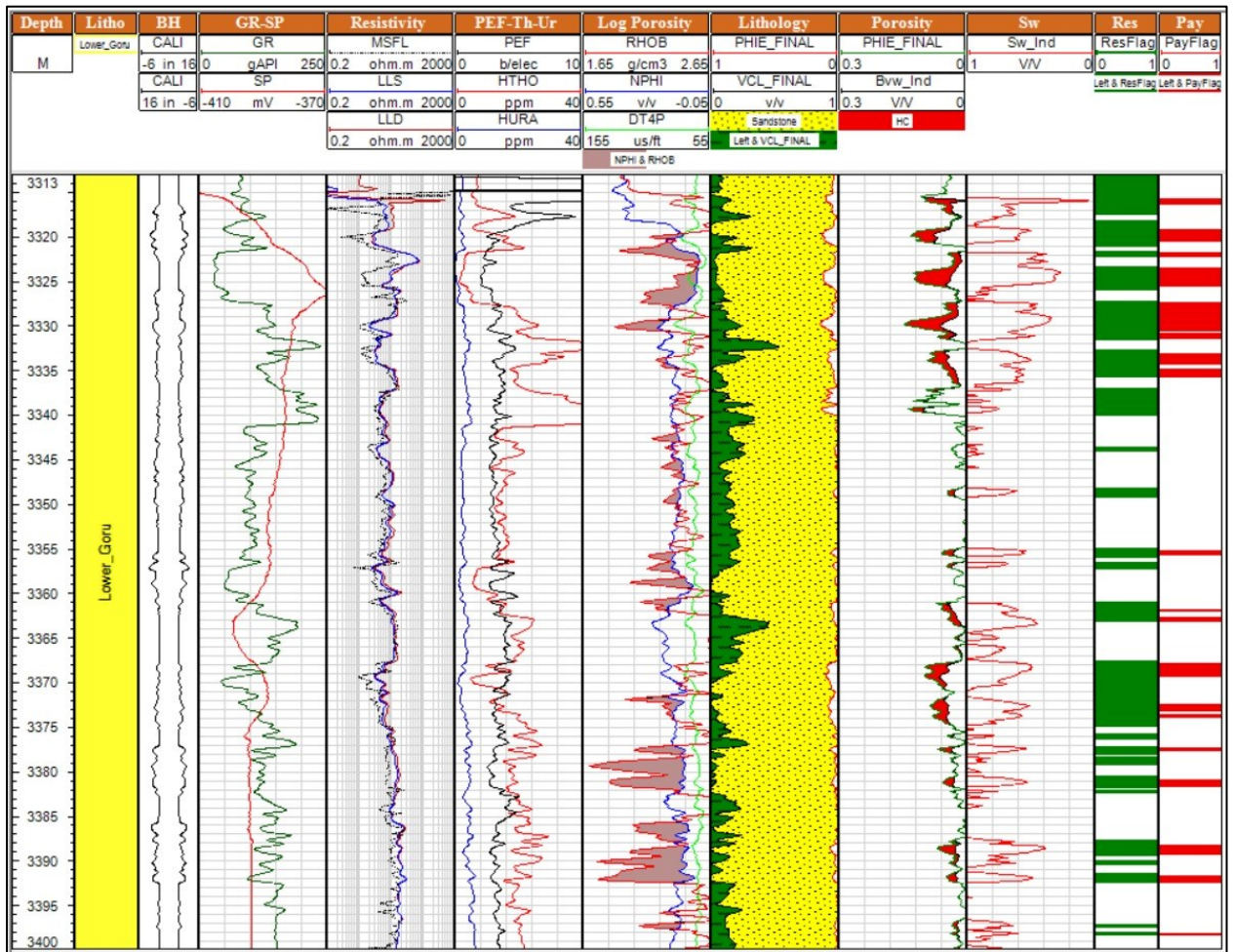
Figure 3.16. Interpretation of Miano-10, lithology; porosity, saturation and pay estimation at Lower Goru Level.

Figure 3.16 shows interpretation of Miano-10, lithology; porosity, saturation and pay estimation at Lower Goru Level.

3.9 Summary and results

Cutoff criteria based on the above analysis:

i. Clay Volume: 40%

ii. Porosity: 6%

iii. Water Saturation: 60% @ Formation Water Salinity - 110PPK.

Table 3.1 Summary and results

Interval	Well	MD		Average Value							
		Top	Bottom	Gross	Net Res.	NTG Res.	Net Pay	NTG Pay	V Clay	Phi	Sw
Lower Goru	Miano-02	3300	3540	240	185	0.7708	12.375	0.0516	0.2601	0.1488	0.2694
	Miano-09	3300	3365	65	53.9378	0.8298	5.493	0.0845	0.3323	0.0882	0.5263
	Miano-10	3313	3400	87	56.8553	0.6535	12.8211	0.1474	0.3496	0.0742	0.4905

Miano-02: Has the highest gross thickness and net reservoir thickness with relatively lower water saturation. This indicates a potentially thicker and more productive zone with good porosity and low clay content.

Miano-09: Shows a smaller gross thickness but a high net-to-gross ratio. However, its high-water saturation may indicate that hydrocarbons are less dominant in this well.

Miano-10: Demonstrates good net pay with relatively low V Clay, suggesting good quality rock, although it has slightly lower porosity compared to Miano-02.

The well interpretation reveals Miano-02 has good NTGR with low clay volume, 14% porosity and ~27% saturation. Miano-09 has the best NTGR with low clay volume and ~9% porosity but has high water saturation. Miano-10 also exhibits good gas potential owing to high NTGR, low clay volume, ~9% porosity, whereas the water saturation is on the higher side ~49%.

From the initial correlation and log motif investigation, we can clearly conclude that flooding surfaces shift marine facies landwards and reduce reservoir quality, however, sands above flooding surfaces (shoreface) have good reservoir potential owing to higher porosities. Due to fluvial ravinement, the reservoir quality is generally affected by variability in depositional architecture, thus porosities are high or chocked depending on the relief and energy of deposition. There is no particular trend for reservoir quality.

However, the base regressive sands onlapping onto the previous prograde have poor reservoir quality due to a transitioning depositional environment (from sand to shale), thus the base sequences have poor reservoir quality.

CHAPTER 4
SEISMIC INTERPRETATION

4.1   Introduction

Apart from science, seismic interpretation can also be deemed as an art, it allows geophysicists and geologists to see the subsurface geology (Badly, 1985). In seismic interpretation, interpreter has to gather information from the seismic section, and he must be familiar with setting of the basin, dominant tectonic regime, major stratigraphic components i.e. shelf breaks, reefs and other major sequence boundaries in order to follow the patterns correctly on the seismic sections and identify zones of interest (Badley, 1985). Seismic contains two different elements the interpreter to study in theory. Firstly, arrival time from a reflected or refracted geologic interface while stratigraphic thickness and velocities of the overlying layers shows the true depth of this interface. Secondly, shape of the reflection which shows strength of signal, frequency distribution and dominant frequency (Brown, 2011). Evaluation of lithology and fluid content of the reflector under observation is done through frequency spectrum. Identification of subsurface structures is dealt with through structural interpretation which fits the geology and based on the inferences drawn, time and depth maps are created. In seismic interpretation, patterns of observed reflections are related to a cyclic depositional model. In seismic sequence analysis, identification of major reflection packages is delineated by identifying surfaces of discontinuity. By interpreting systematic patterns of terminations along surfaces of discontinuity, discontinuities may be recognized (Brown et al., 2011).

A generalized flow-chart of seismic interpretation which can be employed in any exploration campaign is given in Figure 4.1.
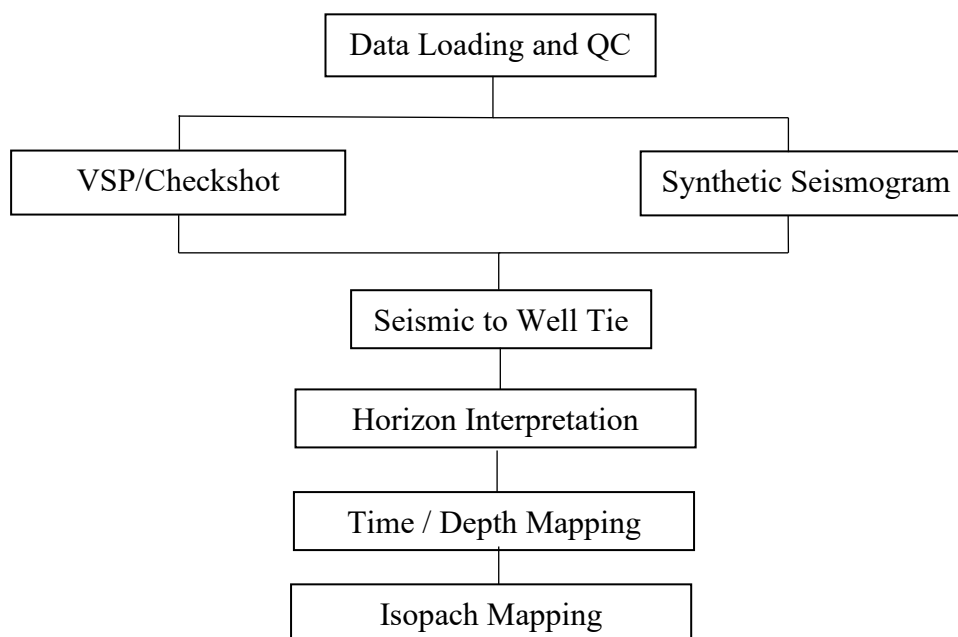

Figure 4.1. Generalized flow chart of seismic interpretation that may be employed in any well-thought exploration campaign.
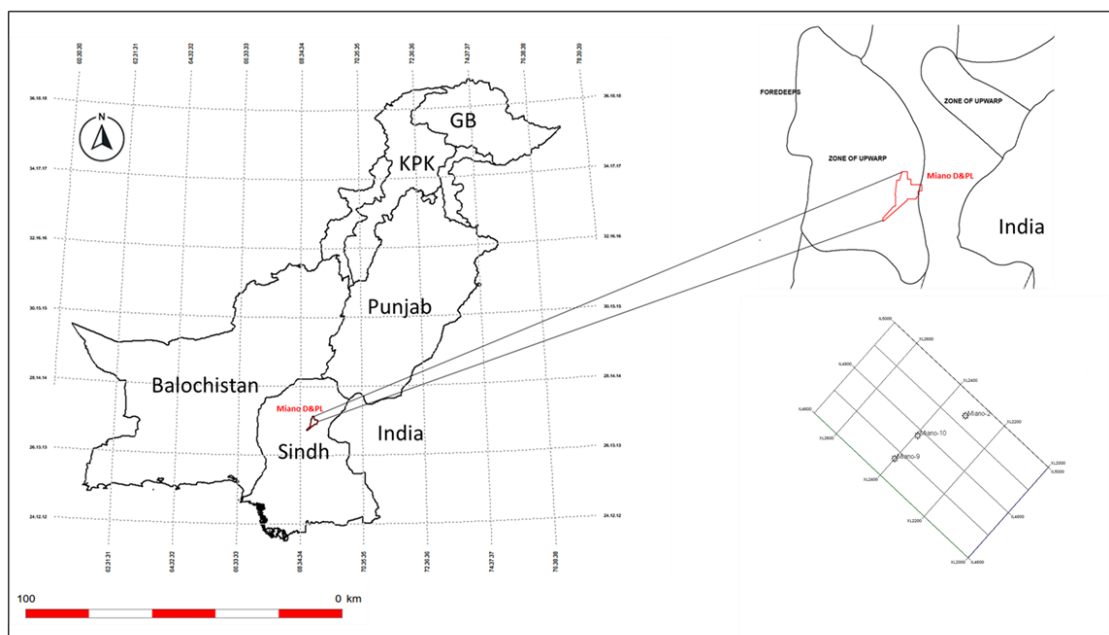

Figure 4.2. Base map of study area (Modified after Yang et al., 2023).

4.2 Data Loading and QC

After verifying header information and data consistency on Seisee, SEGY, LAS well tops and checkshot data was loaded in Petrel using the appropriate

coordinate reference system. The frequency spectrum of Lower Goru was analyzed to check whether it had enough resolution to resolve sand bodies including channels and lenses. The overall quality was good, not needing any Gain filter with an acceptable signal to noise ratio.
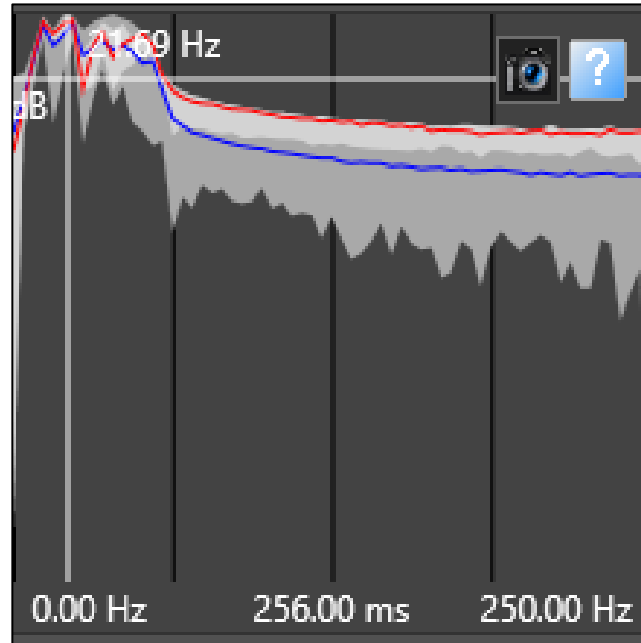
Figure 4.3. Frequency spectrum of Lower Goru Formation, showing a dominant frequency of 21.69 Hz.

4.3   Seismic to Well Tie

Time depth relation (TDR) is established through available VSP data, using OWT/TWT against depth such as a checkshot. In generation of synthetic seismogram, sonic calibration is a vital step. Primary objective of sonic calibration is to reconcile seismic (checkshot) times and integrate sonic times for any given depth in the well. Calibration of sonic log us done for correcting log velocities to time depth (Commonly checkshots), calibration of sonic is vital for obtaining accurate time/depth relationship. Arbitrary stretch to the seismogram is avoided by utilization of sonic calibration (White et al, 2003).

Seismic checkshot times are used as reference for calibration of the sonic log through a mechanism called *Drift Curve* correction (Figure 4.4). The drift can be computed at every depth level, and it is defined as:

i.   **Drift = checkshot time - integrated sonic time**

ii.   **(Tcheckshot - Tlog)**

Positive drift curve shows that the sonic log is too fast.

Negative drift curve shows that the sonic log is too slow.
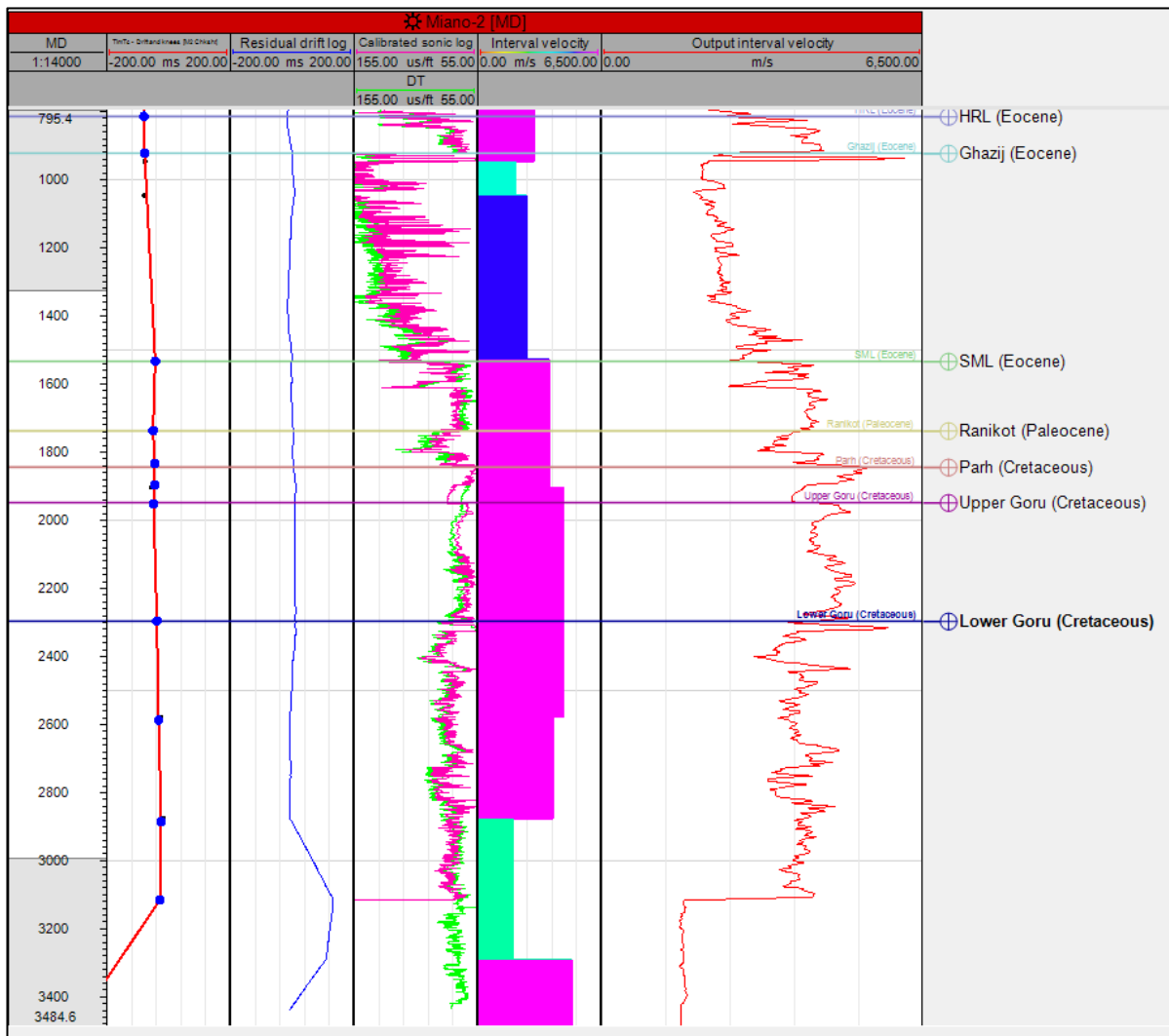
Figure 4.4. Drift curve vs sonic log correction.

Synthetic seismogram is the bridge between geological information (well data in depth) and geophysical information (seismic in time). It allows the interpreter to:

1. Tie the geologic markers to the seismic horizons.

2. Generate accurate time and depth relationships.

3. Develop understanding of the seismic response of lithologies and fluids at well location.

4. Develop understanding of the phase characteristics of the seismic data.

4.3.1 Synthetic generation steps

1. Time converts wells with checkshot data or a sonic log to establish a time and depth relationship.
2. Calculation of acoustic impedance and reflection coefficients from different logs (Density and sonic logs are commonly used).

3. Generate or extract a wavelet.

4. Generate synthetic seismograms from density logs, sonic logs, and a seismic wavelet by calculating acoustic impedance and reflection coefficients. These calculations then are convolved using a wavelet.

The Synthetic generation workflow used in the seismic to well tie procedure featured the ability to tie a synthetic seismic trace with seismic. Gardner patching is used to finish the reflectivity series if there are gaps in the logs between runs. According to Herrera et al. (2014), the Gardner equation establishes a link between velocities and densities. The equation is valid for sedimentary rocks with densities of 2 to 2.8 g/cm3 and velocities of 1500 m/s to 6000 m/s. Gardner patching is used to finish the reflectivity series if there are gaps in the logs between runs. Densities and velocities are related by the Gardner equation (Herrera et al., 2014). For sedimentary rocks with densities of 2 to 2.8 g/cm3 and velocities of 1500 m/s to 6000 m/s, the equation often functions well. The wavelet type that is convolved with the reflectivity series needs to be chosen very carefully.

Finding the one wavelet that best fits the seismic signal requires experimenting with and testing several other wavelets.
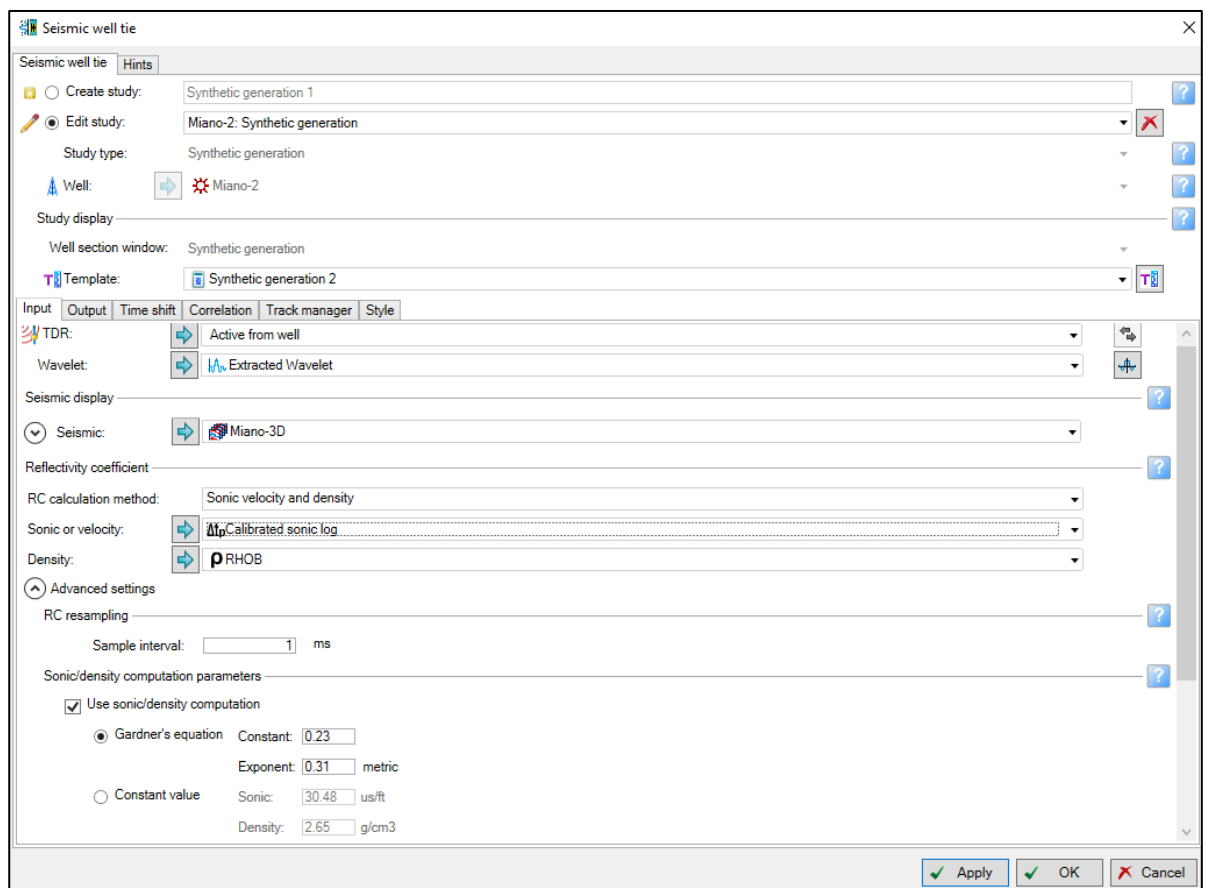
Figure 4.5. Input panel for synthetic seismogram generation.
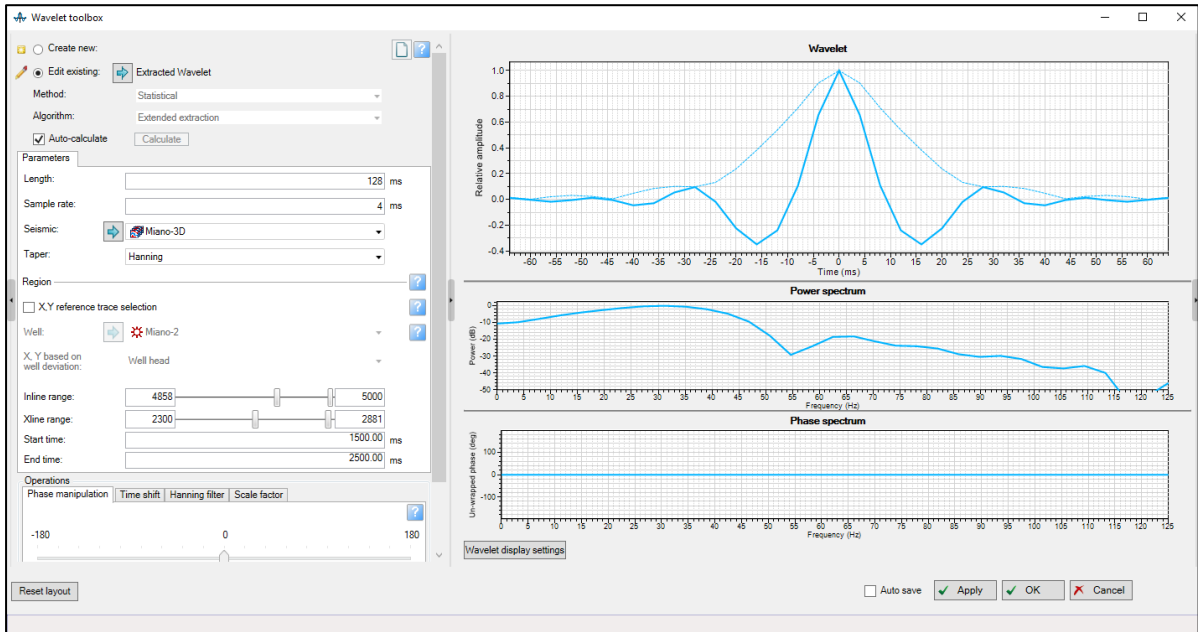
Figure 4.6. Wavelet parameters used in synthetic seismogram.
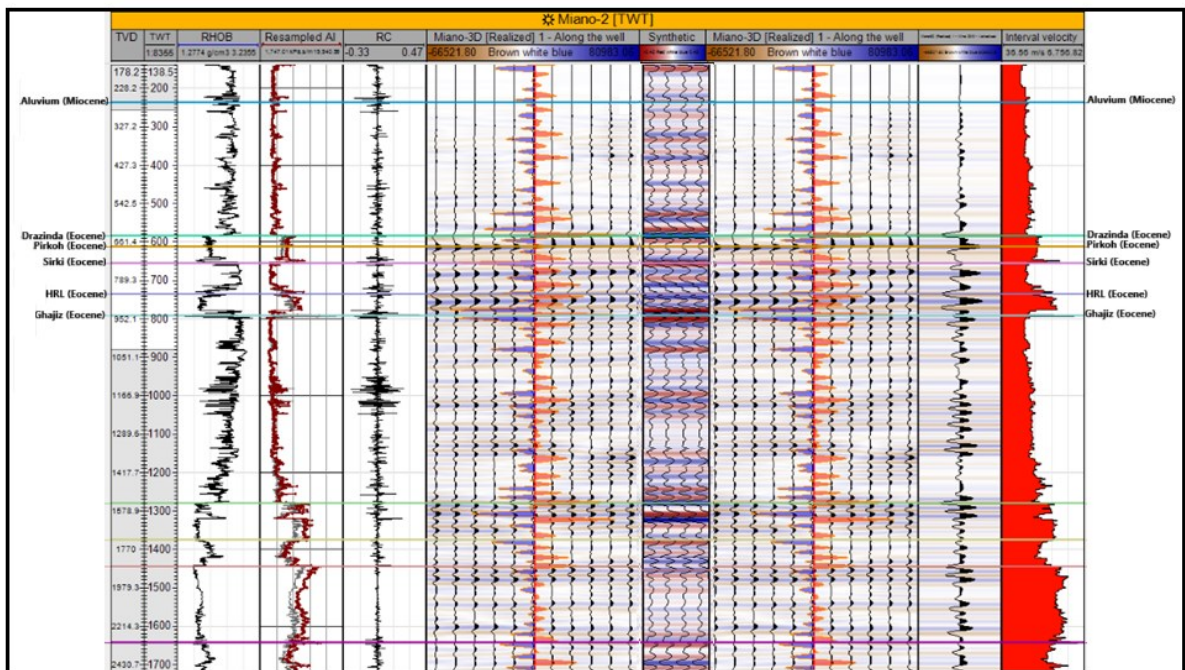
Figure 4.7. Synthetic seismogram on Inline 4396 from well Miano-02.
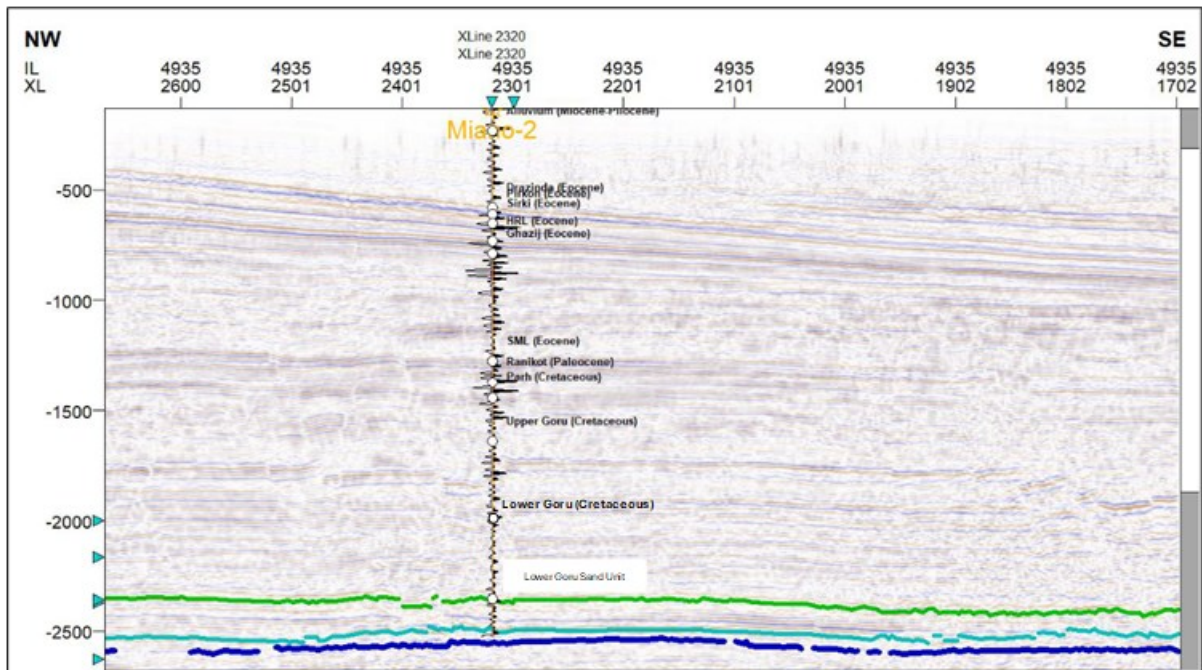
Figure 4.8. Synthetic seismogram on IL 3496 from well Miano-02.

4.4 Horizon Interpretation

Using Inline 3946 as control line, sand units were picked from the cretaceous Sembar prograde system, marking the beginning of the Lowstand System Tract (LST). Jurassic Chiltan Formation was flattened, and rest of the unconformities / discontinuities were marked identifying sand bodies as they were deposited within various depositional settings. Due to sudden fall in sea level due to tectonic highs in the vicinity, the shoreline has been extending basin-wards the deposition has been dominated by wave-tide action.

In order to verify the amplitudes with sand picks, local flatness and semblance attributes were utilized and the sand-units with positive polarity (peaks) were picked accurately.

The local flatness attribute maps the flatness of the local seismic signal in 3D. Flatness is the degree to which features on seismic are planar. It is a very good indicator for stratigraphic features, particularly subtle channel fills in a mixed deposition environment.

Semblance is the measure of later changes in the seismic response which are caused by the variation in different factors such as structure, lithology, stratigraphy, porosity as well as presence of HC. It is unlike the shaded relief maps

which allows us 3D visualization of channels and faults from horizon picks, semblance is bias-free as it operates on the seismic data itself.

Six sand units (SU-1 to SU-6) were picked within Lower Goru Formation above Sembar Fm, which serves as the base for the LST. These sand units were picked according to the amplitude, shape and character of genetically related strata with clear stacking pattern. These parasequence sets vary in terms of depositional character across the 3D volume.
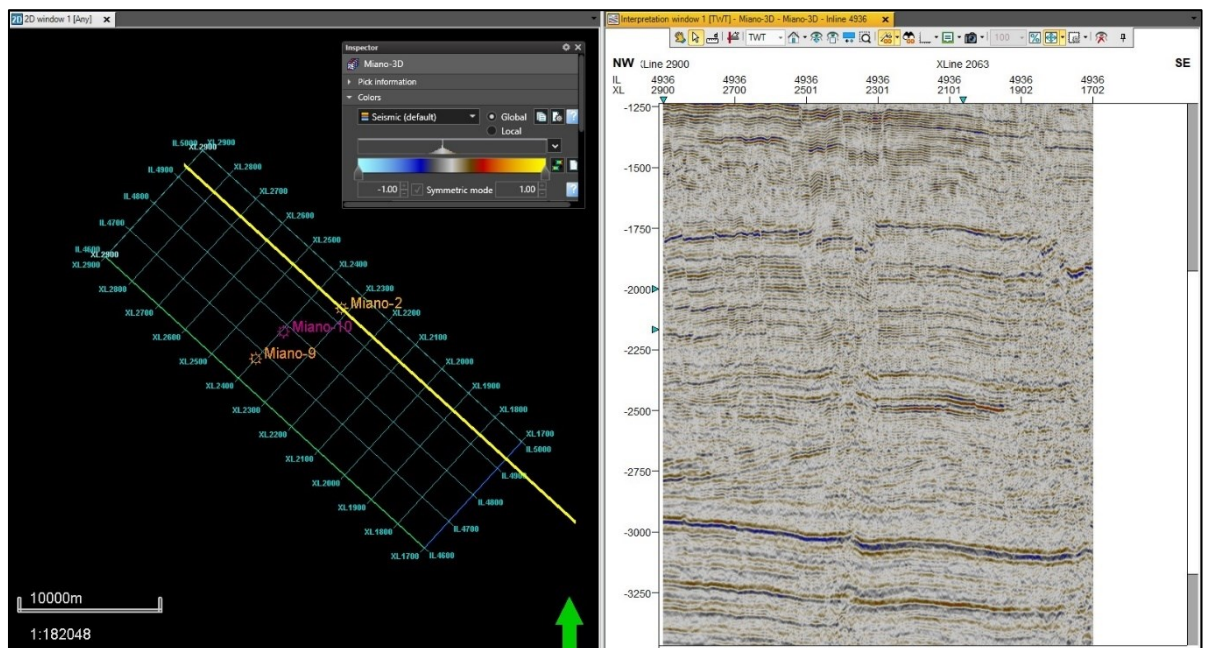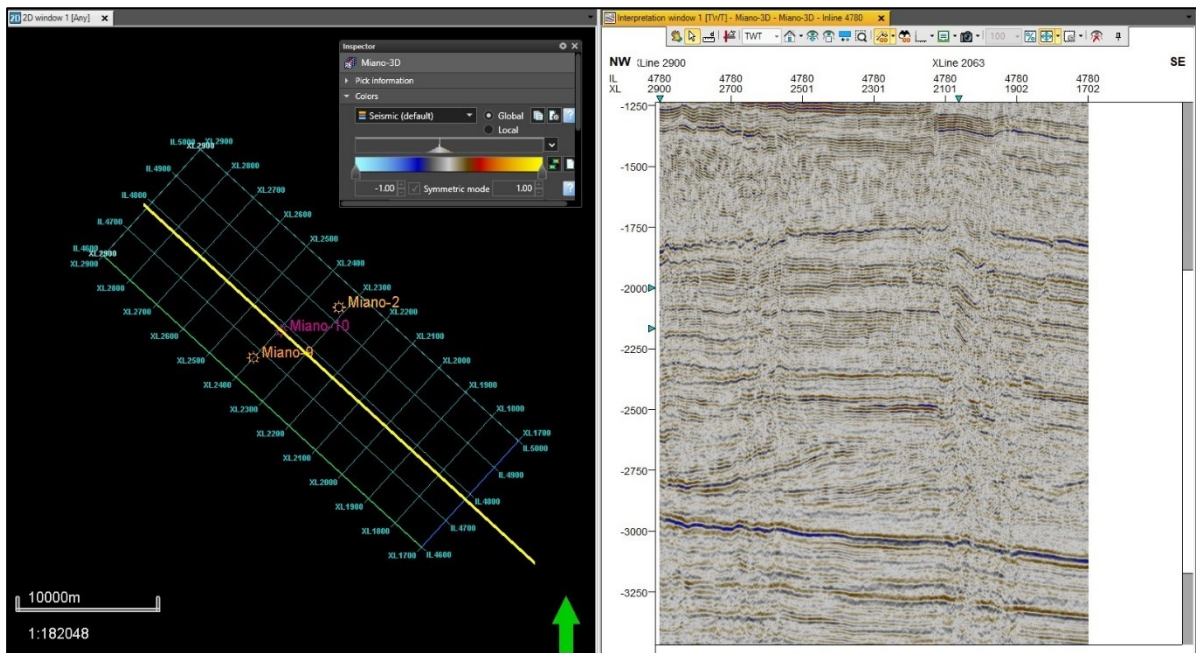

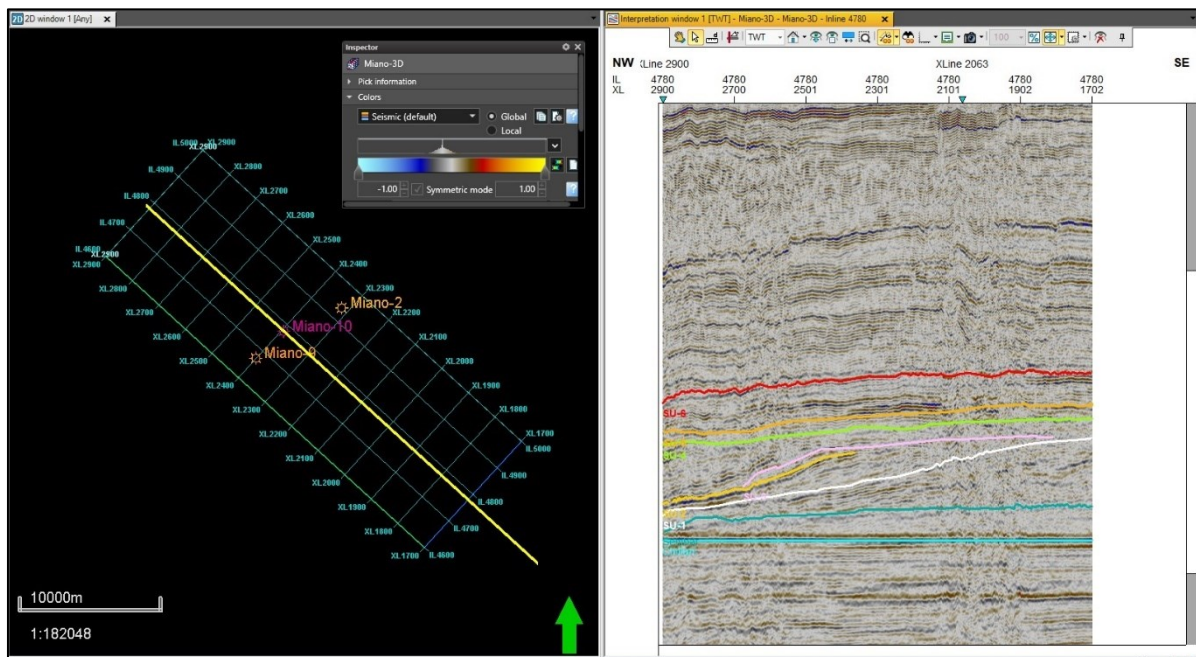Figure 4.9. Un-Interpreted in line 4936.
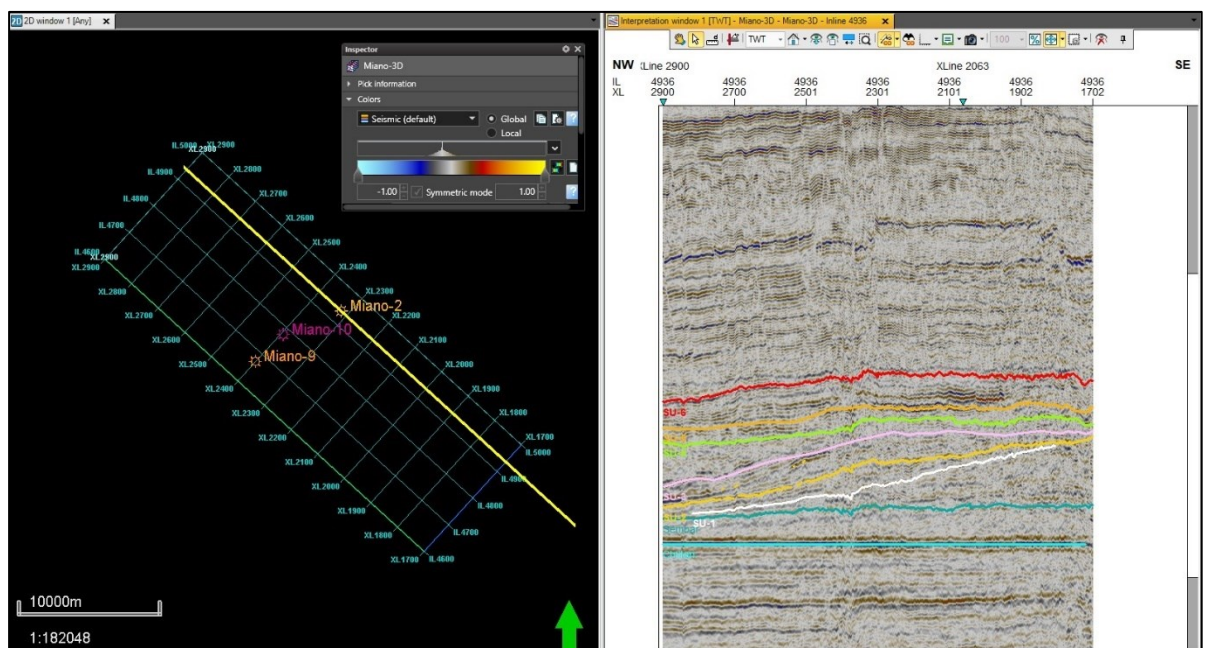
Figure 4.10. Interpreted in line 4936.
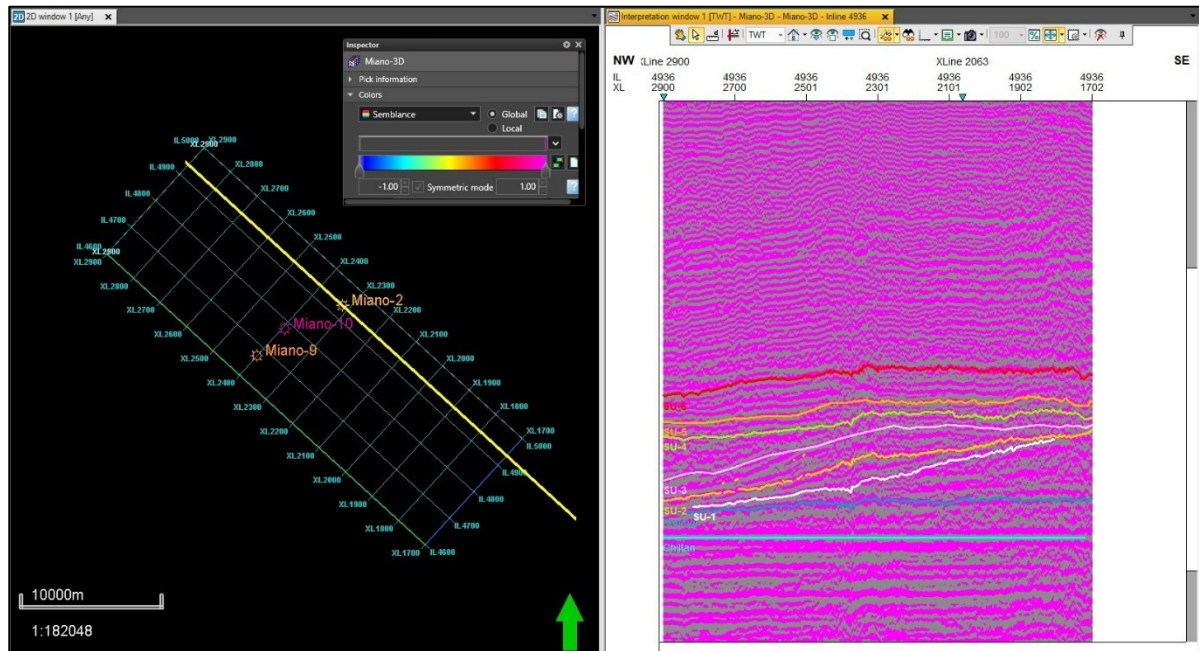
Figure 4.11. Confirmation of the genetically related stacking pattern through the local flatness attribute on inline 4936.

Confirmation of the genetically related stacking pattern through the local flatness attribute on inline 4936 can be seen in fig 4.11.
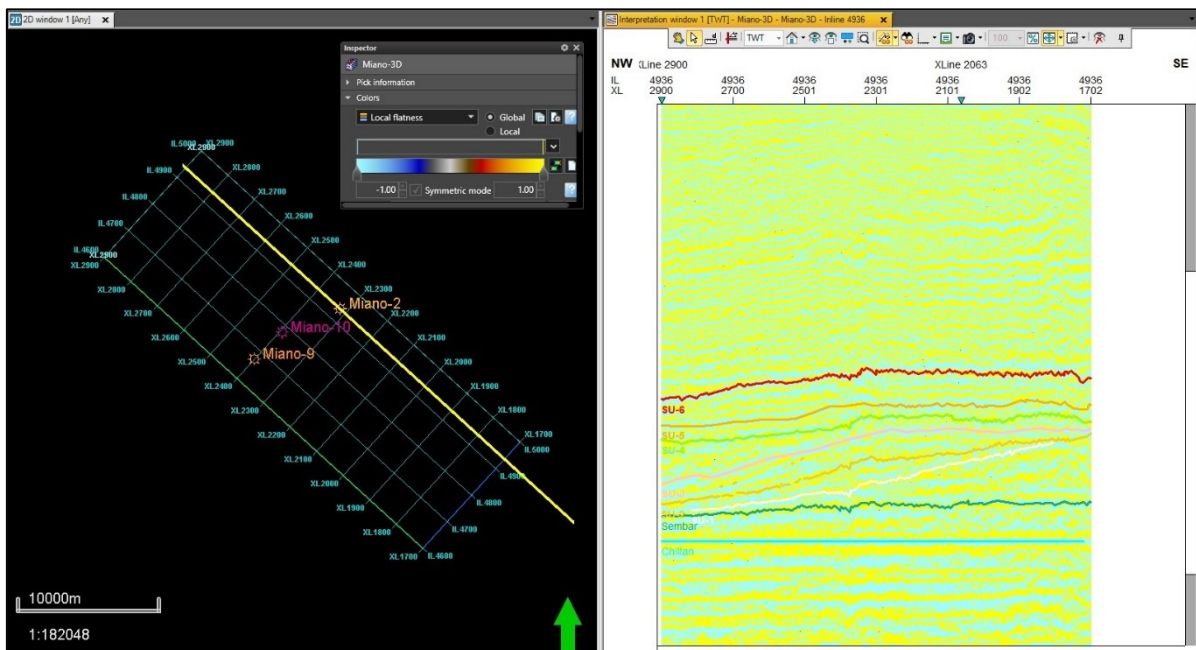
Figure 4.12. Confirmation of the genetically related stacking pattern through the semblance attribute on inline 4936.

Confirmation of the genetically related stacking pattern through the semblance attribute on inline 4936 can be seen in fig 4.12.

Figure 4.13. Un-Interpreted in line 4780.

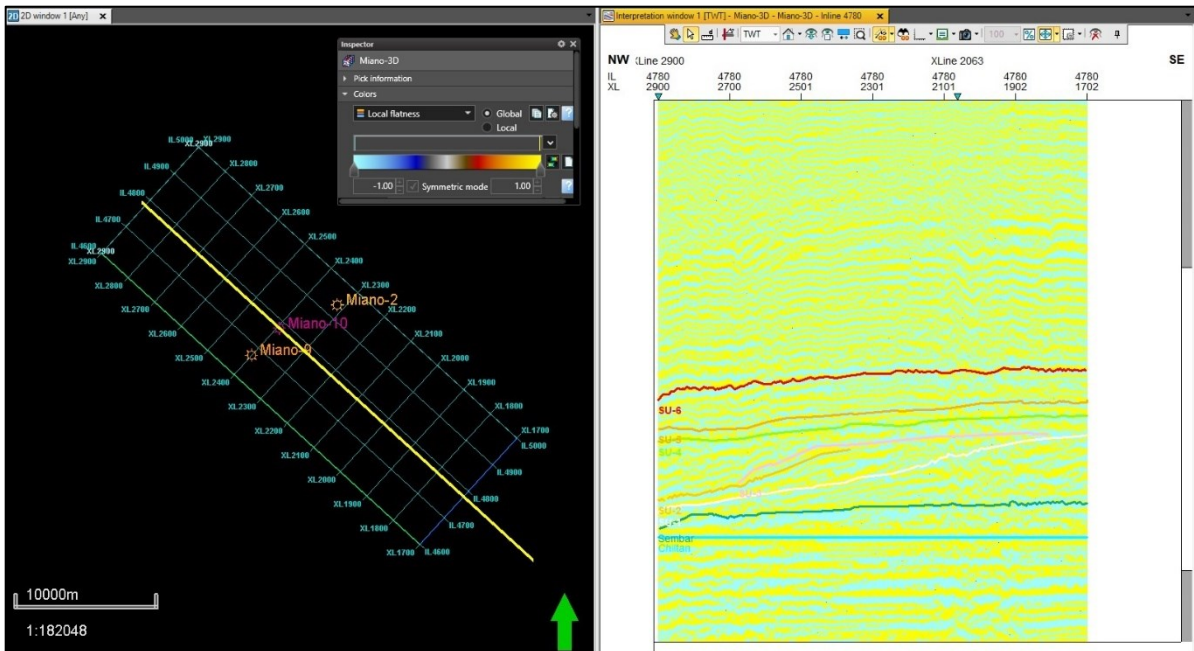Figure 4.14. Interpreted in line 4780.

Figure 4.15. Confirmation of the genetically related stacking pattern through the local flatness attribute on inline 4780.

Confirmation of the genetically related stacking pattern through the local flatness attribute on inline 4780 can be seen in fig 4.15.
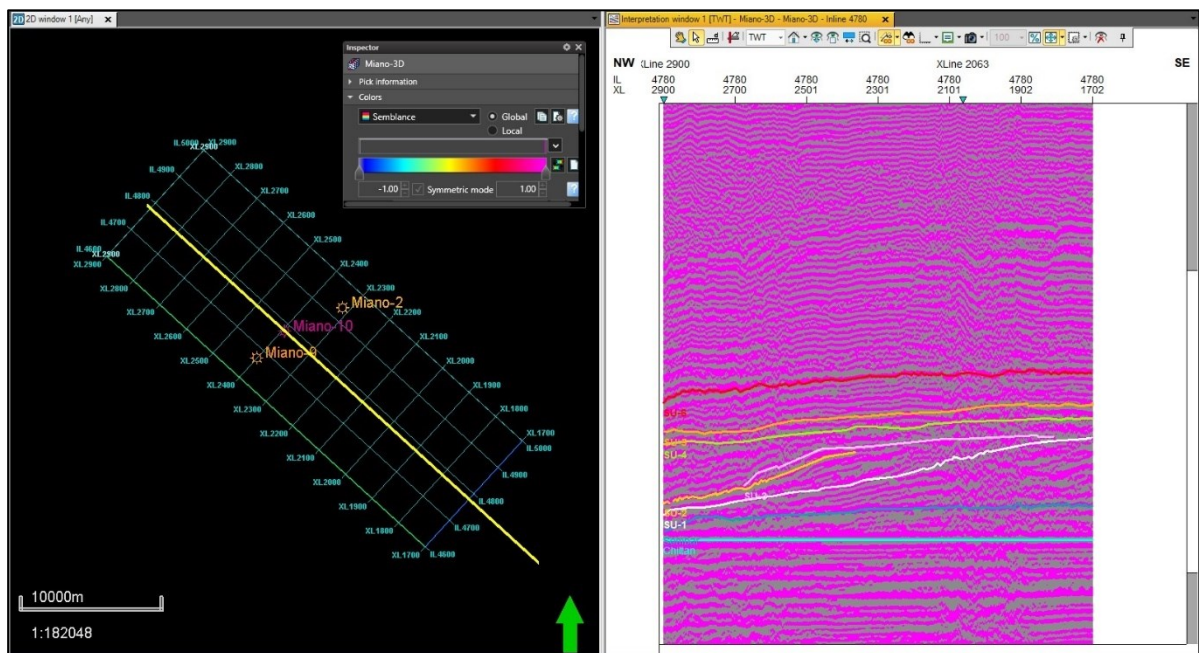

Figure 4.16. Confirmation of the genetically related stacking pattern through the semblance attribute on inline 4780.

.   Confirmation of the genetically related stacking pattern through the semblance attribute on inline 4780 can be observed in fig 4.16.
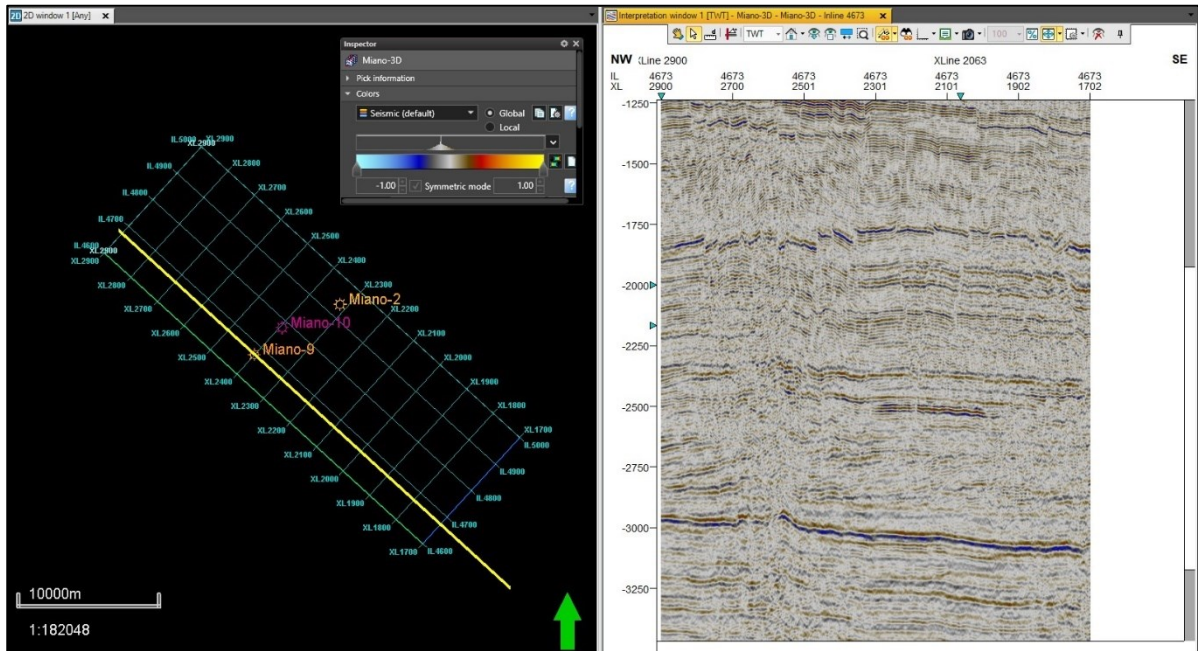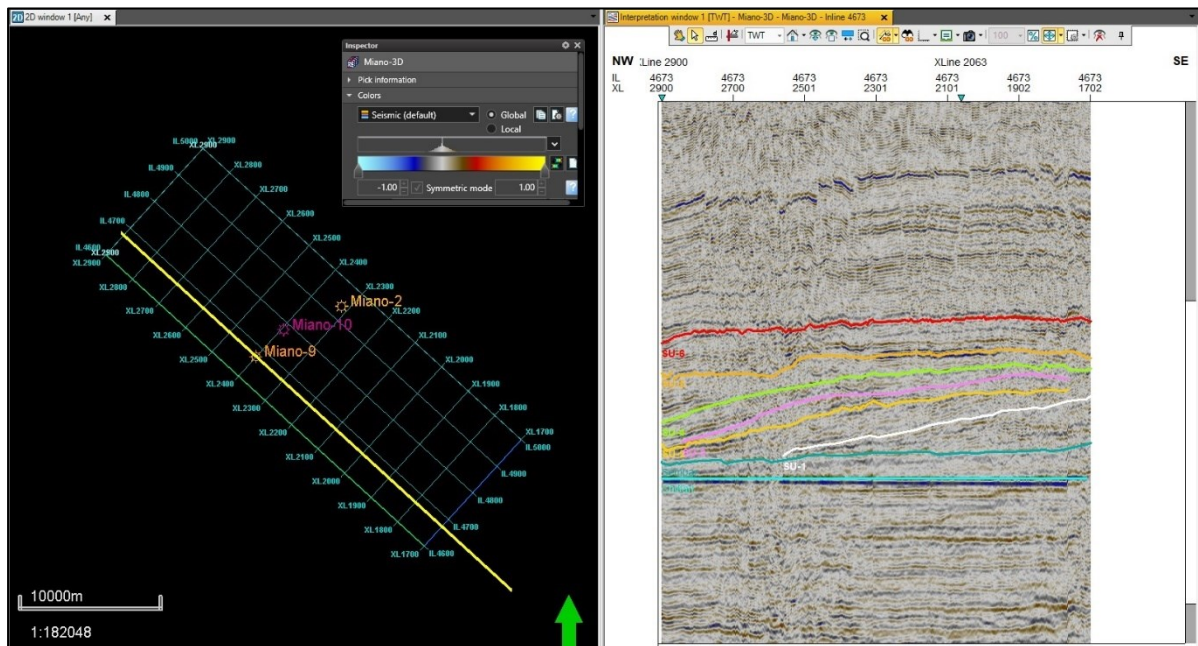

Figure 4.17. Un-Interpreted in line 4673.

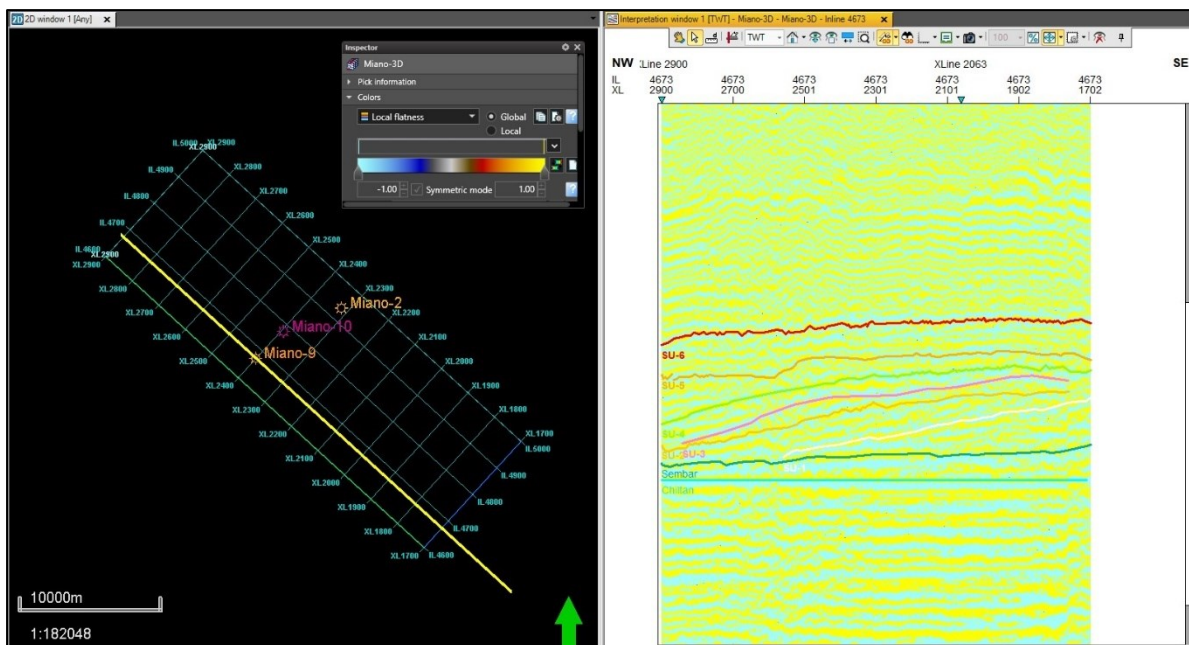Figure 4.18. Interpreted in line 4673.

Figure 4.19. Confirmation of the genetically related stacking pattern through local flatness attribute on inline 4673.
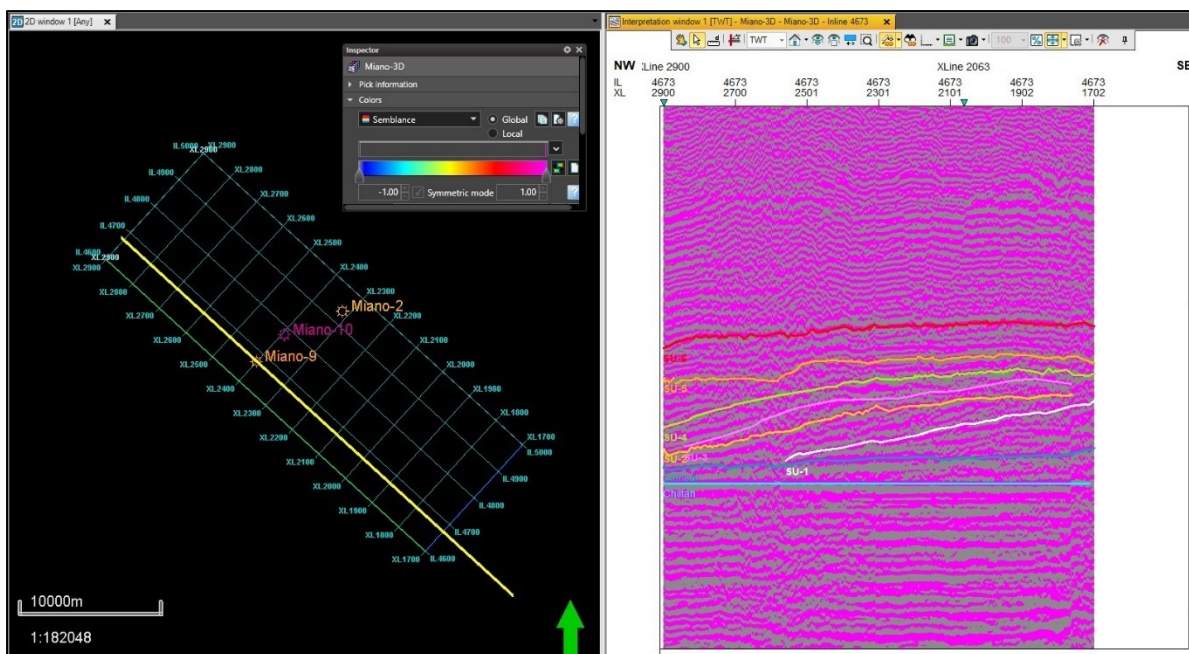

Figure 4.20. Confirmation of the genetically related stacking pattern through semblance attribute on inline 4673.

Confirmation of the genetically related stacking pattern through semblance attribute on inline 4673 can be observed in fig 4.20.

4.5   Time and Depth Mapping

Time maps illustrate the two-way time and spatial arrangement of specific geological horizons beneath the Earth's surface. By analyzing the travel time of seismic waves reflected from subsurface layers, these maps provide insights into the dip and thickness of geological units, essential for applications such as oil and gas exploration, mineral prospecting, and groundwater studies. Time maps help identify stratigraphic variation over the 3D volume and in creation of accurate geological models, guiding drilling operations, and minimizing exploration risks. They offer a three-dimensional perspective crucial for informed decision-making and optimizing resource extraction (Omoja et al., 2019).

Depth maps, similar to time maps, are fundamental in geology for delineating the depth of geological horizons and formations below the Earth's surface. These maps are pivotal for understanding the dip and thickness of geological units, crucial for various applications. They also aid in visualizing the subsurface (Omoja et al., 2019). Additionally, depth maps contribute significantly to geological modeling and simulation efforts, providing accurate representations of Earth's subsurface for scientific research and resource management purposes.

Time and depth maps are instrumental in visualizing reservoir trends. In this study, time and depth maps were generated for each horizon of interest using checkshot velocities. SU-6 and SU-5 were mapped as they were penetrated by Miano-02 well, however, the well was projected over SU-4 for mapping.
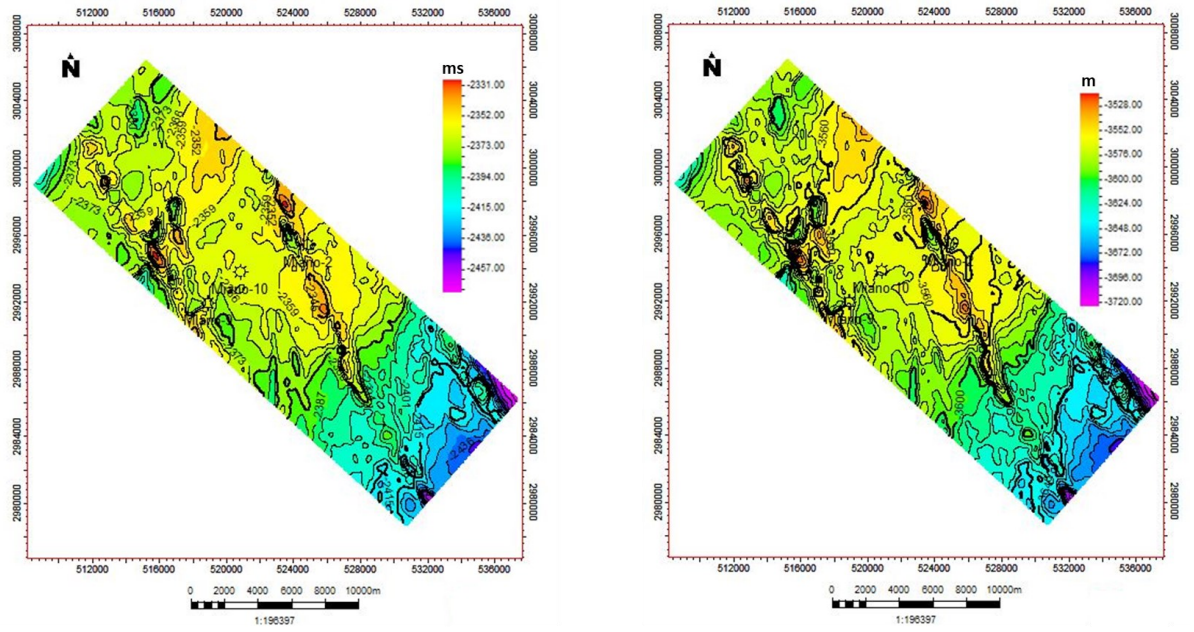
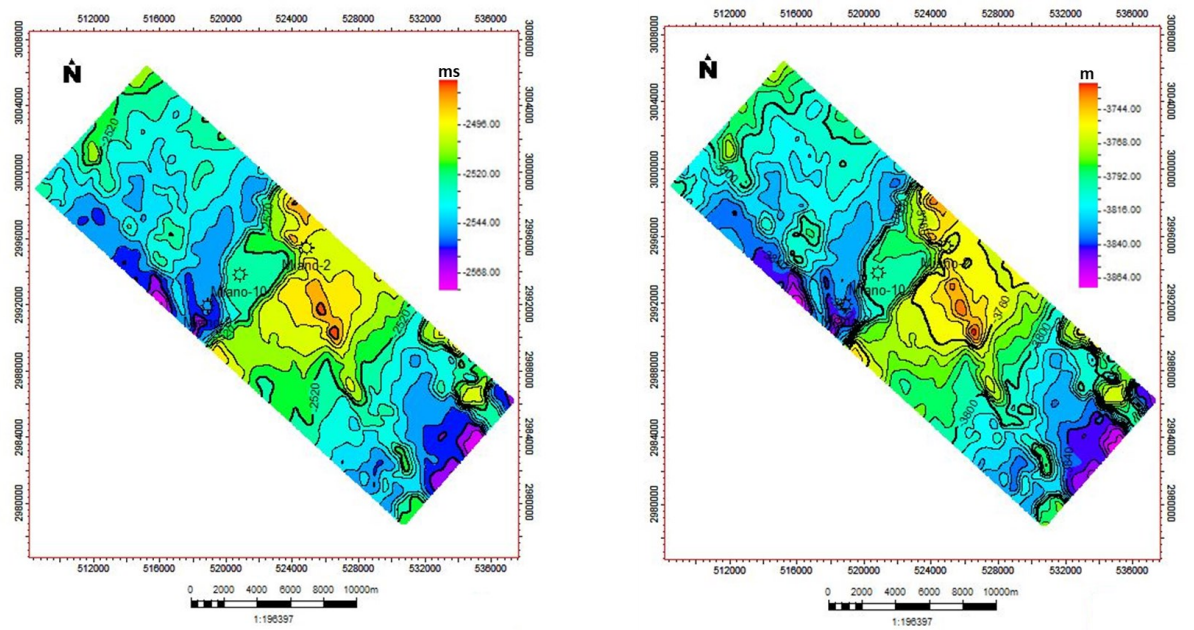Figure 4.21. Time map (left) and depth map (right) of amplitudes for SU-6.

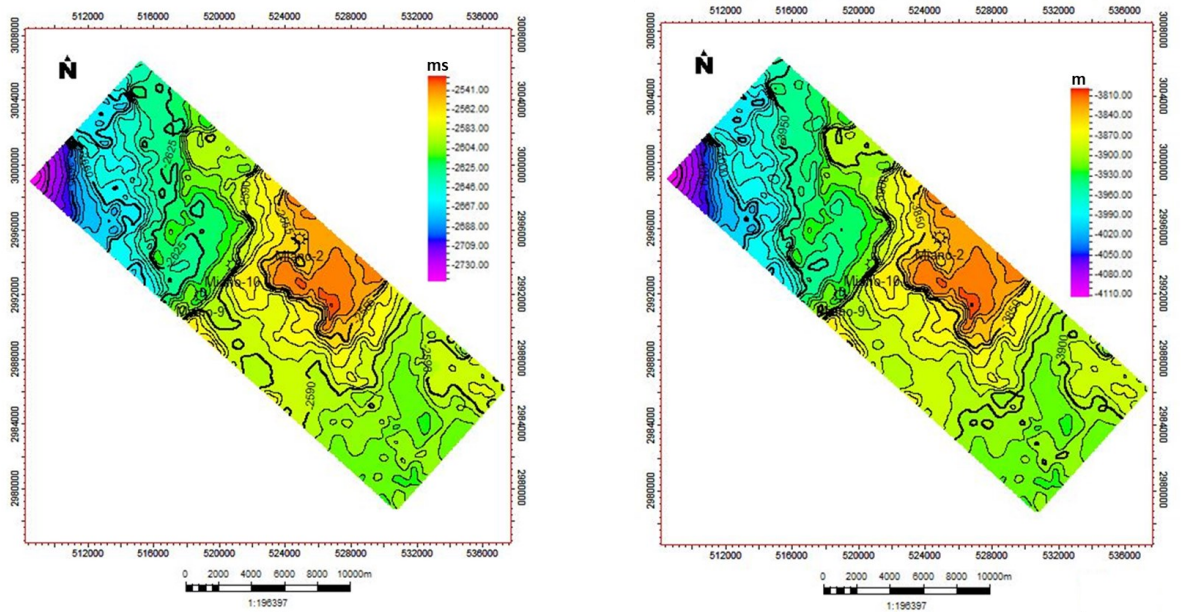Figure 4.22. Time map (left) and depth map (right) of amplitudes for SU-5.

Figure 4.23. Time map (left) and depth map (right) of amplitudes for SU-4.

4.6   Isopach Maps

Isopach maps visualize stratigraphic thickness between upper and lower horizon. It is quantified as minimum separation between the two surfaces. Isopach map offer a more precise representation of stratigraphic thickness as it reflects the thickness of the deposited bed. Isopach maps provide a more geologically precise visualization of stratigraphic interval thickness (Omoja et al., 2019). Isopach maps have been generated between SU-6 / SU-5 and SU-5 / SU-4.
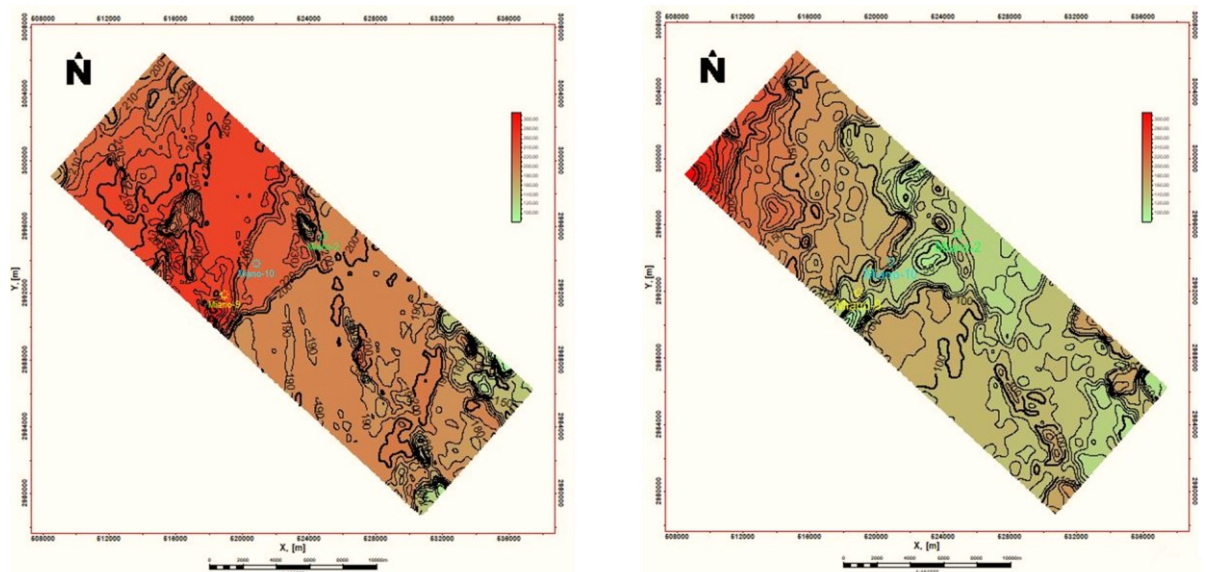

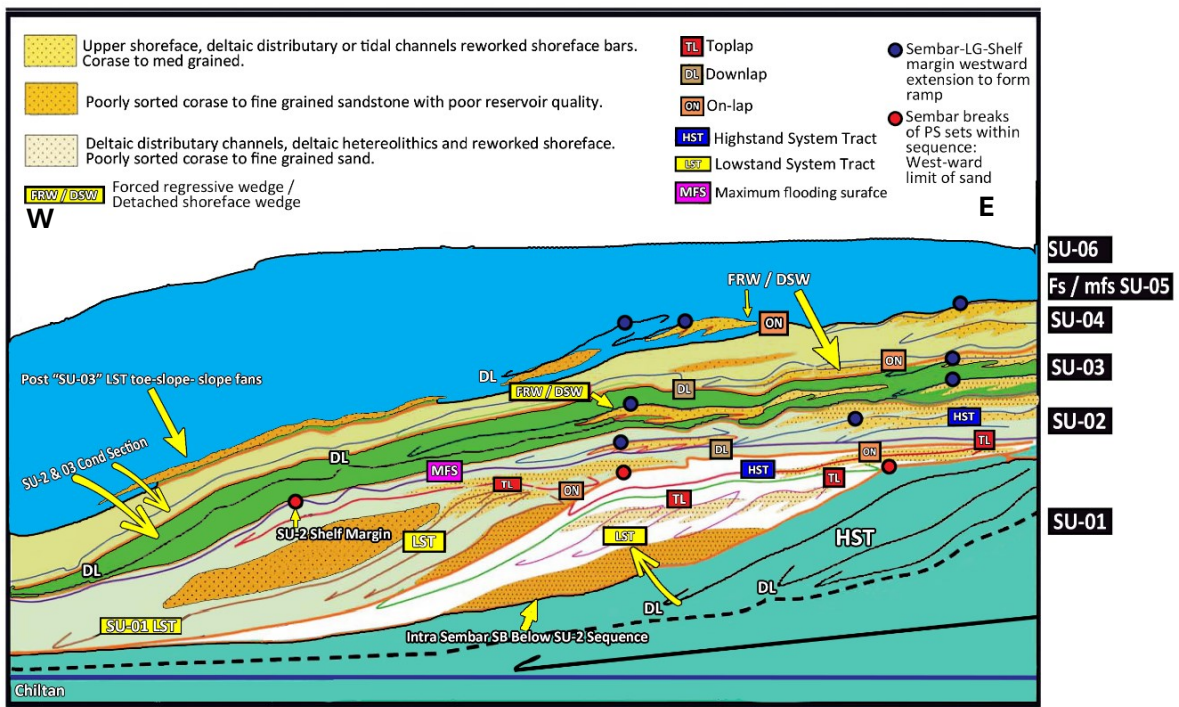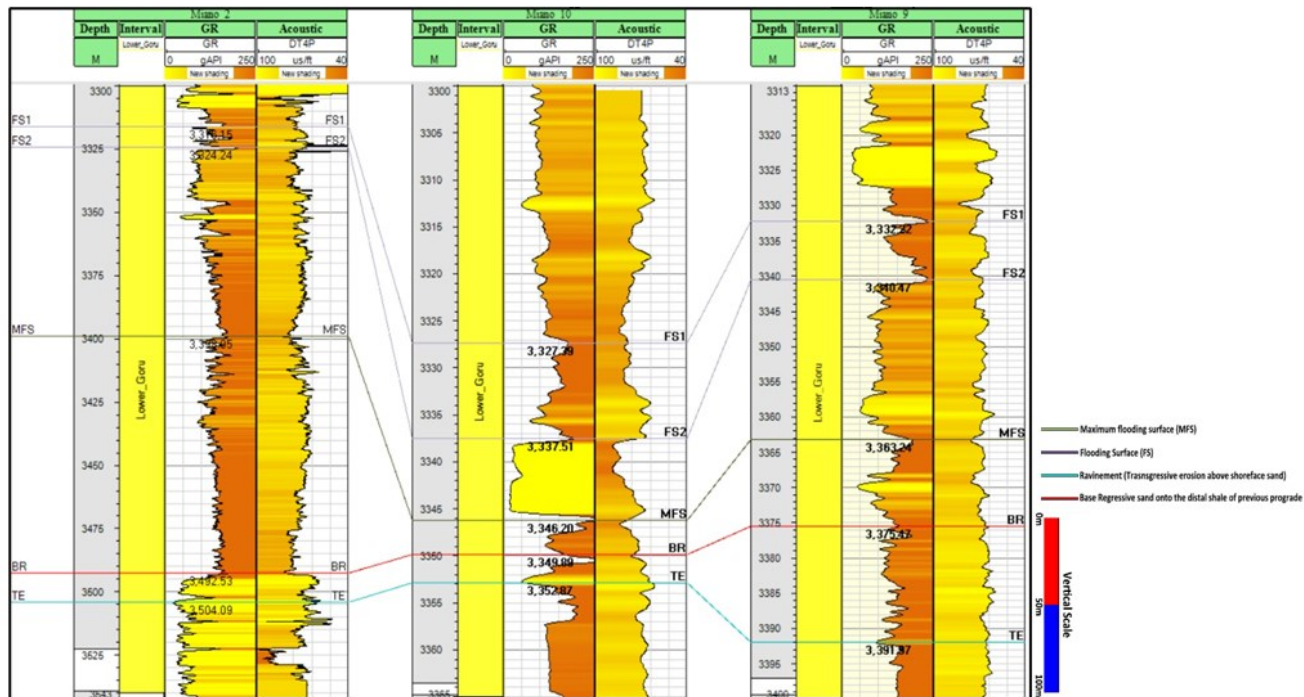Figure 4.24. Isopach maps showing stratigraphic thickness trends between Sand Unit 6 & 5 (left) and 5 & 4 (right).

Figure 4.25. Conceptual sequence stratigraphic model indicating various system tracts and surfaces (Modified after Nadeem et al., 2004).

CHAPTER 5
SEISMIC INVERSION

5.1 Introduction

Seismic inversion, either Pre-Stack or Post-Stack, converts subsurface seismic reflection data into quantitative characteristics that show the subsurface topography. Datasets such as centers and well logs are combined by seismic inversion (Chen et al., 2021). It also makes use of geostatistical techniques, which are related to both stochastic and deterministic approaches. Seismic inversion is helpful because it is efficient and of high quality, and it can be misleading when interpreting seismic data in a simple qualitative manner without including inversion results. This is especially true when looking for tight sands and shale gas reservoirs. By enhancing the accuracy and precision of the data via the calculation of rock characteristics like porosity, net pay, TOC, water saturation, etc., it reduces the risk factors (Pendrel, 2006).

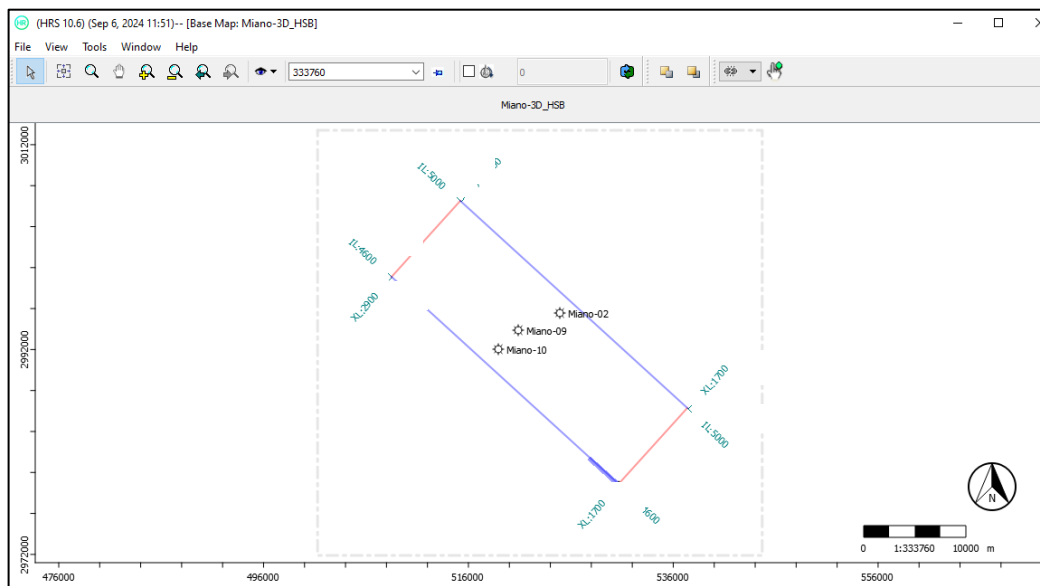Figure 5.1. Basemap of the area under investigation.

5.2 Post Stack Seismic Inversion

Post-stack inversion adds low resolution seismic with high resolution well data in order to create a highly detailed (vertical) model in the vicinity and away from well control; producing supply models having topographically conceivable shapes and evaluates uncertainty to survey chance (Figure 5.1). Accurate

petrophysical models are produced which contributes in reservoir characterization (Barclay et al., 2008).

Post-stack inversion is assumptions based, assuming that lateral variation in velocity is a minimum and average amplitude of stacked trace and is equal to amplitude of a normally reflected trace.

This technique is classified further as given below:

i. Band limited inversion (BLI)

ii. Model-based inversion (MBI)

iii. Linear Programming Sparse Spike Inversion (LPSSI)

If data quality is poor and density is sparse then the Linear Programming Sparse Inversion (LPSSI) is applied in order to estimate porosity and lithology in the study area (Pontnaguine & Castagna, 2005).

5.3 Linear Programming Sparse Spike Inversion (LPSSI)

In our clastic case, the Sparse Spike inversion is very reliable as SSI is based on generalized linear inversion (GLI) algorithm which within acceptable bounds matches the inversion results with seismic data (Zhang & Castagna, 2011). Until the objective function (error) is minimized, the perturbation of the model continues. However, geological knowledge is a pre-requisite to build an initial model (Helgesen et al., 2000). Workflow of LPSSI is given as:
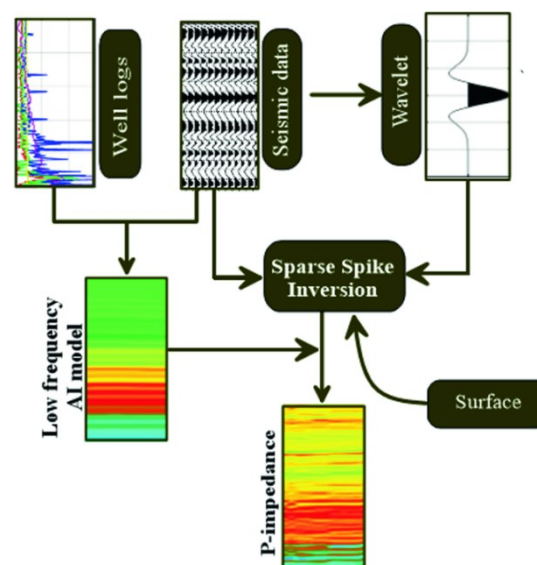

Figure 5.2. Generic inversion workflow.

5.4   Wavelet Estimation

Seismic information is necessary for seismic inversion, and a wavelet is derived from this data using seismic deconvolution. The extraction of the precise wavelet from available data is essential for the implementation of any seismic inversion approach (Abdulaziz et al., 2018). Seismic inversion necessitates seismic data and a wavelet derived from this data, achieved through seismic deconvolution. Extracting an accurate wavelet from the available data is vital for any successful seismic inversion technique. The stage and recurrence of the wavelet are determined by analyzing a reflection coefficient configuration along the borehole. Ensuring the quality of the assessed wavelet is fundamentally significant, as the wavelet's characteristics profoundly influence the inversion outcomes and, thus, directly affect reservoir quality (Yi et al., 2013). Wavelet sufficiency and stage spectra can be quantitatively recorded from either 1) seismic data; or 2) a combination of seismic data and well logs, specifically sonic and thickness variations. Following the estimation of the seismic wavelet, it is employed to calculate seismic reflection coefficients in the seismic reversal (Pendrel et al., 2006).

Distinct statistical wavelets were isolated, and the wavelet exhibiting the highest correlation was computed and later employed for the inversion project.
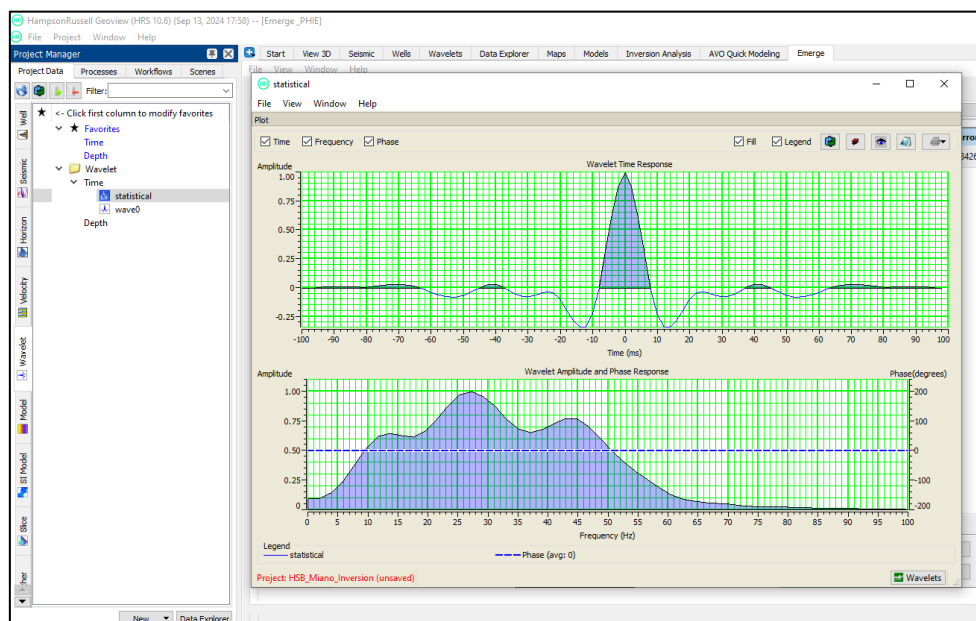
Figure 5.3. Statistical wavelet time, phase and frequence response.

5.5   Inversion Analysis

In the Miano-02 well inversion analysis was carried out as it is the only well that penetrates sand unit 6, the cross-correlation factor in the Miano-02 was about 92.5%, which shows that inversion results are a relatively true depiction of the lithology in the subsurface.

Figure 5.4. Seismic and well correlation.

5.6   P-Impedance Model

The P-Impedance model is a very useful attribute of seismic data for discriminating lithological properties as well as potential reservoir zones (Abdulaziz et al., 2018). The higher impedance zones indicate sand bodies, the lower impedances indicate shale. In case of gas filled sands, the impedance will suddenly drop within a sand body. Here, the impedance shows that the picked horizon has a continuous low impedance over a high impedance indicating gas in the sand body.
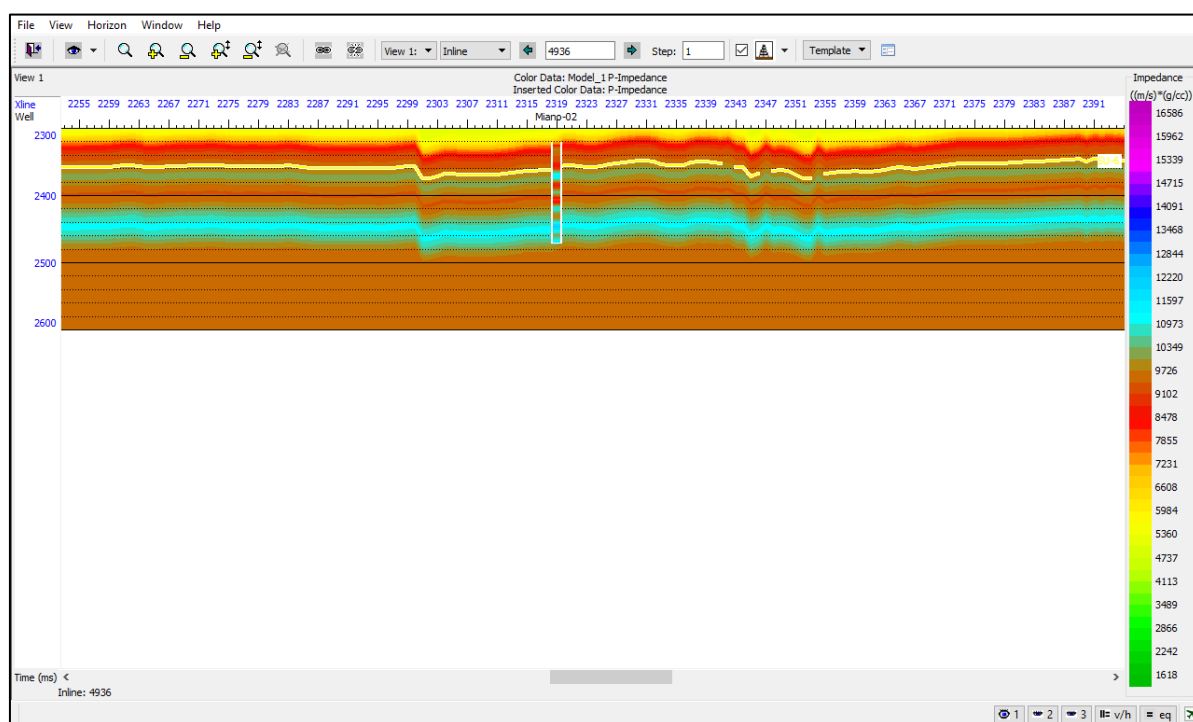

Figure 5.5. P- Impedance model from well Miano-02 on inline 4936.

5.7   Probabilistic Neural Network for Reservoir Quality Prediction

Physical properties were predicted through the use of seismic petrophysics and a geostatistical approach using probabilistic neural network. After PNN was used successfully, shale volume and porosity were calculated using seismic and inverted properties. Since porosity and shale volume are crucial properties for characterizing strata that contain hydrocarbons, they were evaluated using inverted seismic profiles, a geostatistical method. It shows a minimal average error correlation of over 90%.

There is a lot of potential for improving accuracy and resolving even thinner sand bodies when deep learning (DL), or the PNN technique, is applied to

seismic inversion (Abdulaziz et al., 2018). More accurate estimates can be made by combining several seismic parameters with inverted properties, which can offer insightful information on reservoir heterogeneity and fluid content.
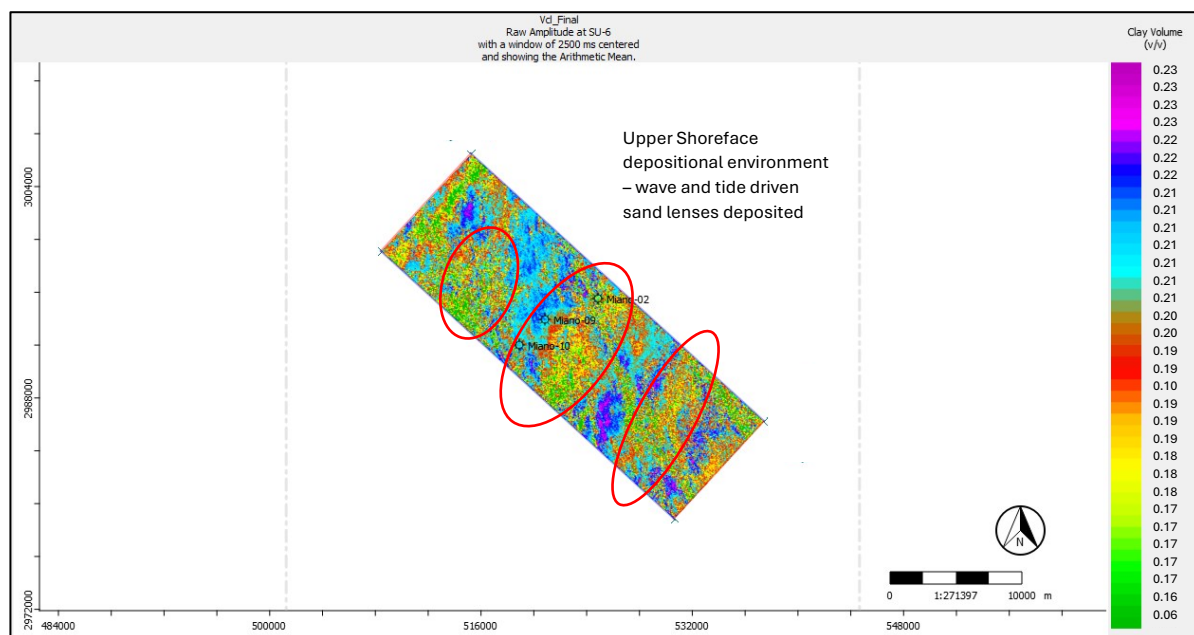

Figure 5.6. Estimated clay volume populated on the inverted seismic discriminating good quality poor quality reservoir sands in the area.
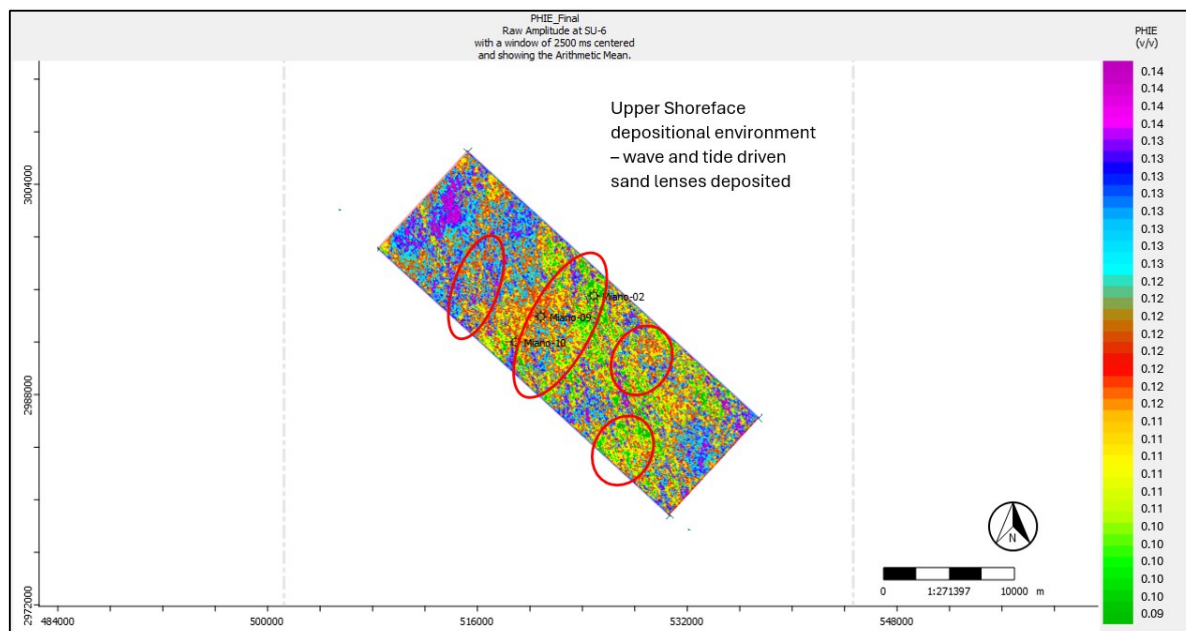

Figure 5.7. Estimated effective porosity populated on the inverted seismic discriminating good quality and poor reservoir sands in the area.

For the gas prospect, the sparse-spike inversion analysis has effectively captured the fluctuations in the reservoir parameter (P-impedance). According to the inversion results, the expected sand lenses are where the comparatively lower P-impedance values are found. Geostatistical methods, such as probabilistic neural network (PNN) analysis and multi-attribute regression, are used to estimate the reservoir's effective porosity in order to better define it. In contrast, the PNN analysis applied its estimations to the full seismic volume and predicted the desired property more effectively. Additionally, the reservoir candidate zones were considerably anticipated by the geostatistical predictions of PNN analysis, which also validated the sand channel's role as a key contributor to the gas accumulation in the area.

CHAPTER 6

SEISMIC ATTRIBUTES AND MACHINE LEARNING BASED FACIES CLASSIFICATION

6.1   Seismic Attributes

Seismic attributes can be described as "quantities that are measured, computed, or inferred from seismic data." The primary purpose of attributes is to offer precise and comprehensive insights to interpreters regarding the structural, stratigraphic, and petrophysical characteristics of a seismic prospect (Oumarou et al., 2021).

Seismic attribute analysis involves breaking down seismic data into various distinct attributes. This disintegration of seismic data lacks formal guidelines for attribute computation or defining their nature. In fact, any geological or geophysical parameter derived from seismic data can be considered an attribute. Amplitude is an inherent attribute of seismic data (Barens, 2001). Seismic attributes play a crucial role in offering qualitative insights for understanding both structural and stratigraphic features, such as channels, meanders, pinch-outs, thin bed tuning etc. They can also provide indicators for rock types and fluid content, contributing to a more comprehensive understanding of reservoir characteristics (Oumarou et al., 2021).

Attributes are primarily employed to detect various features and changes in the subsurface. These include the identification of distinct bright spots, areas of gas accumulation, and demarcations of sequences. They can also highlight significant shifts in depositional settings, effects arising from thin-bed tuning, and discrepancies such as unconformities. Additionally, they can point out notable lithological transitions, localized alterations suggesting fault presence, and spatial relationships related to porosity (Oumarou et al., 2021).

6.2   Attribute Analysis and Blending

Four stratigraphic attributes include General Spectral Decomposition (GSD), Grey Level Co-Variance Matrix (GLCM), 3D Curvature and Variance.

Seismic attributes are used to support interpretation at all scales, ranging from analyzing regional depositional systems to mapping fine details of structure, stratigraphy, and rock properties.
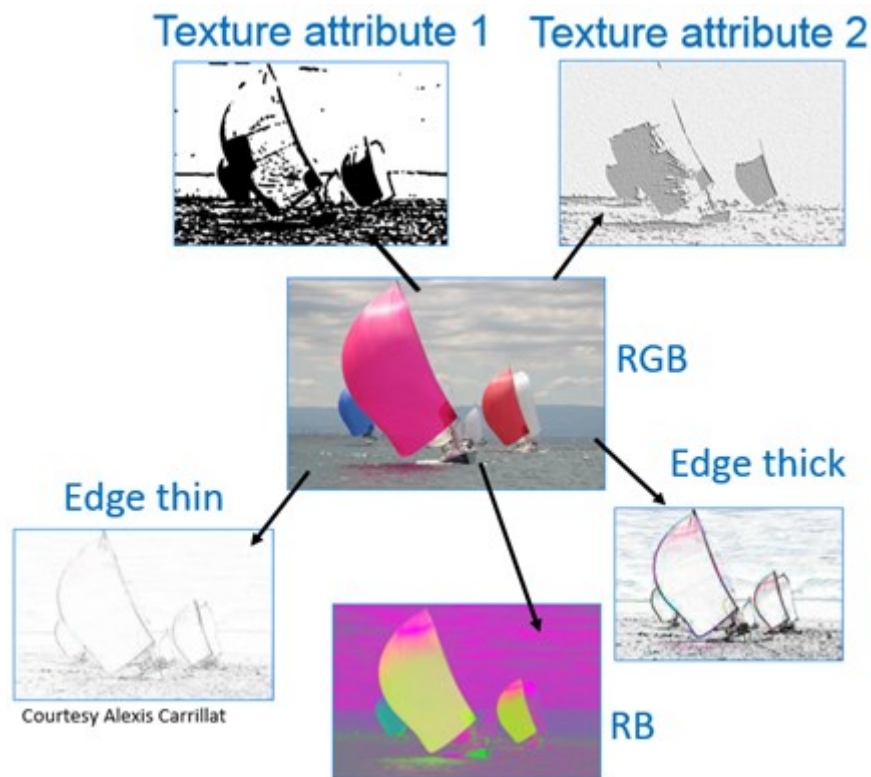

Figure 6.1. Your choice of an attribute depends on the dataset and what you want to highlight (Shen et al., 2020).
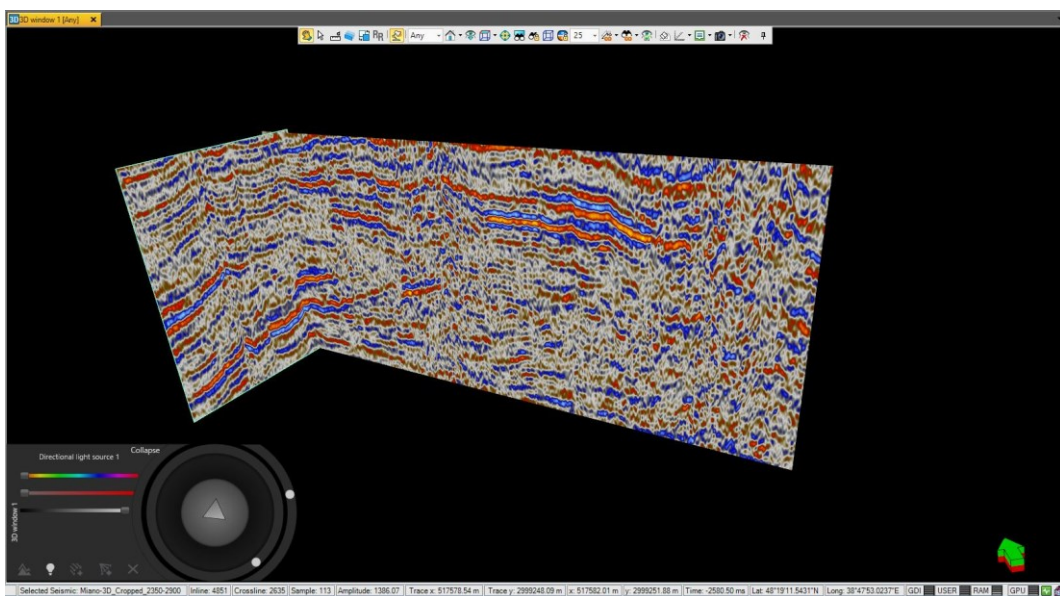

Figure 6.2. 3D seismic volume displayed without filtering or attribute rendering.

The sequences are clear in figure 4.25 but in order to glean further insights, attributes will play a significant role.

Textural attributes such as the grey level co-occurrence matrix (GLCM) and its derived attributes are able to describe the spatial dependencies of seismic facies. GLCM and its derived attributes are tools for image classification that were initially described by. Principally, the GLCM is a measure of how often different combinations of pixel brightness values occur in an image (Haralick et al., 1973).

Spectral decomposition separates the seismic signal into its constituent frequencies. It allows the interpreter to delineate subtle geologic features (amplitude and/or phase) tuned at a specific frequency (Chopra et al., 2007).

A popular attribute for qualitative and quantitative interpretation workflows, it is commonly used for seismic geomorphologic analysis, layer thickness determination, and direct hydrocarbon indicator for gas charged reservoirs (Chopra et al., 2007).

3D Curvature represents a sophisticated approach in the analysis seismic data, leveraging the phase and amplitude characteristics inherent in seismic waveforms. By decomposing seismic signals into their in-phase and quadrature components, these attributes facilitate the extraction of vital facies change information that is instrumental in illuminating subsurface geology. The process of attribute extraction involves calculating instantaneous frequency, amplitude, and phase from the quadrature components (Chopra et al., 2007).

Variance (edge detection) estimates trace-to-trace variance (1-semblance). It is amplitude invariant (but not orientation invariant); i.e., it will produce the same response for the same seismic signature, whether in a low- or high-amplitude region (Chopra et al., 2007).

Its utility includes revealing discontinuities in seismic data either related to stratigraphic terminations or structural lineaments, it can discriminate between low and high continuity of seismic. It is useful in interpreting progradational vs aggradational stacking patterns on stratal slices. Also, Variance is a good

discriminator for seismic facies analysis. The attribute analysis is run on a 100 ms time shift from 2350 to 2650 ms time window.
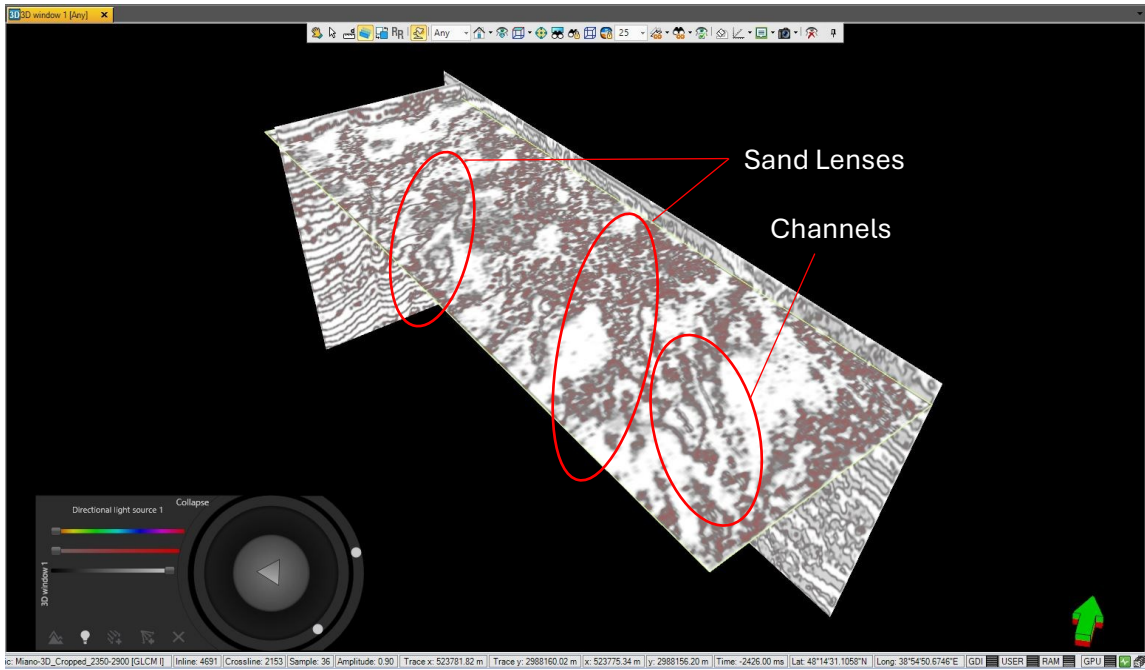

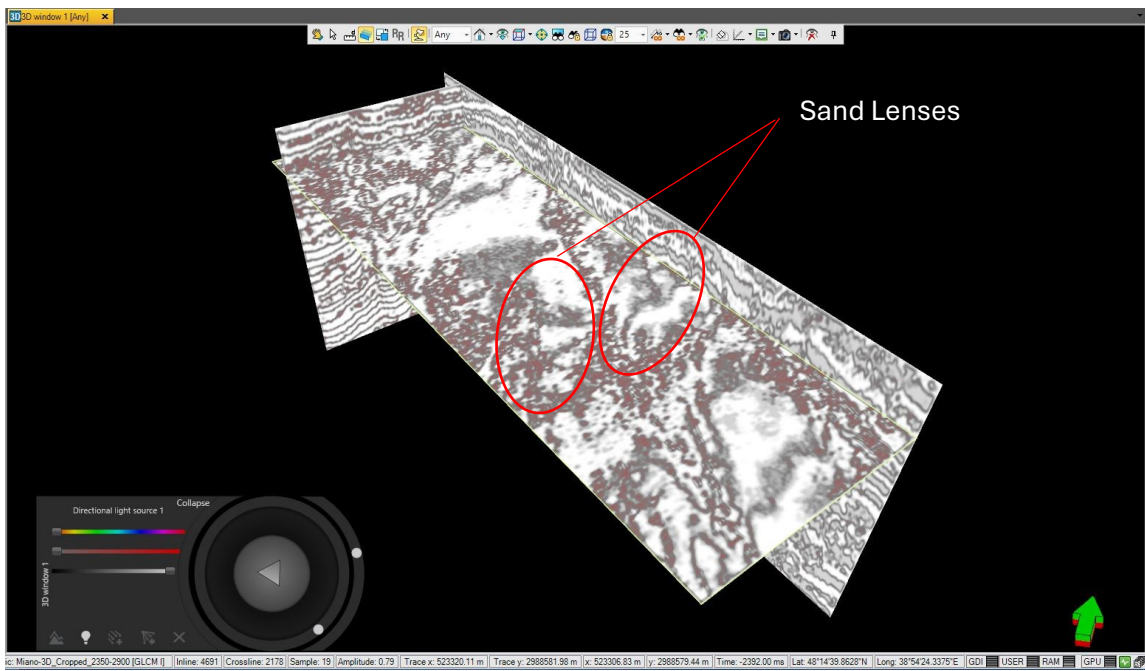Figure 6.3. GLCM at 2350 ms, highlighting upper shoreface sand deposition.

Figure 6.4. GLCM at 2450 ms, highlighting upper shoreface sand deposition.
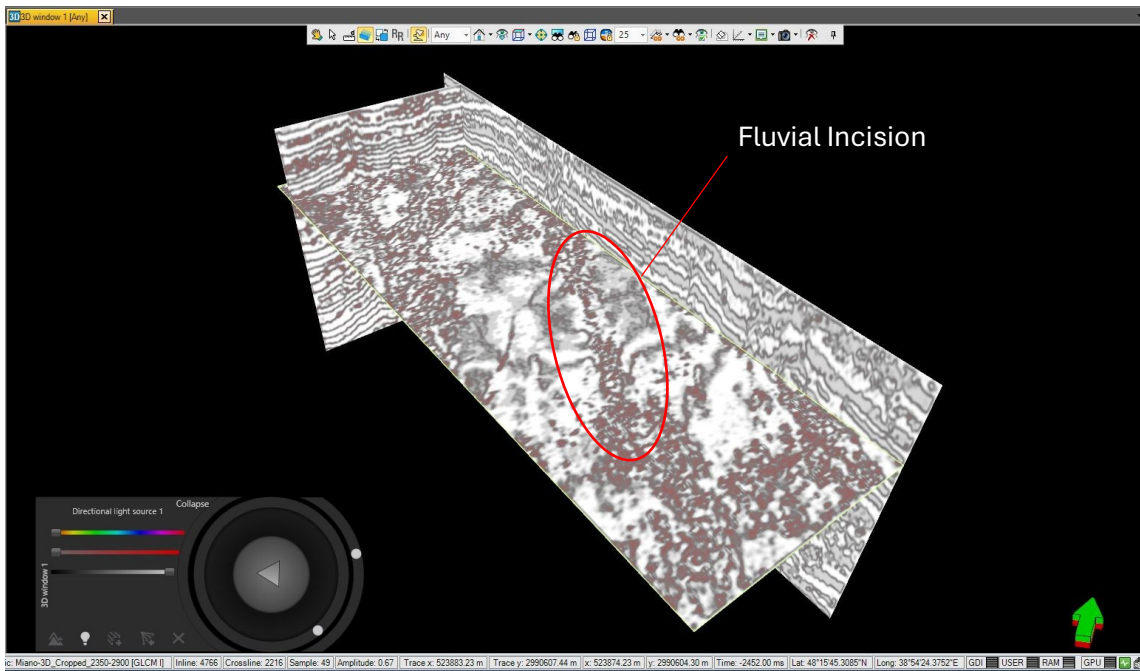
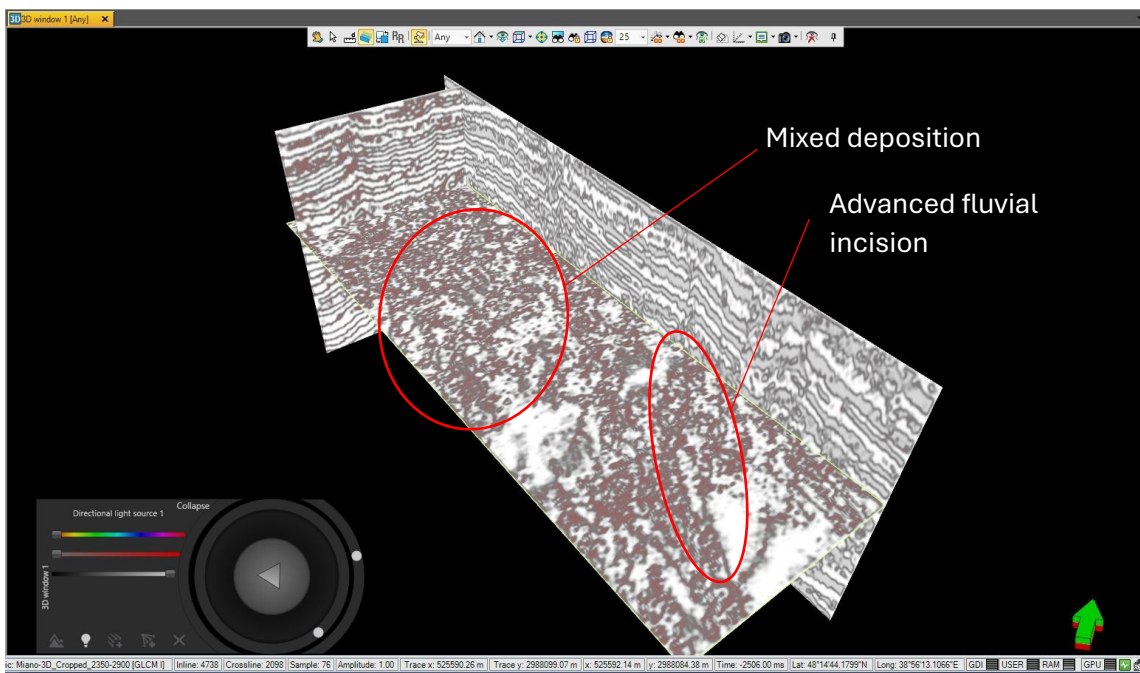Figure 6.5. GLCM at 2550 ms, highlighting channels and river incision.

Figure 6.6. GLCM at 2650 ms, indicating deeper incision and further channels translating to mixed deposition.
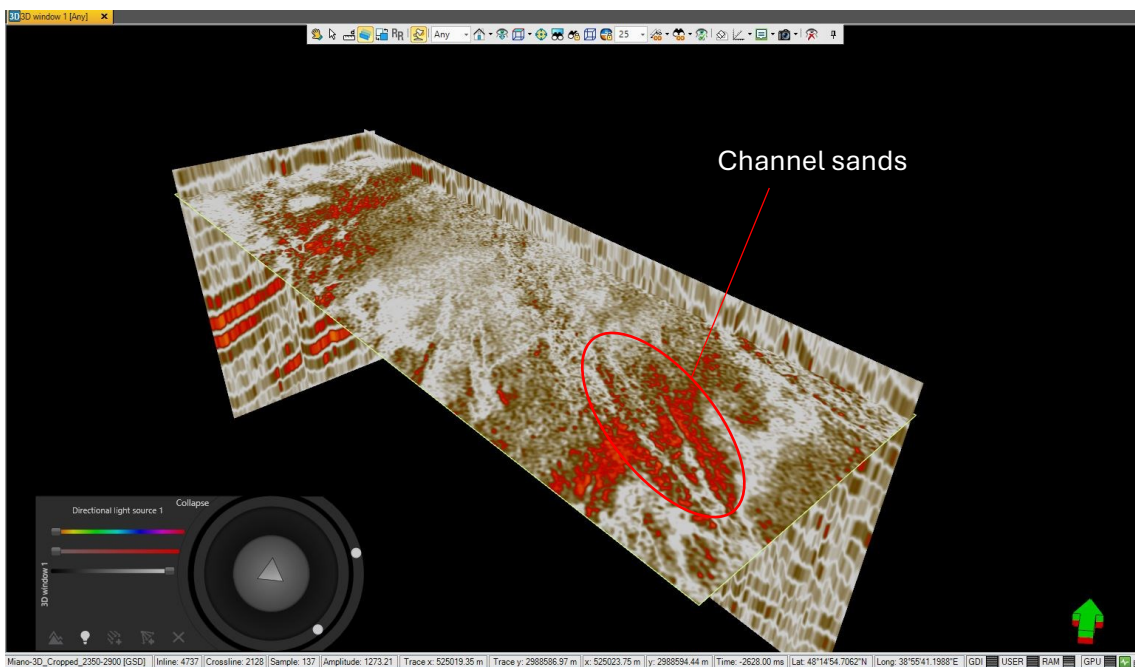
Figure 6.7. GSD at 2350 ms, showing channel geometries and sand deposition (lobes around the channels).
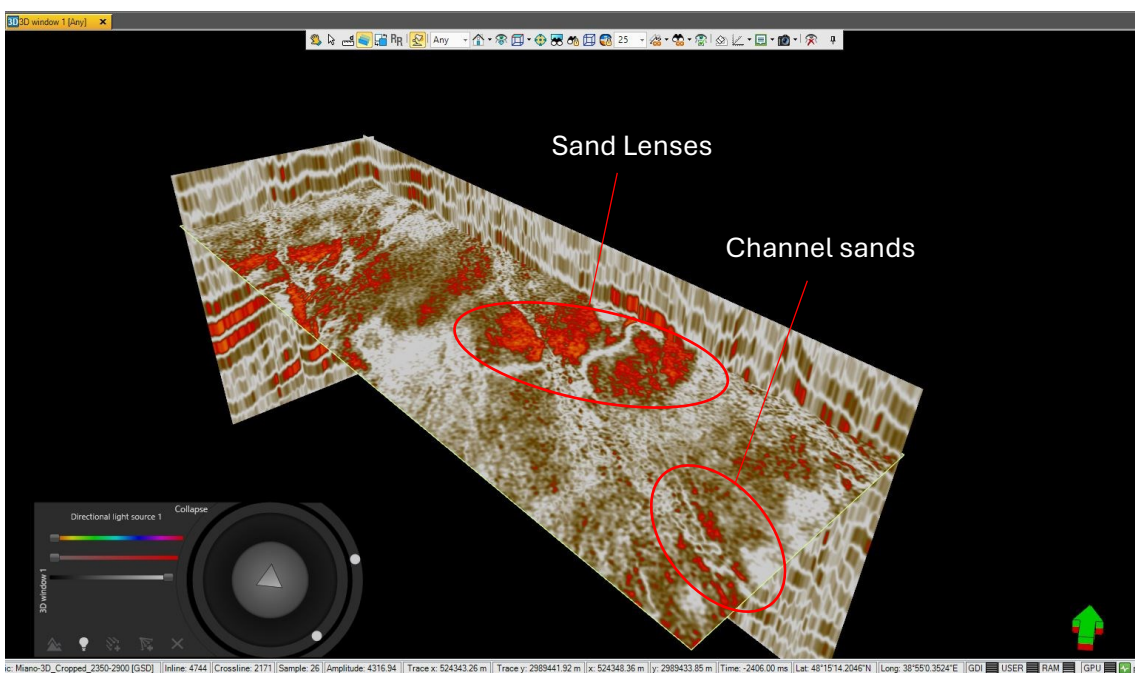
Figure 6.8 GSD at 2450 ms, highlighting channel paths and sand lens geometries (wave-tide deposition).
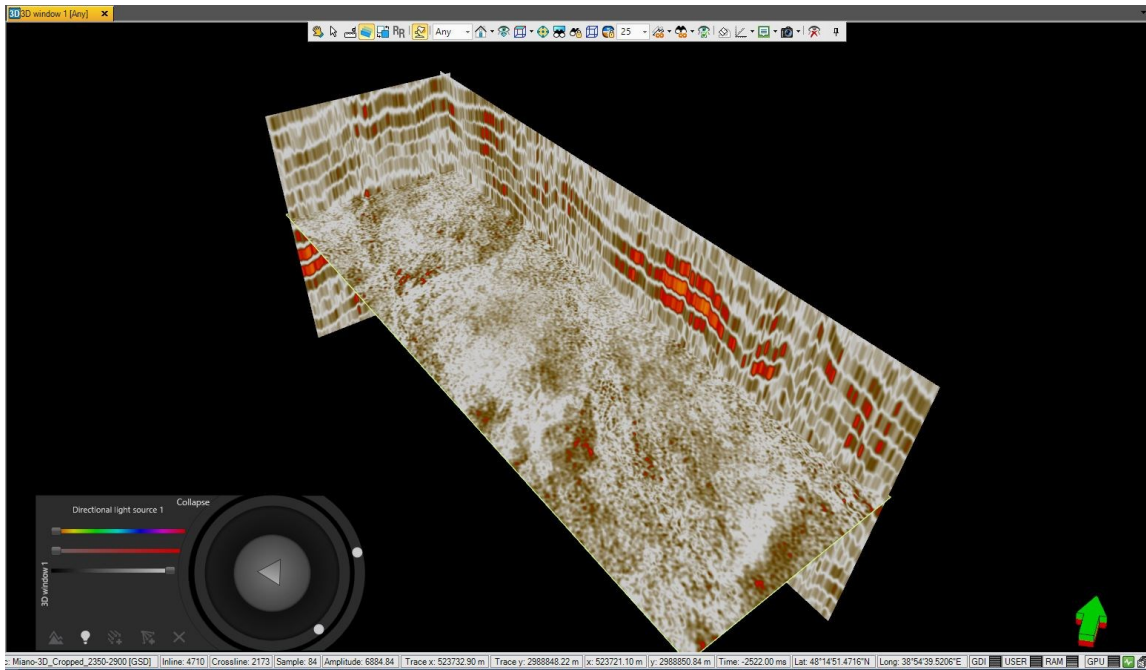
Figure 6.9. GSD at 2550 ms, highlighting channel paths and sand lens geometries along with a hint of mixed facies, i.e. river dominated / wave-tide dominated deposition.
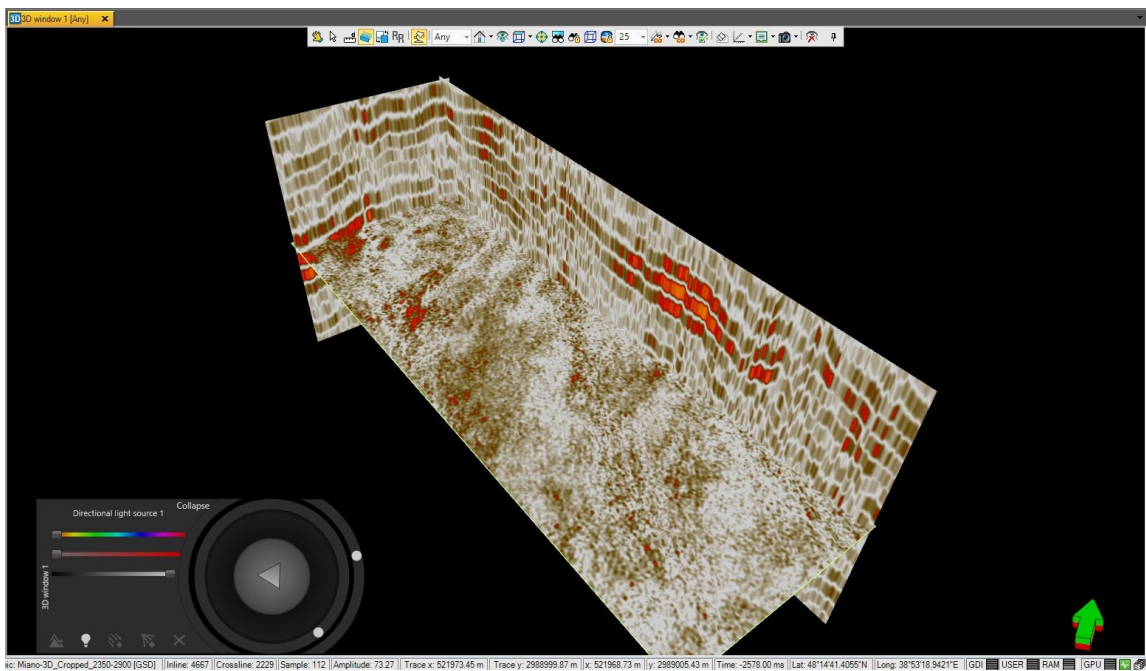
Figure 6.10. GSD at 2650 ms, highlighting channel paths and sand lens geometries along with a hint of mixed facies, i.e. river dominated / wave-tide dominated deposition.
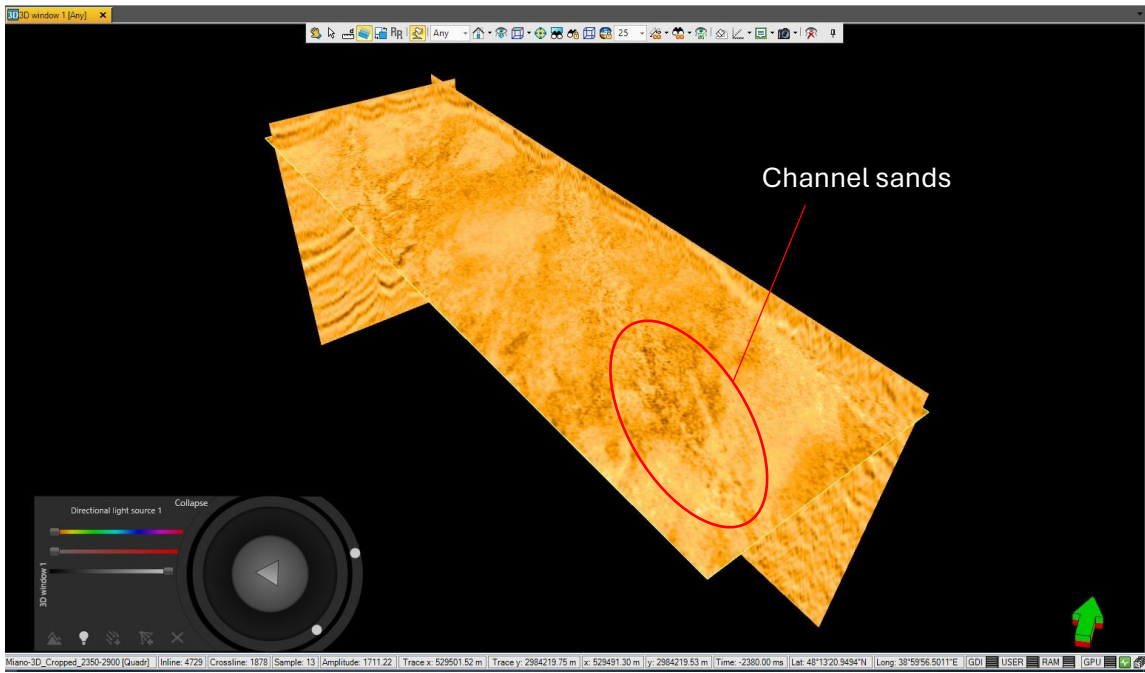
Figure 6.11. 3D Curvature at 2350 ms, highlighting channel pathways.
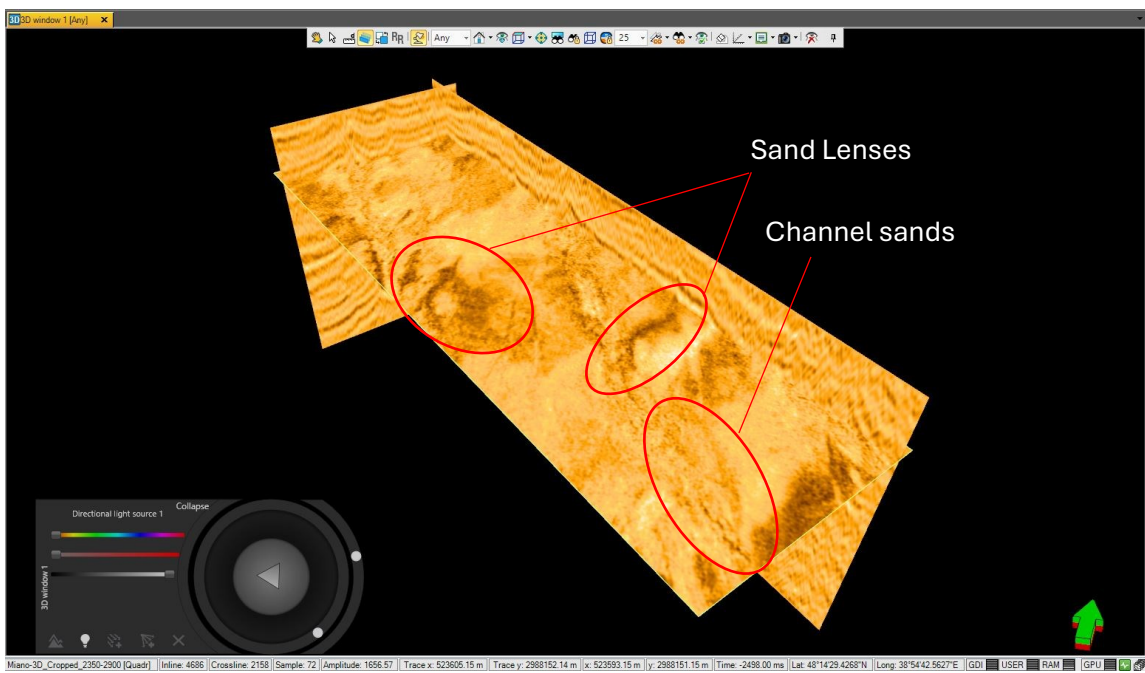
Figure 6.12. 3D Curvature at 2450 ms, highlighting sand lenses.
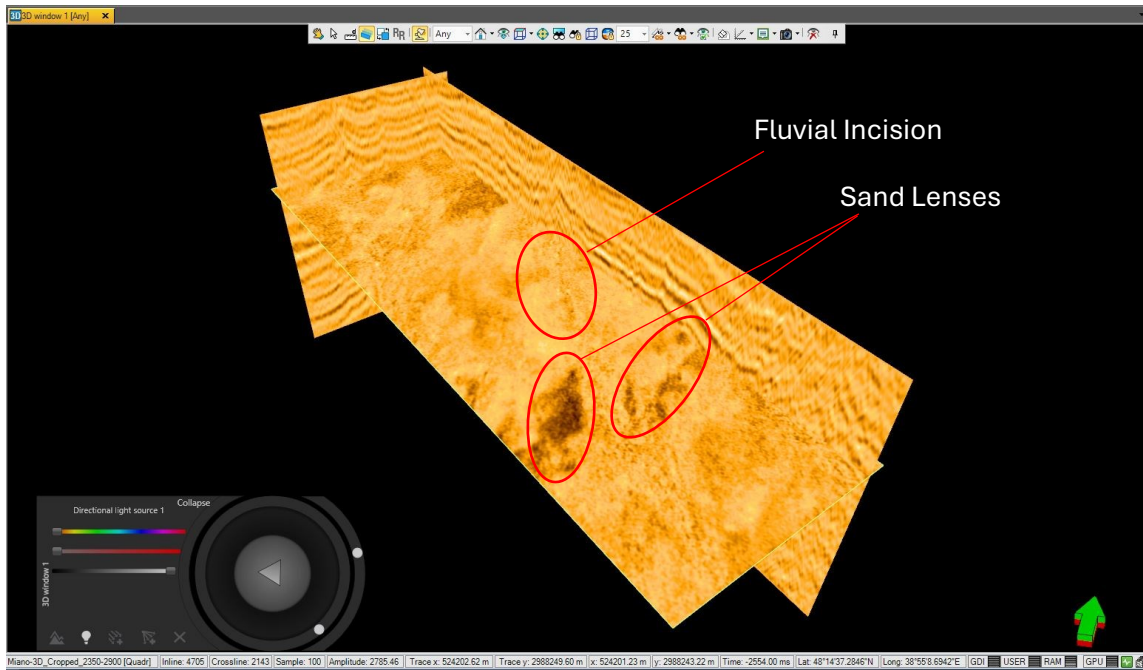
Figure 6.13. 3D Curvature at 2650 ms, showing start of fluvial incision and mixed deposition due to sudden changes to depositional environment owing to rapid sea level drop.
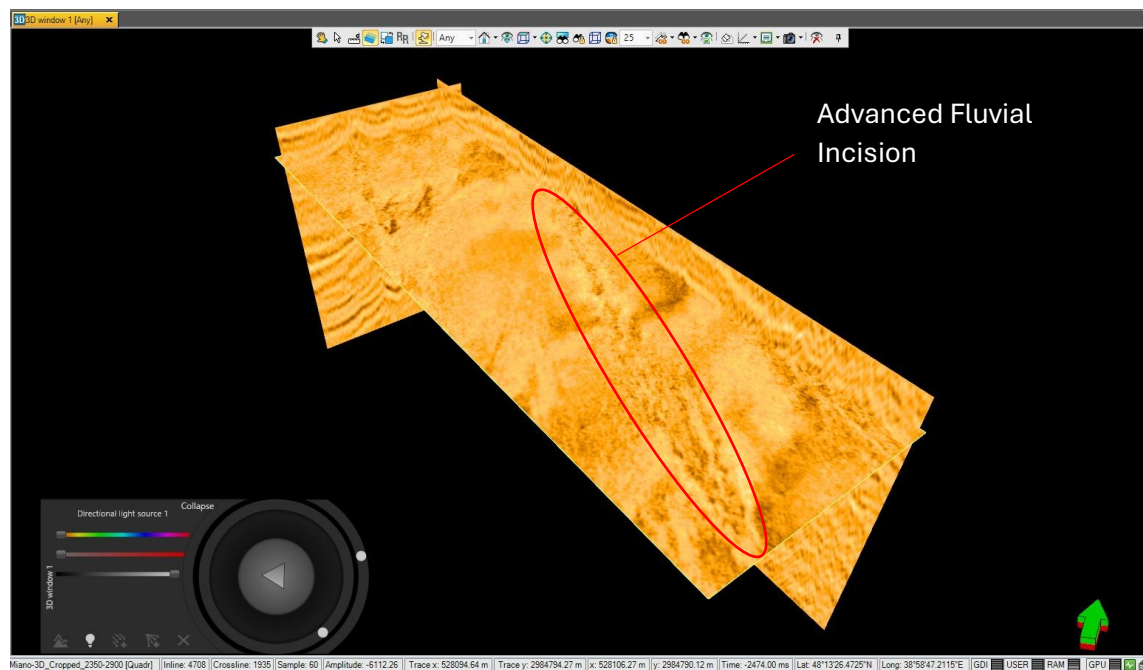
Figure 6.14. 3D Curvature at 2650 ms, showing advanced fluvial incision and mixed deposition due to sudden changes to depositional environment owing to rapid sea level drop.
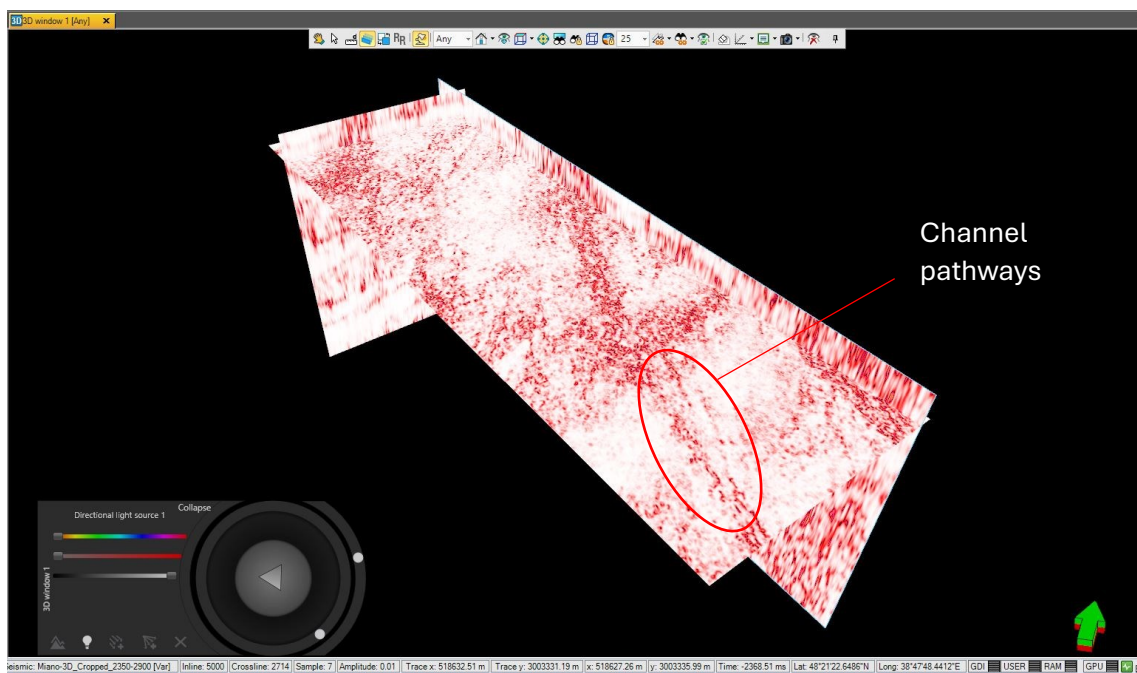
Figure 6.15. Variance at 2350 ms, highlighting channel deposition.
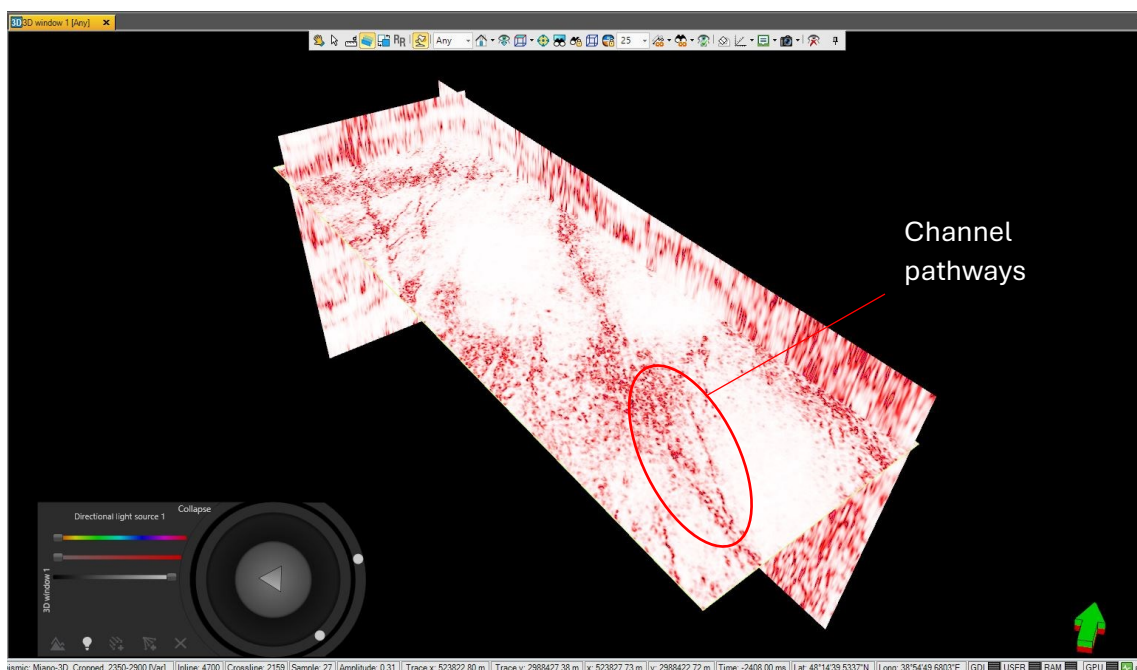
Figure 6.16. Variance at 2450 ms, highlighting channel pathways.
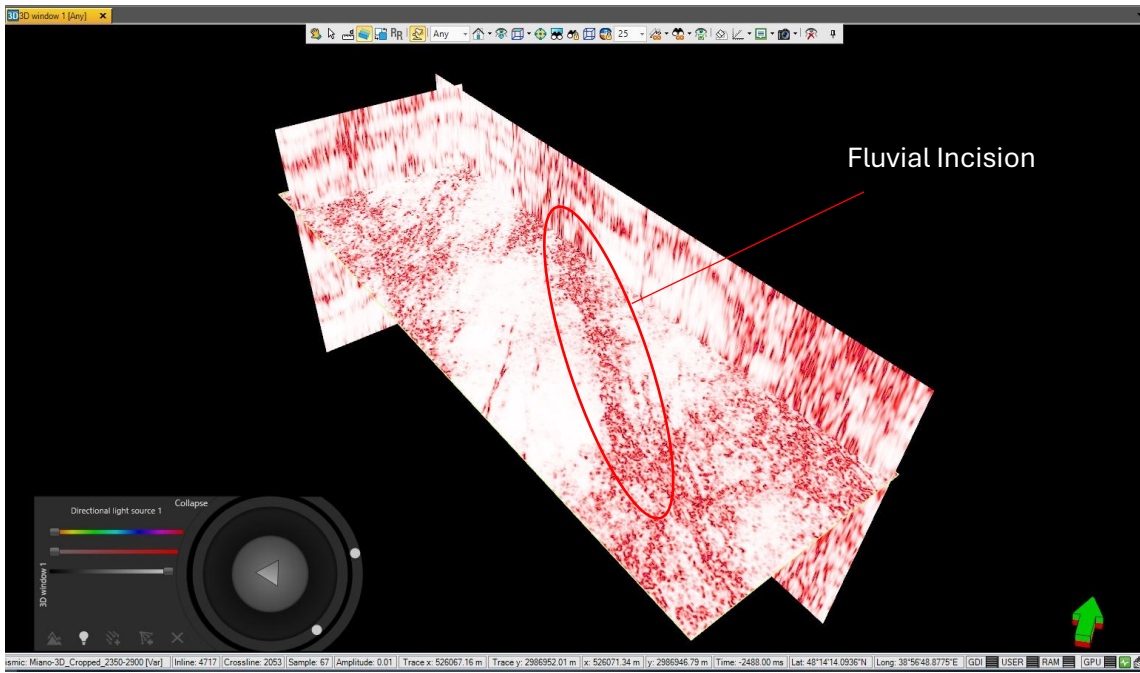
Figure 6.17. Variance at 2550 ms, showing fluvial incision.
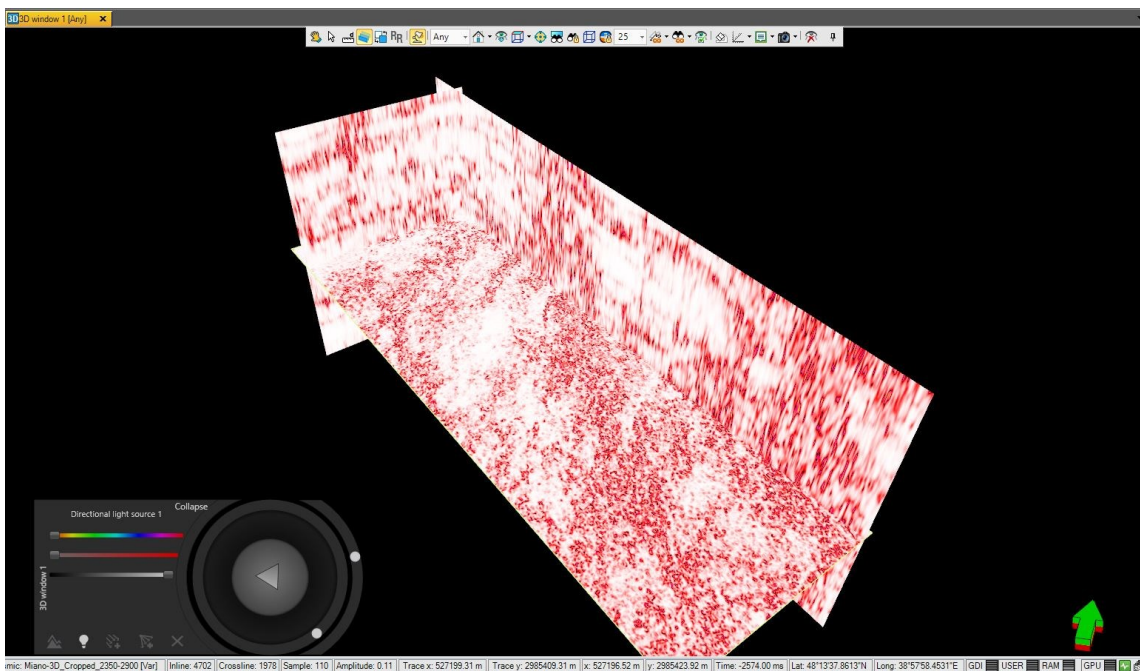
Figure 6.18. Variance at 2650 ms, showing inconsistent trends due to mixed deposition.

6.2.1 Attribute Blending

In terms of viewing multiple potentially helpful seismic volumes, the attribute blending enables us to widen the color spectrum in a dynamic and visually impressive way, allowing us to make various conclusions regarding the color changes indicating, for example, changing facies, or pore fill. It helps to accurately identify stratigraphic features and later red, green, and blue are the additive primary colors of the color spectrum. For blending magnitude volumes from the frequency decomposition, the RGB (red, green and blue) color scheme is the best one (Ruan et al., 2018).
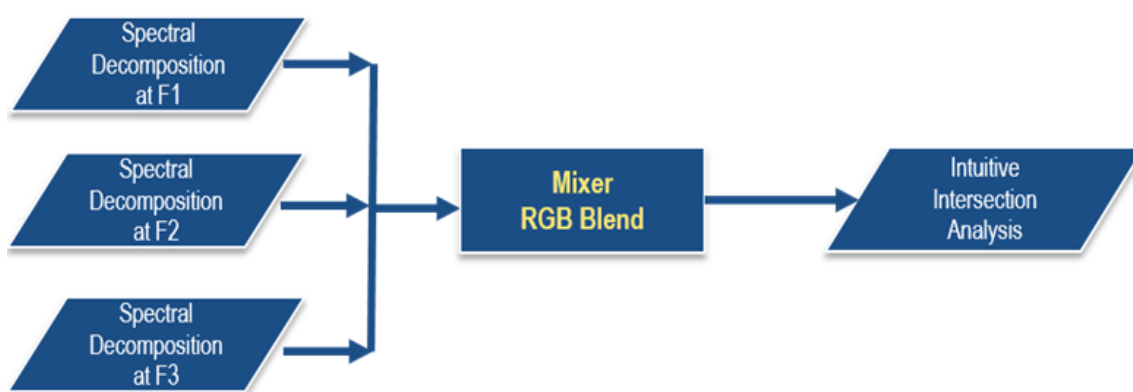
Figure 6.19. Schematic of spectrally decomposed attribute blending (Ruan et al., 2018).

One of the most successful and highly effective techniques for visually combining the multiple attributes is the RGB blending color model (Ruan et al., 2018). Figure 6.19 shows three relevant inputs. Attribute blending using the General Spectral Decomposition (GSD), Grey Level Co-Variance Matrix (GLCM), 3D Curvature and Variance is carried out for the Miano 3D volume.
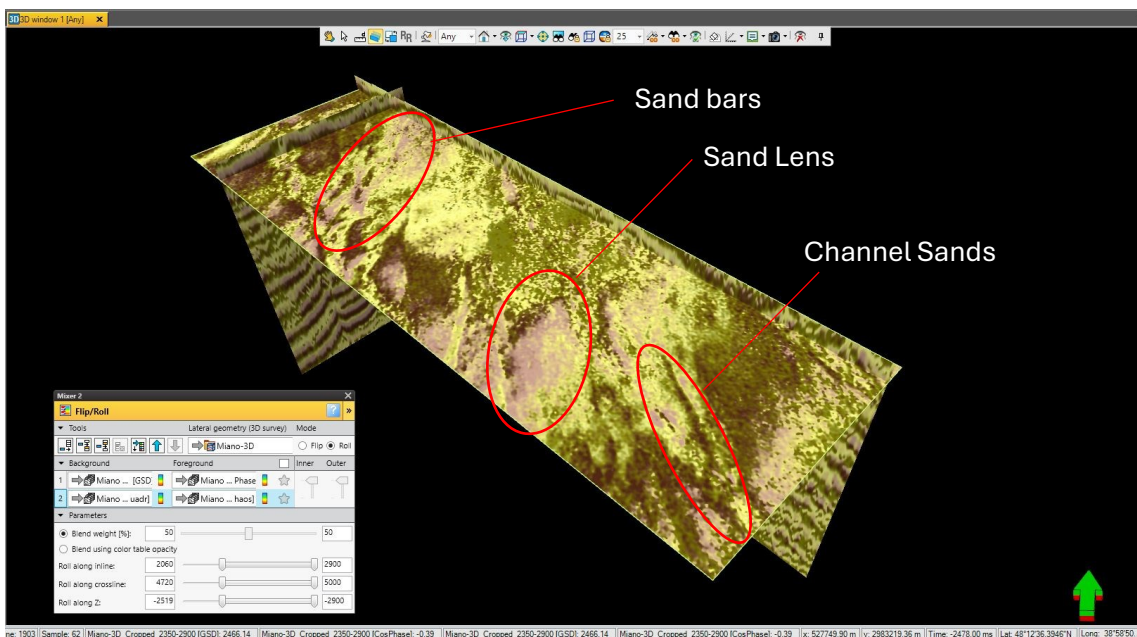
Figure 6.20. High resolution attribute blending resolves channels and sand lenses at 2350 ms.
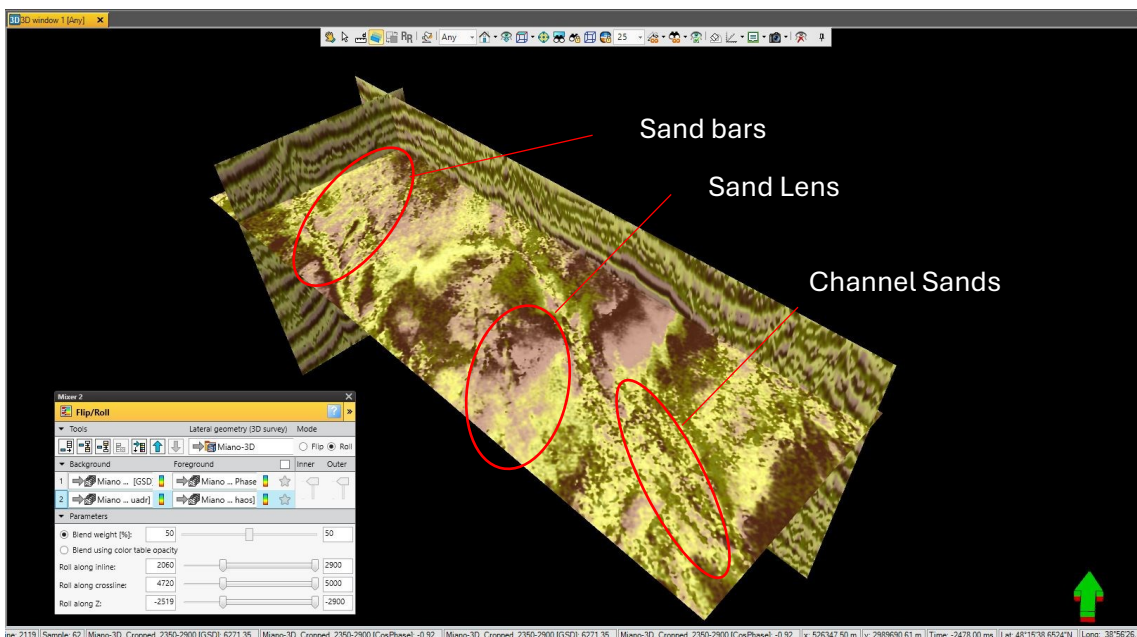
Figure 6.21 High resolution attribute blending resolves channels and sand lenses at 2450 ms.
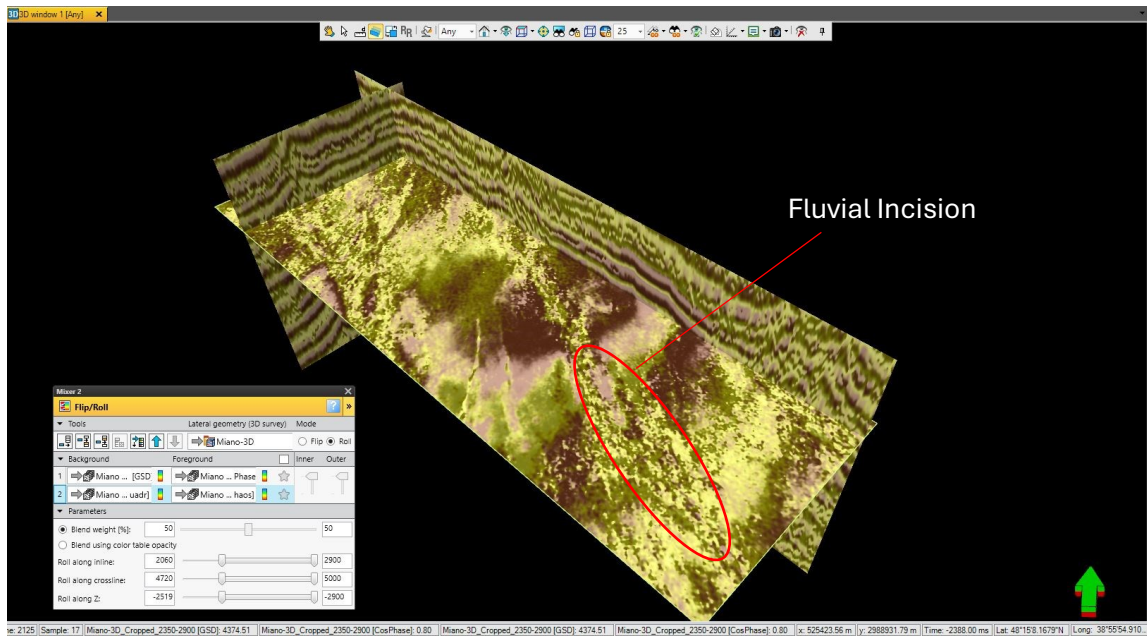
Figure 6.22 High resolution attribute blending resolves fluvial incision and sand lenses at 2550 ms.
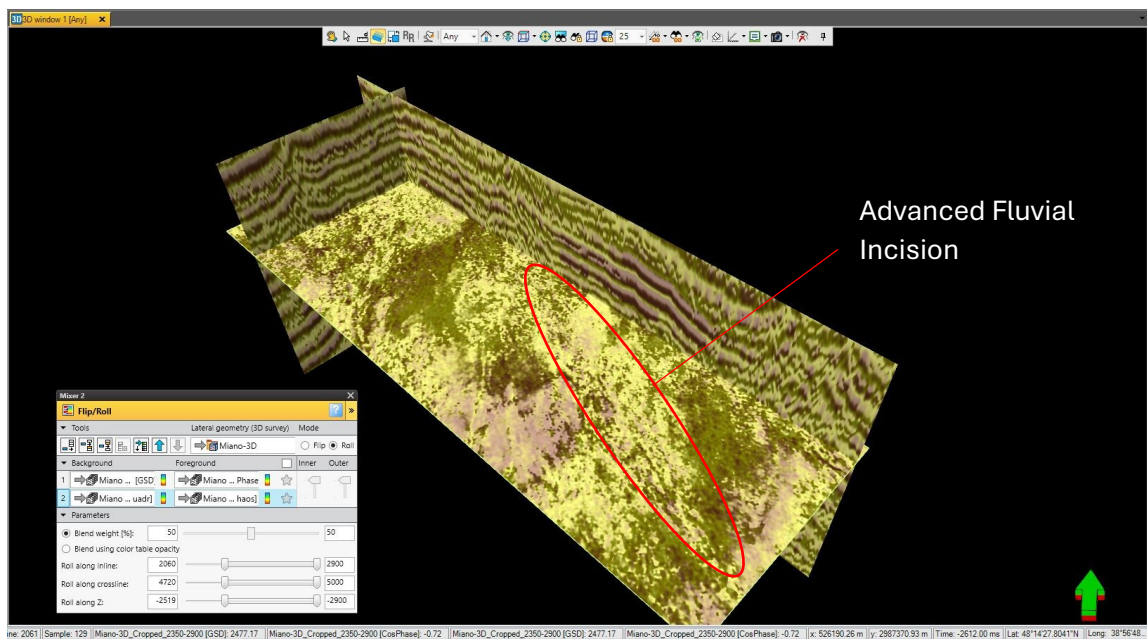
Figure 6.23. High resolution attribute blending resolves channels mixed deposition at 2650 ms.

6.3   ML Based Facies Clustering from Well Logs

In order to gain control for facies classification on seismic (coarse scale), we use the open hole log interpretation (fine scale) for facies discrimination and then match that with facies encapsulated by attributes (Bestagini et al., 2017). These attributes are ideally suited to subtle stratigraphic discontinuities unconformities. Here we present the methodological controls for a multi-step approach leading to assessing the sub-seismic scale facies prediction prowess of machine learning algorithms. Open-hole log interpretation of the wells Miano 2, 9 and 10 classified lithology of the reservoir into 5 lithotypes Lithotype 1 was Sand, Lithotype 2 was Sandy Shale, Lithotype 3 was Silt, Lithotype 4 was Shaly-sand and Lithotype 5 was Shale. Well data was preprocessed NaN values were removed in training and testing data and the data was merged into a single data-frame. Skewness was removed in curve data required through machine learning algorithms and the dataset was normalized using yeo-johnson normalization. The outliers were subsequently removed. Miano 2 was used as a blind well and two machine learning algorithms (Random Forest Classification and Gradient Boosting Classification) were used to train well Miano-9 and predict facies on Miano-10. Random Forest predicted facies with little more accuracy than Gradient Boosting. Randon Forest classifier had an accuracy of 87.1% and accuracy of each lithology column were Sand 92%, Sandy Shale 88%, Siltstone.

First and foremost, an Exploratory Data Analysis (EDA) is performed. EDA stands as a compass in the initial QC of a dataset, serving as a guide through the intricate details of the data. This exploratory step focuses on revealing underlying patterns, trends, and irregularities within the dataset. Summary statistics take center stage in this process, providing a quick overview of the central tendencies, dispersions, and distributions of the dataset, setting the foundation for a comprehensive understanding. Visualizations such as histograms, scatter plots, and box plots complement the numerical summaries, offering a visual representation of the data's narrative. These visual aids play a vital role in identifying outliers, discerning relationships between variables, and elucidating the overall structure of the dataset. Essentially, EDA functions as a preliminary investigative phase preceding the modeling stage, enabling practitioners to make informed decisions about data preprocessing, feature

engineering, and the selection of suitable machine learning algorithms. Moreover, EDA extends beyond being a one-time detective process; it is dynamic and iterative, adapting to the unique characteristics of each dataset. It involves a thorough examination of missing values, scrutiny of feature relationships, and the identification of potential transformation needs. The insights gained during EDA often prompt additional refinements in data cleaning, preprocessing, or the creation of new features. This iterative approach ensures that a deep understanding of the intricacies of the data are gained, facilitating well-informed decisions in subsequent stages of the machine learning pipeline (Bestagini et al., 2017).

Exploratory Data Analysis (EDA) is performed on well logs to assess petrophysical parameters derived from log data (Bestagini et al., 2017). The mean and variance of the red, green, blue, and greyscale pixel channels for each pixel row in the aligned core photographs are computed. These computations are then depth registered to produce RGB Logs (RGBL). This foundational calculation generates a pseudo- lithology log directly from the images, capturing shifts in log values corresponding to changes from sand to mud. The RGBL log and petrophysical analysis of well logs are used to train models at wells (Bestagini et al., 2017).

The dataset underwent rigorous preprocessing to ensure data quality and to make it suitable for machine learning analysis:

1. **Data Cleaning**: Any missing values (NaN) are removed to avoid inconsistencies. Removing NaNs ensures the models are trained on complete data without gaps, improving model reliability.

2. **Data Merging**: Different datasets from various sources are combined into a single cohesive table, or data frame, for unified processing. This merged data frame provides a comprehensive basis for training and testing ML models.

3. **Normalization and Skewness Removal**: Skewness in the dataset is removed, and Yeo-Johnson normalization is applied to standardize the distribution of data values. This normalization is crucial as it scales data to a range that ML models can handle effectively, enhancing the accuracy of predictions.

4. **Outlier Removal**: Outliers, or anomalous values, are identified and removed. This step prevents the models from being biased by extreme values that could otherwise degrade performance.
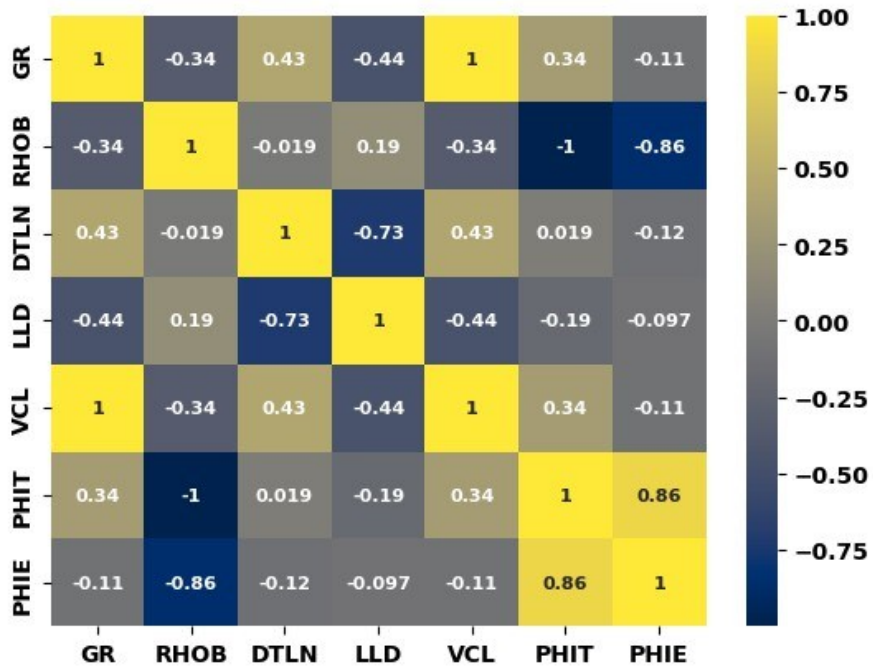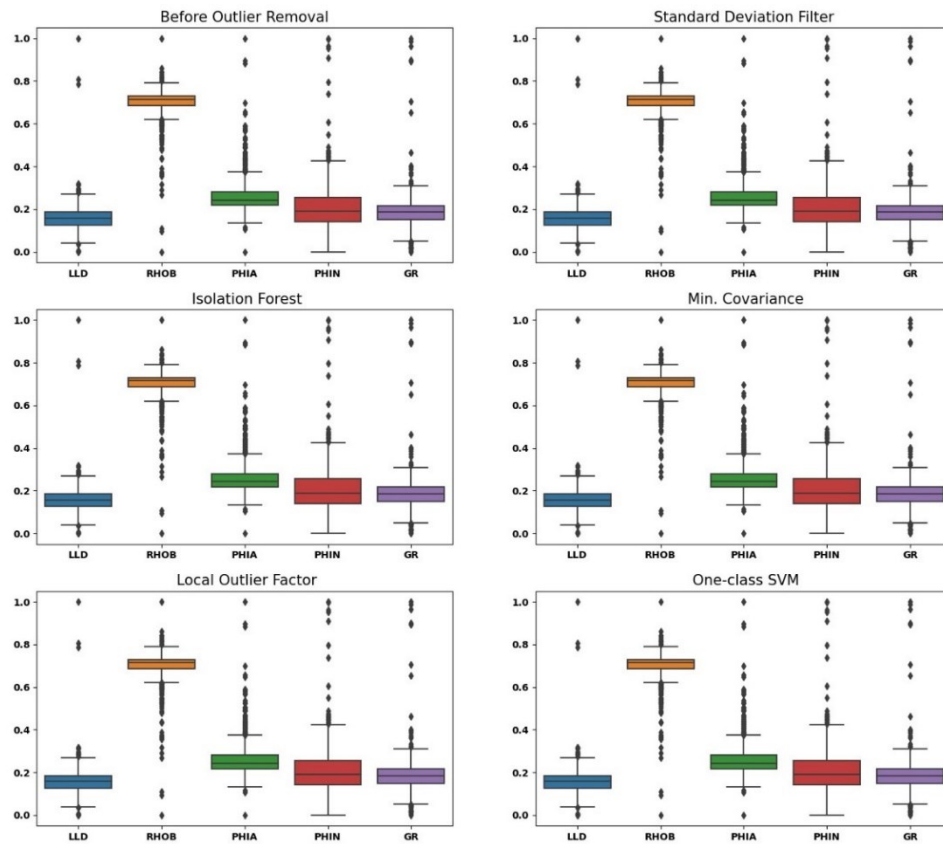
Figure 6.24 Exploratory Data analysis of Miano-02.
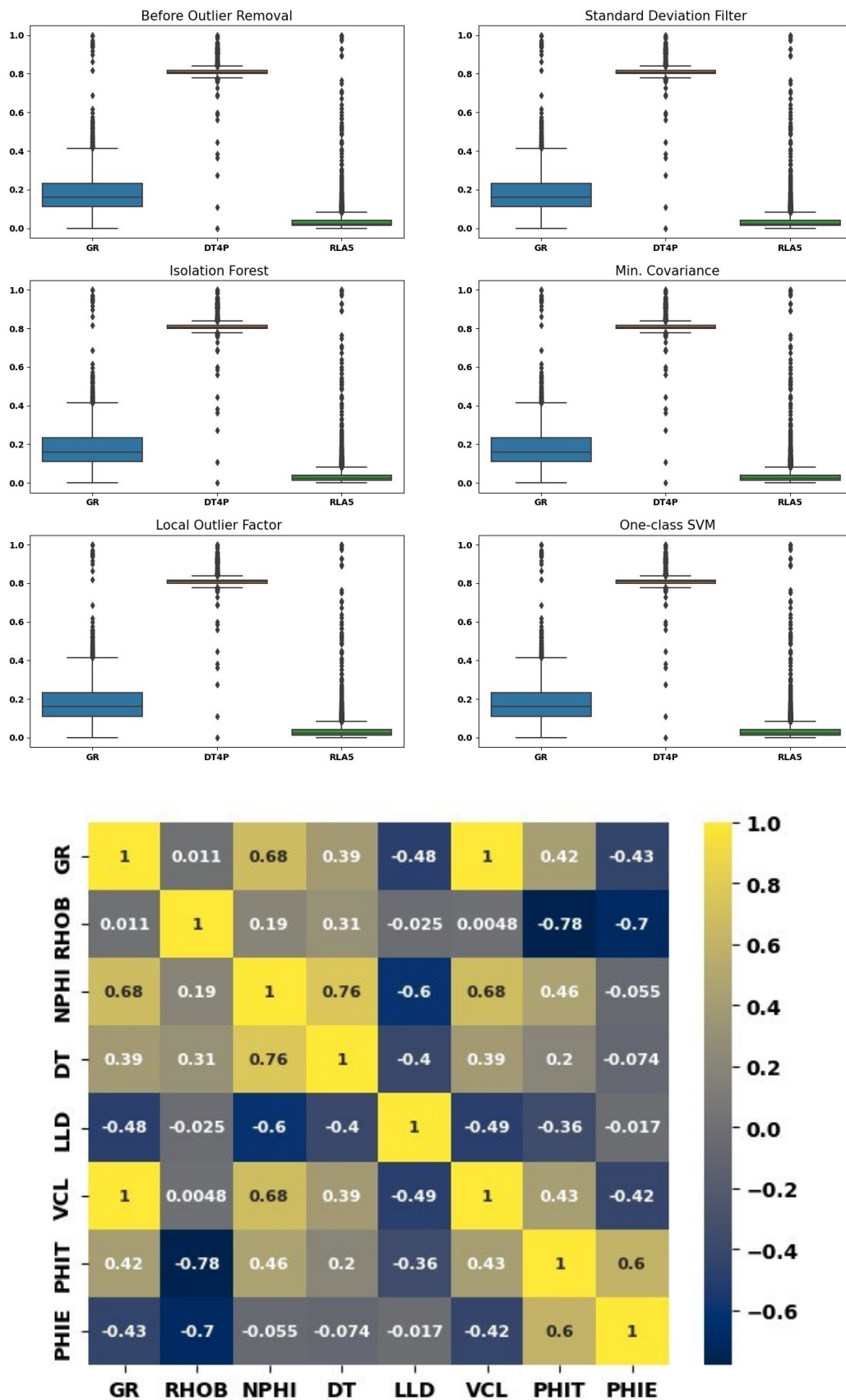
Figure 6.25 Exploratory data analysis of Miano-09.
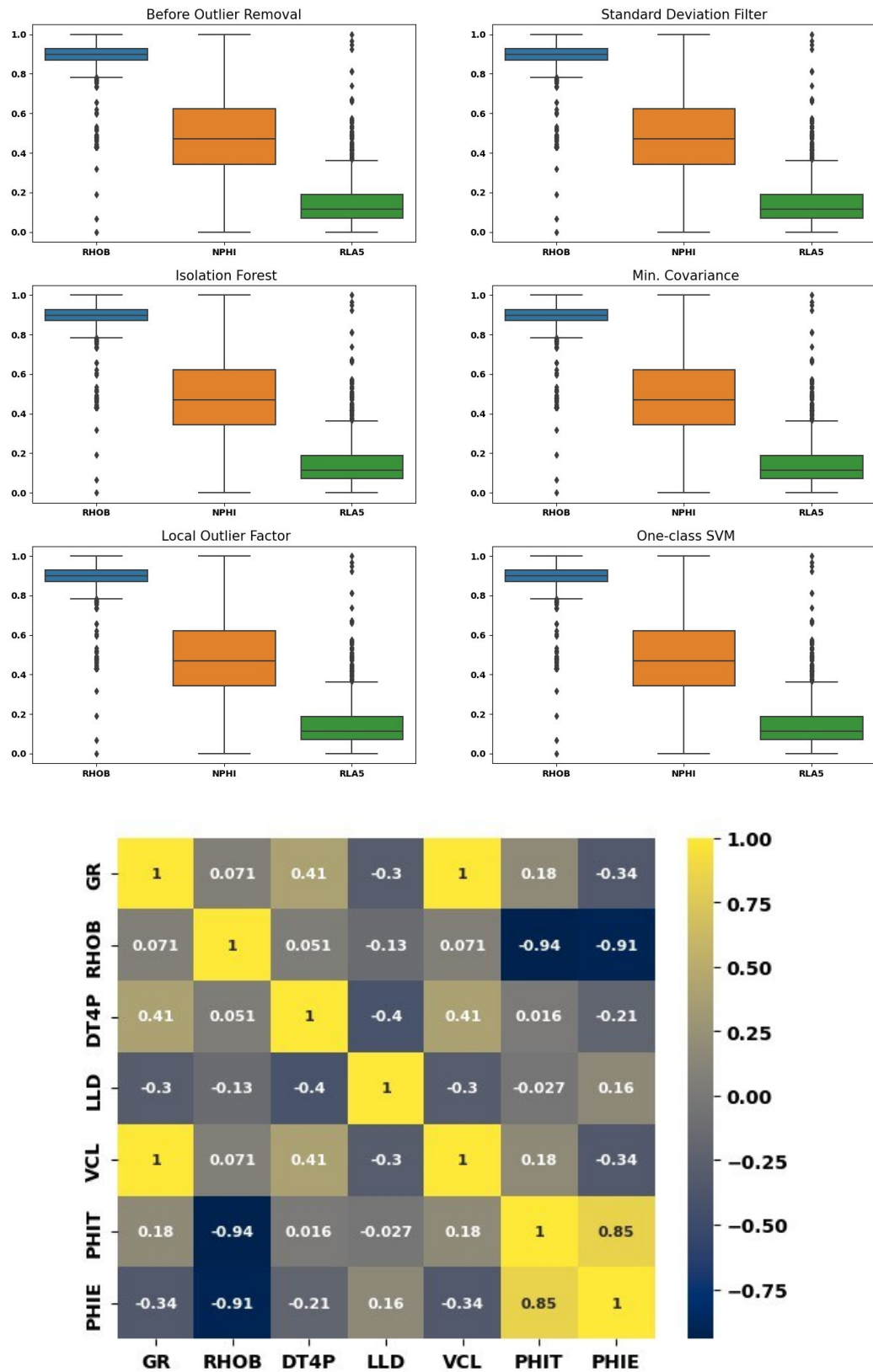
Figure 6.26. Exploratory data analysis of Miano-10.

The use of the MLP-SVM model for predicting lithofacies based on RGB logs is a new approach to understanding oil and gas reservoirs. By using machine learning techniques, the model achieved an impressive total accuracy of 92.31%. This successful application of MLP-SVM showed the utility of machine learning in improving lithofacies prediction and reservoir characterization. The comparison of Random Forest Classification and Gradient Boosting Classification provided valuable insights into their performance in lithofacies prediction. Both algorithms were effective at finding patterns in the data, but Random Forest had slightly higher accuracy compared to Gradient Boosting. This difference highlights the importance of selecting the right algorithm for the specific dataset. GR logs were split into RGB components the red, green and blue pixel rows were average to plot it as a pseudo litho-log, yeo-johnson normalization was used to normalize the RGB logs from 0-255 to 0-1 per channel (red green blue) representing the mean value for each channel across the core. the RGB logs capture fine-scale detail that the GR log does not. MLP-SVM (Multilayer Perception Support Vector Machines) was used to predict facies using RGB log instead the GR log.
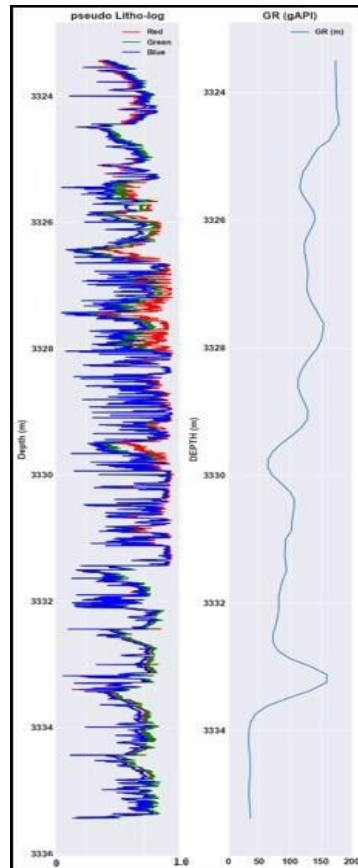
Figure 6.27. RGB log (left), and gamma ray log (GR, right) (depth in meters).

To represent the mean value for each channel across the core, we normalize the RGB log's scale from 0–255 values to 0–1 on a per-channel basis (i.e., red, green, blue, and gray) (Bestagini et al., 2017). Keep in mind that the GR log lacks fine-scale detail, but the RBG log does. The results from using Multilayer Perception Support Vector Machines (MLP-SVM) to predict rock layers (lithology facies) based on RGB log data show an impressive total accuracy rate of 92.31%. This demonstrates the exceptional effectiveness of MLP-SVM in accurately predicting rock layers using the comprehensive information extracted from the RGB logs. The high accuracy suggests the model was well-trained on the RGB log data, allowing it to effectively identify the complex patterns and relationships in the dataset, leading to precise predictions of the rock layers.
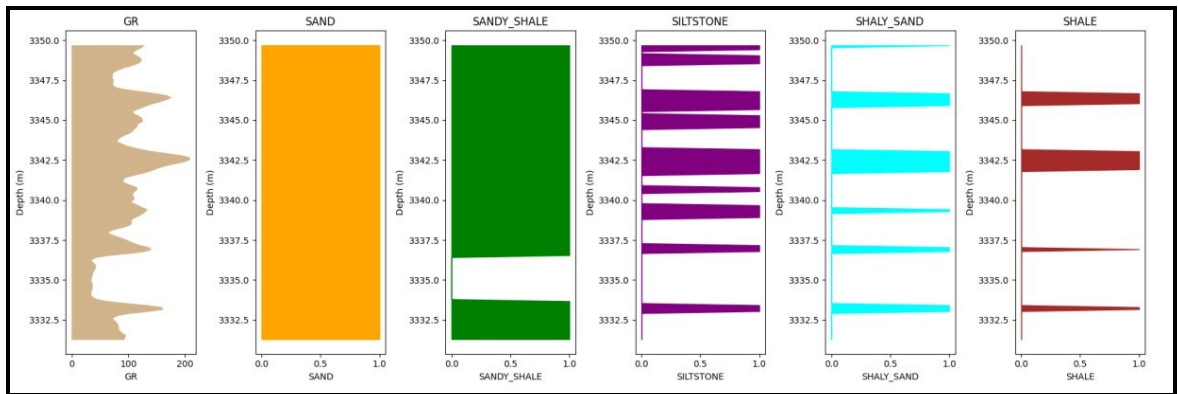
Figure 6.28 Actual interpreted litho-facies of Miano-2
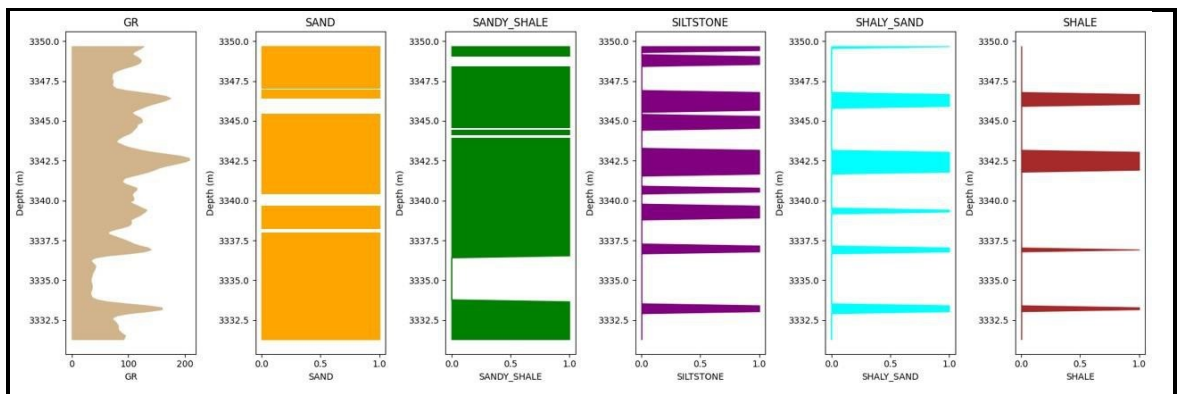
Figure 6.29 K Means lithofacie prediction of Miano 2.
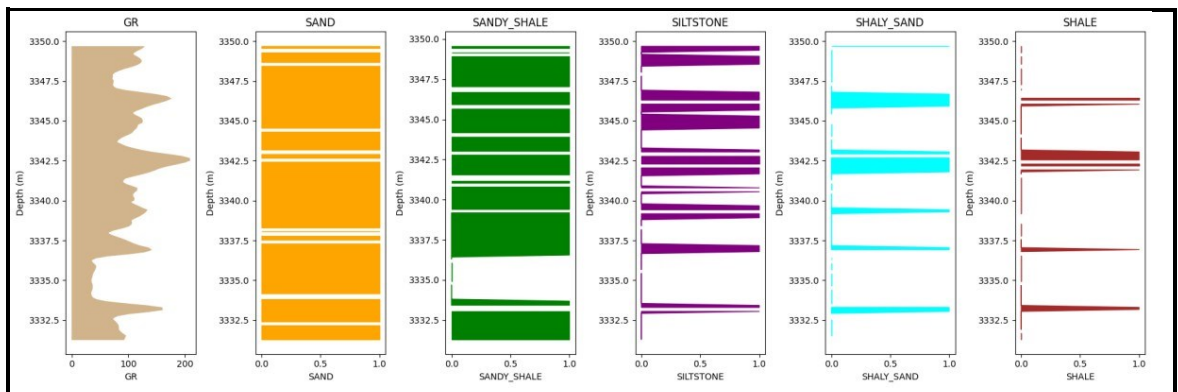
Figure 6.30 Actual interpreted litho-facies of Miano-10.

6.4   SOM Steered Seismic Attribute Analysis

From the well based control points and rendered attributes, facies clustering is performed through Self Organizing Map, a type of unsupervised machine learning algorithm. Initially, using the well based facies clusters (SOM-1) and attributes-based

clusters are parameterized and transformed to a color log. An initial neighborhood radius is kept at 1.2 and training iterations are constrained to 5 (Wen et al., 2011). The grid spacing for the cluster projection space is kept at 150 at a Eucilidian threshold of 80 and threshold for spectral angle mapping is limited to 45 degrees. EarthVision grid is employed for volumetric classification of facies clusters (Wen et al., 2011).
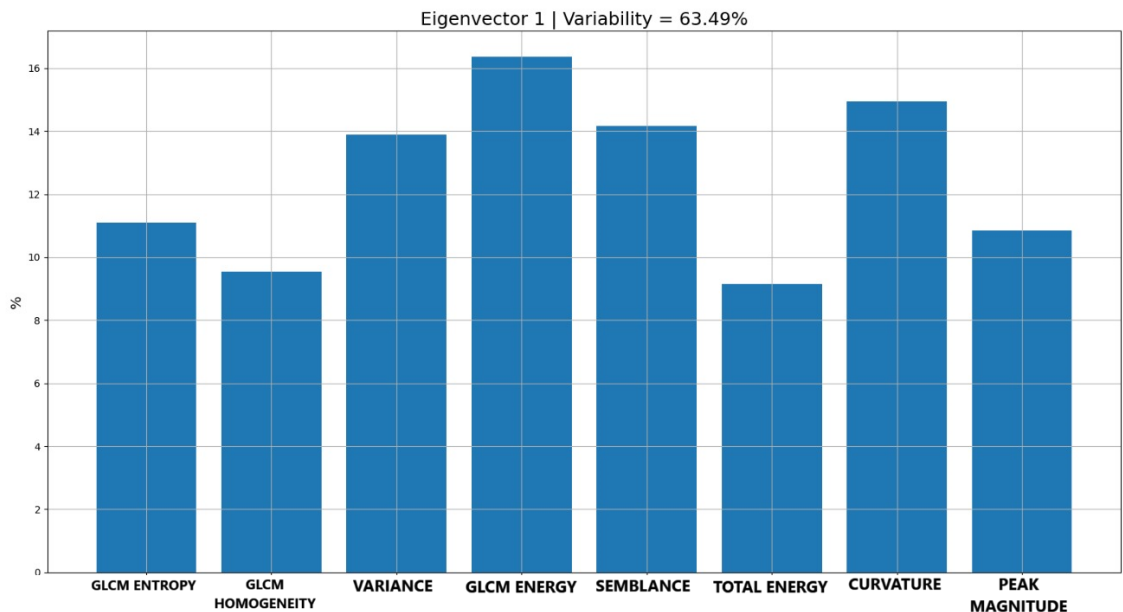
Figure 6.31. Principal component analysis, unsupervised machine learning.

Fig 6.31 represents the contribution of various attributes to the first principal component, or Eigenvector 1, in a data set, where Eigenvector 1 captures 63.49% of the total data variability. The attributes such as GLCM Entropy, Variance, and Curvature are shown with bars indicating their percentage contribution to this primary component, with GLCM Energy, Curvature, and Variance being the most significant. In this context, Eigenvector 1 highlights the direction in which the data varies the most, meaning it captures the dominant patterns across all attributes. By analyzing these contributions, the attributes with the highest variability are identified, allowing us to select the most informative features for input to a Self-Organizing Map (SOM). This step is essential for dimensionality reduction, focusing the SOM on the attributes that best represent the data's underlying structure, thereby improving clustering and interpretation efficiency.
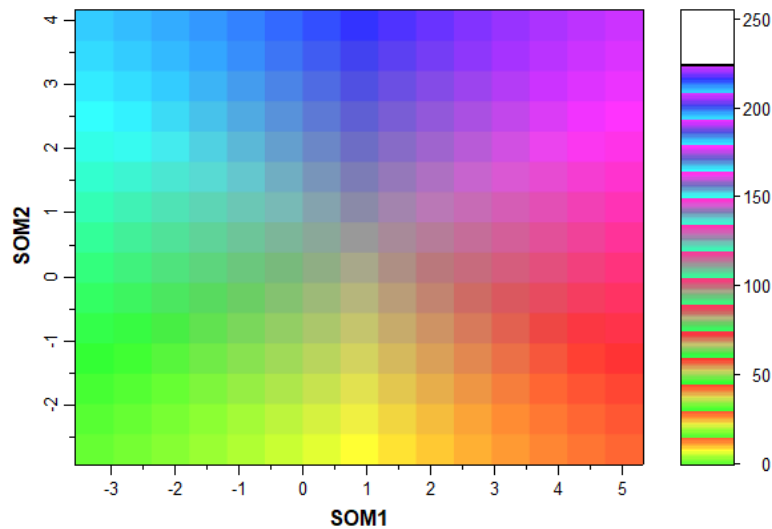
Figure 6.32. Parameterization cross plot with the color log for well-based and attributes driven facies.

Fig 6.32 shows a 2D Color Legend for a Self-Organizing Map (SOM). It shows a color-coded grid, where each square represents a node or cluster within the SOM. The axes, labeled SOM1 and SOM2, correspond to two dimensions in the SOM's reduced feature space, where similar data points are grouped close together. The colors vary across the grid, indicating different clusters or regions with distinct patterns. The color scale on the right provides a reference for these clusters, with colors ranging from blue to pink, green, and orange, each representing different values or classes in the dataset. This color map helps in visually interpreting the clustering results, allowing users to identify clusters or zones with similar attributes based on the color coding.
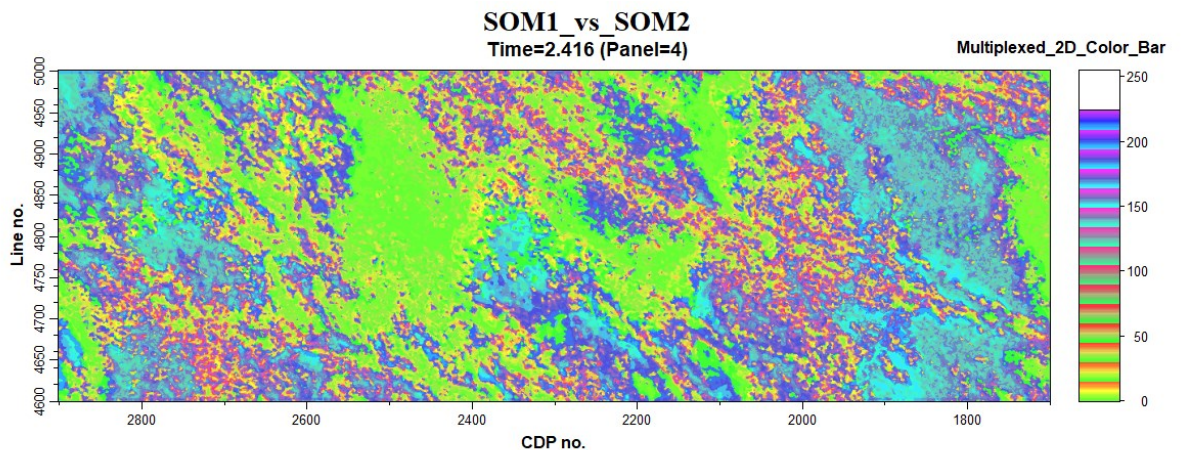
Figure 6.33. Sand lenses and depositional trends at 2416 ms.
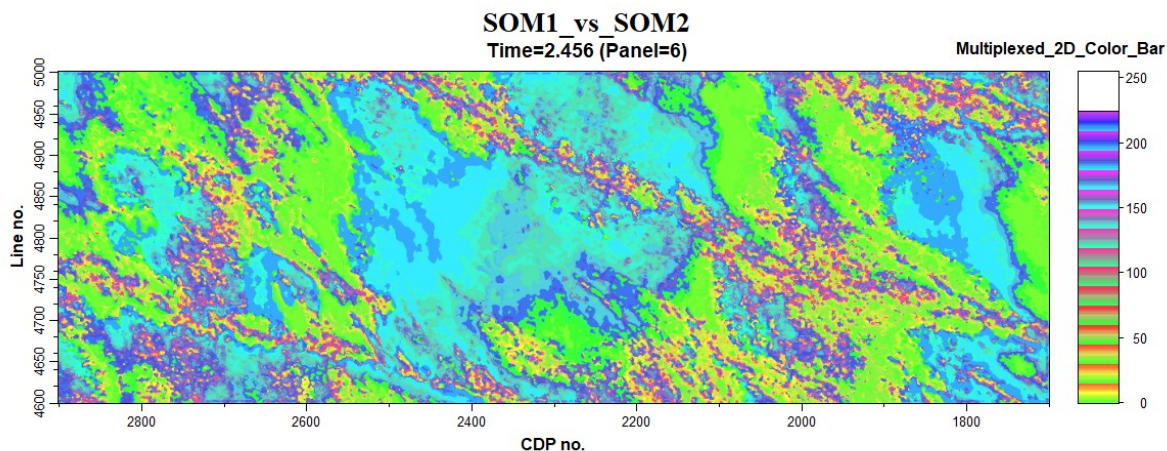
Figure 6.34. Fluvial ravinement and depositional trends at 2456 ms.
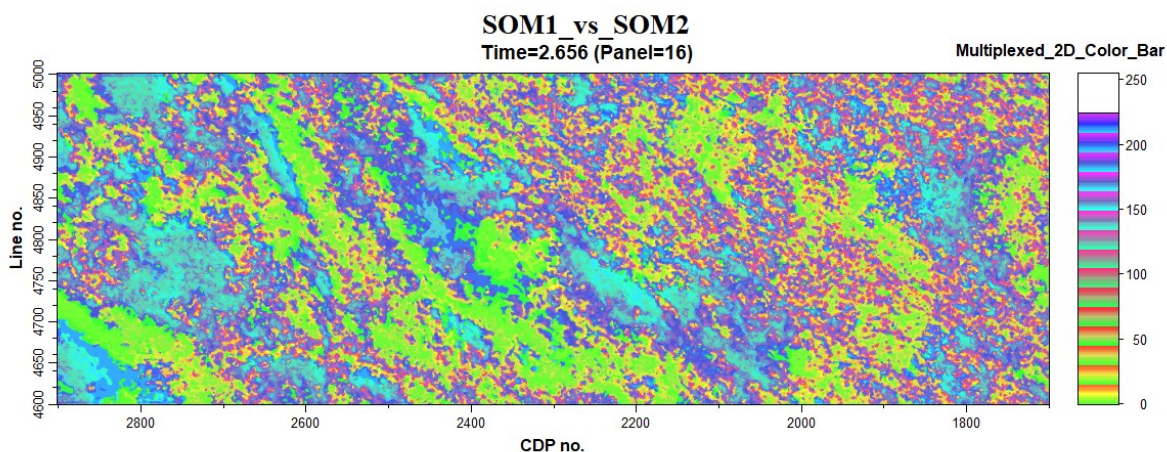
Figure 6.35. Sand channels and chaotic depositional trend at 2656 ms.

Seismic attributes, well based facies classification and attributes-based facies clustering does a remarkable job in evaluating and predicting reservoir candidate sands within the study area (Qi et al., 2019). At upper sequences, all attributes are in agreement that sand lenses above the flooding surface are good quality whereas silty sands / shaly sands around these lenses and at the edges of river channels downgrade the reservoir quality by choking porosities.

With high resolution attributes blending and good confidence in edge detection / stratigraphic boundary discrimination, we can assess that below the flooding surface, the transgressive sands have mixed variation in terms of reservoir potential owing to the fact that due to rapid sea level fall, deep fluvial incision and transitioning

depositional environments. Forced progradation has been a consistent feature over the Late Cretaceous (Qi et al., 2019).

Furthermore, the lower regressive facies indicate poor reservoir quality as the sands onlap shaly strata, thus deeper sands are enveloped with higher reservoir quality risk and challenging characterization.

This multi-method approach integrating well log data, machine learning algorithms, RGB log transformations, and SOM-based seismic clustering enables a detailed analysis of facies distribution and reservoir quality. Random Forest, MLP-SVM, and SOM collectively enhance the accuracy of lithofacies prediction and reservoir assessment, demonstrating the power of machine learning for subsurface characterization. The insights gained can inform drilling decisions, optimize production, and support effective reservoir management in complex geological settings.

CHAPTER 7
RESULTS AND DISCUSSION

7.1   Results and discussions

Clastic depositional environments are diverse, heterogeneous and have massive potential for being hydrocarbon reservoirs. Facies prediction is a critical yet challenging endeavor for oil and gas field development, particularly at centimeter scale. Since the deposition does not happen randomly and depends entirely on the energy of water at different stages of sea level rise and fall, there are patterns in nature. The effort to integrate core-based facies to reservoir scale models is especially complicated while trying to capture the thin-bedded heterogeneity that is common to deposition via interacting dynamic processes (wave energy, tidal regime, currents etc.; each with different energy), which re- work and disperse fluvial clastic sediments in a deltaic setting. Depositional morphology in deltaic environments include distributary channels, river-mouth bars, inter-distributary bays, tidal flats, shore-face, beaches, swamps, marshes, and evaporite flats. Identifying facies (the characteristics of a rock that reflect its origin and differentiate it from other rocks in its vicinity) within the morphologies is the key to understanding how the hydrocarbon reservoir will perform in its lifecycle. The lower Indus basin still has huge upside gas potential. With exploration efforts dating back to 1980s, Miano Gas Field was discovered at upper sand interval of the early Cretaceous Lower Goru Formation in August 1994 and is something of a geological puzzle. The sands which were supposed to flow gas proved to be either low porosity (tight) or produced water. This relates directly to facies variation within the Lower Goru Formation. With only upper sand interval producing commercially viable gas, other sand bodies were extensively tested but due to a poor understanding of depositional geomorphology, most models were inconclusive in evaluating the true potential of Lower Goru Formation. However, the upper sequence sand interval has been exploited thoroughly for commercial gas flow for the past three decades. A lack of facies control and understanding in the deltaic and pro-deltaic environment have hindered subsequent exploration endeavors. This is precisely where machine learning driven workflows with a high level of detail can be of immense value.

Control of depositional trends is first obtained from the wells. Gamma ray log is used in conjunction with the acoustic slowness log to interpret the depositional environments and sequence boundaries. Due to a lack of well control beyond 3600 meters, a model-based approach is taken for the middle and lower sand sequences. We build upon the work of Nadeem et al., 2012 and interpret the depositional environments sequentially using seismic and advanced ML driven attributes.

In terms of seismic stratigraphy as indicated in Figure 5.25, SU-1 can be sub-divided in lower sequence and upper sequence. The Lowstand wedge's base of slope is called "SU-2" Sequence LS. SU-1 sequence progrades maximum till the last offlap break. Downward shift in the coastal onlap defines a sequence boundary as sea level is dropping below the SU-1 (lower sequence) shelf margin, by downlap of steep post-SU-1 reflections by the onlapping truncations against the slope of the upper sequence boundary, as well as the low-angle SU-1 lower boundary and base-of-slope reflectors. The chaotic to drape-like geometries stacked against the lower sequence's slope and base-of-slope describe the SU-2 sequence. These could be explained as turbidite lobes that shifted as a result of a significant ravinement event. In a traditional topsets geometry, these submarine fans are overlain by progradational geometries typical of shelf-edge deltas. The clinoforms of a westward prograding system are represented by the seismic reflections in this package (upper series), which have an oblique shape and a rather high angle. This upper sequence wedge's offlap break displays sub-horizontal topsets after a mild aggradational trend (end of section, east). The base-of-slope and higher sequence slope of the lowstand system are stacked up against by another forced-regressive wedge. The "SU-2" Sequence's lowstand may very well be this wedge. This wedge is mapped as a component of the Sembar Formation in practice. This wedge serves as a crucial interface to limit the westward sand movement in the overlying sequences and specifies the maximum westward displacement of the Sembar shelf margin.

A widely distributed regional seismic event (toplap surface) above the lowstand wedge in the basinal part and on top of the SU-1 upper sequence boundary in the proximal areas towards east can be inferred as the flooding surface of the SU-2 Sequence. The high GR log motif on the logs from Miano field and other wells connects with this occurrence. These shales and the lag associated with erosion in the

basal ravinement can be understood as a transgressive surface created during a significant flood and reversing the ramp created by the SU-2 lowstand wedge and SU-1 upper sequence highstand. The nature of this sequence (Type-I vs. Type-II) varies within the survey area and is controlled by local uplift (e.g., thermal doming) and the magnitude of resulting sea level fall.

SU-1 upper sequence provide evidence that this is a depositional remnant of the fluvio-deltaic progradation from which the uppermost better reservoir quality sands were lost either during the subsequent regression or during transgressive ravinement erosion of the overlying SU-2 sequence. In view of that the areas bearing higher accommodation space, such as the distal end of the ramp, should be explored for the shelf edge deltaic topsets and shoreface depositional remnants of SU-1 upper sequence.

As gleaned from the interpreted seismic, large proportions of the SU-3, 4, 5 and 6 lap out near the lowstand shelf margin beneath. Within geometries of LG sequences, it is shown that good quality shoreface sands are in the shelf margin eastwards.

Near the SU-1 upper sequence shelf margin, there are two major breaks in the ramp's slope that may be seen. Where seismic imaging quality permits, these breaks can be plotted. This portion of the ramp, known as the outer ramp, is viewed as a distally steepened ramp and is situated between the margin made outwardly by the SU-2 lowstand wedge and the SU-1 upper sequence shelf margin. Sands deposited very thick aggradational stacked parasequences on the proximal ramp (SU-2 and SU-3), thinning across the distally steepened slope. The SU-4 and early SU-5 regressions most likely represent stacked forced regressive sand wedges that are bound by sequence boundaries and maximum flooding surfaces. It is more probable that the fluvial tracts that fed into the SU-6 forced regressive systems later on converted into a distinct noticeable shelf edge delta and disconnected shoreface systems because they incised significantly deeper into the underlying SU-5 highstand on the proximal ramp. Stratigraphic attributes including Spectral Decomposition, Grey Level Co-Variance Matrix, 3D Curvature and Variance highlight the subtle features and facies variation. Time correlating these with rapid sea level fall due to uplift in the vicinity

(Kandra High, Jacobabad High) reveal three different levels of deposition. The deposition above the flooding surfaces has shoreface facies which translates to sand lenses deposited by wave-tide action. These high energy deposited lenses have good reservoir potential. As the sea receded in an earlier time, fluvial incision and channels dominated the depositional ecosystem as the facies shifted basinwards. These channels have good to medium quality reservoir sands. Furthermore, as we go deeper, the sea level falls further causing the fluvial incision to advance. At this stage, the reservoir quality drops drastically due to the fact that the sands are now regressively onlapping shales and mixed deposition is widespread. Facies transition quickly chaotic deposition occurs as can be seen in time slices >2550 ms. Petrel rendered attributes, machine learning driven facies clustering and seismic inversion agree in terms of system tracts, flooding surfaces and depositional variations in the Cretaceous sands of Lower Goru Formation. The robust workflow employed has been successful in delineating reservoir quality and charts a way forward for further exploration in an already de-risked area.

7.2   Conclusion and Recommendations

In this research, we can see a new era of exploring and characterizing the subsurface for hydrocarbon exploitation. This is thanks to the powerful combination of machine learning and traditional geological expertise. By employing a data-driven workflow, we can now better understand reservoir quality of Miano. This will direct explorationists and future researchers to more advanced strategies for optimized gas recovery. As we venture into this new frontier of discovery, the blend of technology and human creativity will reveal fascinating insights about our planet's geology. This will build resilience and sustainability for the future.

Expanding on these remarkable achievements, the future holds exciting research directions with promises of further innovation and advancement. Exploring advanced modeling techniques, such as neural networks, self-organizing maps, high resolution color blending, these advanced methods can capture intricate spatial and temporal patterns within geological data, leading to more precise insights. Furthermore, integrating seismic data and well logs promise a more comprehensive understanding of reservoir characteristics. This holistic approach can help overcome the limitations of individual datasets, ultimately enhancing the accuracy and reliability

of predictive models. Furthermore, the investigation of techniques for integrating data in real-time provides a chance to develop dynamic lithofacies prediction models. These models can continuously update their forecasts to adapt to changing reservoir conditions, enhancing reservoir management practices.

As the boundaries of subsurface exploration expand, the combination of cutting-edge technology and interdisciplinary collaboration will continue to shape the future of geological research and resource management. Proper data preparation is crucial for building effective machine learning models. Exploring new preprocessing methods, like tailoring feature engineering to geological data or using advanced outlier detection, can enhance data quality and model performance. Additionally, incorporating domain expertise into the preprocessing stage can help reduce biases and improve the interpretability of predictive models.

Carefully testing and comparing different models is crucial for understanding how well lithofacies prediction models work in various geological areas. Doing detailed analyses to see how the new models stack up against existing methods and standard datasets can reveal the strengths and weaknesses of each modeling approach. Additionally, scientists working together and agreeing on standard ways to evaluate these models can help ensure the results are reliable and can be built upon, speeding up progress in predictive modeling for geoscience.

REFERENCES

Aadil, N. and Sohial, G.M.D., 2011. Stratigraphic Correlation and Isopach Maps of Punjab Plateform, Middle Indus Basin, Pakistan.

Abdulaziz, Abdulaziz & Mahdi, Hameeda & Sayyouh, Mohamed. (2018). Prediction of reservoir quality using well logs and seismic attributes analysis with artificial neural network: A case study from Farrud reservoir, Al-Ghani field, Libya. Journal of Applied Geophysics.

Afzal, J., Kuffner, T., Rahman, A. and Ibrahim, M., 2009. Seismic and Well-log Based Sequence Stratigraphy of The Early Cretaceous, Lower Goru "C" Sand of The Sawan Gas Field, Middle Indus Platform, Pakistan. Thomas Kuffner, Attiqueur Rahman, Muhammad Ibrahim, SPE/PAPG Annual Technical Conference.

Ahmad, Nadeem, et al. Sequence Stratigraphy as Predictive Tool in Lower Goru Fairway, Lower and Middle Indus Platform, Pakistan. (2004).

Allen, P.A., and Allen, J.R. "Basin Analysis: Principles and Applications." John Wiley & Sons, 2013.

Ashcroft, W. A. (2011). Seismic interpretation of layer-oriented impedance for reservoir models.

Aziz M.Z. and Khan M.R., 2003. A Review of InfraCambrian Source Rock Potential in Eastern Sindh, an analogue to Huqf Group of Oman. Infra – Cambrian play of Eastern Sindh, Pakistan.

Barclay, F. & Bruun, A. & Rasmussen, K.B. & Alfaro, J.C. & Cooke, A. & Cooke, D. & Salter, D. & Godfrey, R. & Lowden, D. & McHugo, S. & Ozdemir, Huseyin & Pickering, S. & Pineda, F.G. & Herwanger, Jorg & Volterrani, S. & Murineddu, A. & Rasmussen, A. & Roberts, R. (2008). Seismic inversion: Reading between the lines. Oilfield Review. 20. 42-63.

Bestagini, Paolo & Lipari, Vincenzo & Tubaro, Stefano. (2017). A machine learning approach to facies classification using well logs.

Carr, M., Cooper, R., Smith, M., Taner, M.T. and Taylor, G., 2001, October. The generation of rock and fluid properties volume via the integration of multiple seismic attributes and log data. In 7th International Congress of the Brazilian Geophysical Society (pp. cp-217). European Association of Geoscientists & Engineers.

Chen, Yuqing & Saygin, Erdinc. (2021). Seismic Inversion by Hybrid Machine Learning. Journal of Geophysical Research: Solid Earth.

Chopra, S., & Marfurt, K. J. (2007). Seismic attributes for prospect identification and reservoir characterization. Society of Exploration

Christopher, Octavian, Catuneanu & Galloway, (2011). Sequence Stratigraphy: Methodology and Nomenclature.

Dar, Qamar Uz Zaman & Pu, Renhai & Baiyegunhi, Christopher & Ghulam, Shabeer & Ali, Rana & Ashraf, Umar & Sajid, Zulqarnain & Mehmood, Mubashir. (2021). The impact of diagenesis on the reservoir quality of the early Cretaceous Lower Goru sandstones in the Lower Indus Basin, Pakistan. Journal of Petroleum Exploration and Production Technology. Geophysicists.

Delaplanche, J. & Lafet, Y. & Sineriz, B. & Gil, m. (2006). Seismic reflection applied to sedimentology and gas discovery in the Gulf of Cadiz. Geophysical Prospecting. 30. 1 - 24. 10.1111/j.1365-2478. 1982.tb00411. x.

Dietz, R. S., and Holden, J. C., 1970. Reconstruction of Pangaea: Breakup and Dimroth, E., and Kimberley, M. M., 1976.

Gale, A.S., et al. "Integrated stratigraphy and correlation of the Cenomanian stage in western Europe." Cretaceous Research 19.4 (1998): 625-667.

Gradstein, F.M., et al. "A Geologic Time Scale 2004." Cambridge University Press, 2004.

Hao Wu, Zhen Li, Naihao Liu, Bo Zhang, improved seismic well tie by integrating variable-size window resampling with well-tie net, Journal of Petroleum Science and Engineering, Volume 208, Part A, 2022, 109368, ISSN 0920-4105,

Haq, B.U., et al. "Mesozoic and Cenozoic chronostratigraphy and cycles of sea-level change." Sea-level changes: an integrated approach. SEPM Society for Sedimentary Geology (1987).

Helgesen, Jan & Magnus, Ingrid & Prosser, Sarah & Saigal, Girish & Aamodt, Geir & Dolberg, David & Busman, Sito. (2000). Comparison of constrained sparse spike and stochastic inversion for porosity prediction at Kristin Field. The Leading Edge. 19. 400-407. 10.1190/1.1438620.

Helmberger, Don & Burdick, L. (2003). Synthetic Seismograms. Annual review of earth and planetary sciences. Vol. 7. 7.

Herrera, R.H., Han, J. and van der Baan, M., 2014. Applications of the synchrosqueezing transform in seismic time-frequency analysis. Geophysics, 79(3), pp.V55-V64.

Iqbal M. W. A. and Shah, S. M. I., 1980. A guide to the stratigraphy of Pakistan, Geological survey of Pakistan.

Kear, B.P., et al. "Late Cretaceous fish from the Mangrullo Formation of Uruguay." Cretaceous Research 27.1 (2006): 103-114.

Khalid, Perveiz & Qayyum, Farrukh & Yasin, Qamar. (2014). Data-Driven Sequence Stratigraphy of the Cretaceous Depositional System, Punjab Platform, Pakistan. Survey in Geophysics.

Krois, Peter & Mahmood, Tariq & Milan, Gerhard. (1998). Miano Field, Pakistan, a case history of model driven exploration. Proceedings of the Pakistan Petroleum Convention; Pakistan Association of Petroleum Geologist. 1998. 111.

Loeblich, A.R., and Tappan, H. "Foraminiferal genera and their classification." Van Nostrand Reinhold, 1988.

Mitchum, R. M., Vail, P. R., & Thompson, S. (1977). Seismic stratigraphy and global changes of sea level, Part 4: Global cycles of relative changes of sea level. AAPG Memoir, 26, 83-97.

Molnar, P., and Tapponnier, P. "Cenozoic tectonics of Asia: Effects of a continental collision." Science 189.4201 (1975): 419-426.

Omoja, Uzochukwu & Obiekezie, Theresa. (2019). Application of 3D Seismic Attribute Analyses for Hydrocarbon Prospectivity in Uzot-Field, Onshore Niger Delta Basin, Nigeria. International Journal of Geophysics. 2019. 1-11. 10.1155/2019/1706416.

Oumarou, Sanda & Mabrouk, Djeddi & Tabod, & Tabod, Charles & Ngos, Simon & Abate Essi, Jean Marcel. (2021). Seismic attributes in reservoir characterization: an overview. Arabian Journal of Geosciences. 14. 10.1007/s12517-021-06626-1.

Pendrel, John. (2006). Seismic Inversion - Stillthe Best Tool for Reservoir Characterization. CSEG Recorder. 31.

Posamentier, H. W., & Vail, P. R. (1988). Eustatic controls on clastic deposition II—Sequence and systems tract models. In Sea-level changes—An integrated approach (pp. 125-154). SEPM Special Publication No. 42.

Poulsen, C.J., et al. "Cretaceous Ocean circulation and climate sensitivity." Geology 29.2 (2001): 103-106.

Pringle, M.S., et al. "The sedimentology of the lower Eocene Nummulitic limestone at Gais, southeast Turkey." Journal of Sedimentary Petrology 51.3 (1981): 955-970.

Qi, Jie & Zhang, bo & Lyu, Bin & Marfurt, Kurt. (2019). Seismic attribute selection for machine learning based facies analysis. GEOPHYSICS. 85. 1-95. 10.1190/geo2019-0223.1.

R. M. Haralick, K. Shanmugam and I. Dinstein, "Textural Features for Image Classification," in IEEE Transactions on Systems, Man, and Cybernetics, vol. SMC-3, no. 6, pp. 610-621, Nov. 1973, doi: 10.1109/TSMC.1973.4309314.

Raza, H.A., Ali, S. M. and Riaz, A., 1990. Petroleum Geology of Kirthar Sub-Basin and Part of Kutch Basin Pakistan. Journal of Hydrocarbon Research, no.1, 29-73.

Ruan, Fengming & Yang, Shucai & Huang, Guoping. (2018). Seismic attributes blending analysis for structural interpretation and geobody delineation. 840-843. 10.1190/IGC2018-205.

Schlager, W. "Carbonate sedimentology and sequence stratigraphy." SEPM Concepts in Sedimentology and Paleontology 8 (2005): 1-357.

Schlanger, S.O., et al. "Cenomanian–Turonian anoxic events in the South Atlantic Ocean." Nature 305.5933 (1983): 19-22.

Scotese, C.R. "A continental drift flipbook." Journal of Geology 112.6 (2004): 729-741.

Shekaili, Fatema & Chacko, Soman & Din, Samy & Yin, Yahui & Pujol, Aurelie & Lecante, Gael. (2012). Well Log Conditioning for Quantitative Seismic Interpretation. 10.2118/161382-MS.

Shen, Shian & Chi, Siqi & Chen, Wenchao & Wang, Xiaokai & Wang, Cheng & Binke, Huang. (2020). Texture attribute analysis based on strong background interference suppression. Interpretation. 8. 1-55. 10.1190/int-2019-0101.1.

Skelton, P.W., et al. "The evolutionary history of rudist bivalves." Annual Review of Earth and Planetary Sciences 36 (2008): 217-243.

Smewing, John & Warburton, John & Daley, Tim & Copestake, Philip & Ul-Haq, Nazir. (2002). Sequence stratigraphy of the southern Kirthar Fold Belt and Middle Indus Basin, Pakistan. Geological Society, London, Special Publications. 195. 273-299. 10.1144/GSL.SP.2002.195.01.15.

Szczepan J. Porębski, Ronald J. Steel, Shelf-margin deltas: their stratigraphic significance and relation to deepwater sands, Earth-Science Reviews, Volume 62, Issues 3–4, 2003, Pages 283-326, ISSN 0012-8252,

Vail, P. R., Mitchum, R. M., & Thompson, S. (1977). Seismic stratigraphy and global changes of sea level, Part 3: Relative changes of sea level from coastal onlap. AAPG Memoir, 26, 63-81.

Vine, F. J., Matthews, D. H., & Morley, L. W. (1963). Magnetic anomalies over oceanic ridges.

Wegener, A. (1915). The Origin of Continents and Oceans.

Wen, Renjun. (2011). Interactive Seismic Attribute Analysis for Reservoir Characterization. 10.5724/gcs.11.31.0473.

Yang & Ruan, Fengming, Shucai & Huang, Guoping. (2018). Seismic attributes blending analysis for structural interpretation and geobody delineation. Qi, Jie & Zhang, bo & Lyu, Bin & Marfurt, Kurt. (2019). Seismic attribute selection for machine learning based facies analysis. GEOPHYSICS. 85. 1-95. 10.1190/geo2019-0223.1.

Yi, Boyeon & Lee, Gwang & Kim, Han-Joon & Jou, Hyeong-Tae & Yoo, Dong-Geun & Ryu, Byong-Jae & Lee, Keumsuk. (2013). Comparison of wavelet estimation methods. Geosciences Journal. 17. 10.1007/s12303-013-0008-0.

Yin, A., and Harrison, T.M. "Geologic evolution of the Himalayan-Tibetan orogen." Annual Review of Earth and Planetary Sciences 28.1 (2000): 211-280.

Zachos, J.C., et al. "Trends, rhythms, and aberrations in global climate 65 Ma to present." Science 292.5517 (2001): 686-693.

Zhang, Rui & Castagna, John. (2011). Seismic sparse-layer reflectivity inversion using basis pursuit decomposition. Geophysics. 76. 147-. 10.1190/geo2011-0103.1.

Hamza Shah MS Thesis

1	**Submitted to Higher Education Commission Pakistan** Student Paper	**4**%
2	www.researchgate.net Internet Source	**2**%
3	www.searchanddiscovery.com Internet Source	**2**%
4	www.sepmstrata.org Internet Source	**1**%
5	Bourget, Julien, R. Bruce Ainsworth, and Sophie Thompson. "Seismic stratigraphy and geomorphology of a tide or wave dominated shelf-edge delta (NW Australia): Process-based classification from 3D seismic attributes and implications for the prediction of deep-water sands", Marine and Petroleum Geology, 2014. Publication	**1**%
6	link.springer.com Internet Source	**1**%